

# Design of Small Water Turbines for Farms and Small Communities

---

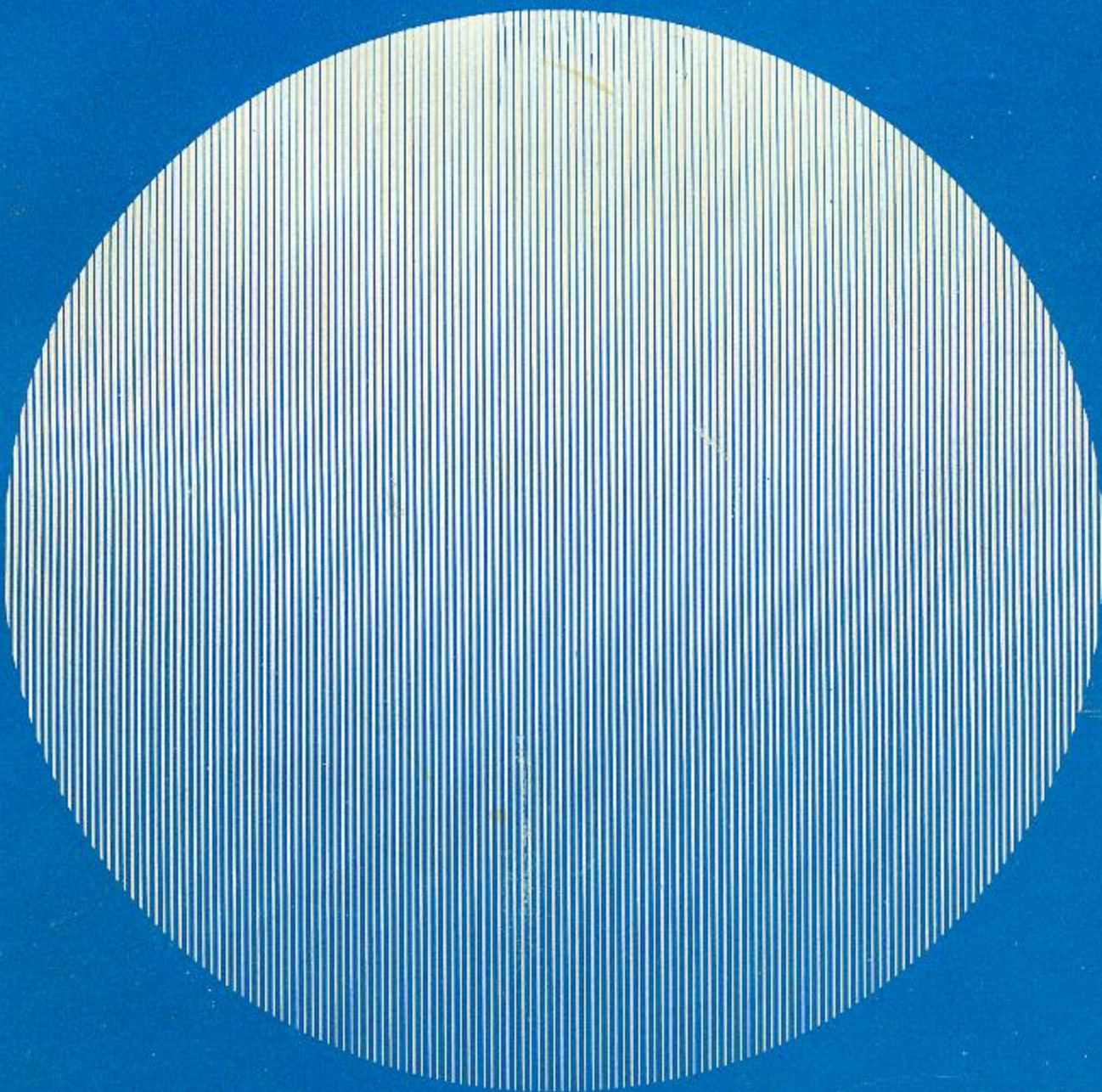
By  
Mohammad Durali

Project Supervisor:  
David Gordon Wilson

Prepared for the  
Office of Science and Technology  
United States Agency for  
International Development

By the  
Technology Adaptation Program  
Massachusetts Institute  
of Technology  
Cambridge, Massachusetts  
02139

---



DESIGN OF SMALL WATER TURBINES FOR  
FARMS AND SMALL COMMUNITIES

by

Mohammad Durali

Project supervisor:

David Gordon Wilson

Spring 1976

TECHNOLOGY ADAPTATION PROGRAM

Massachusetts Institute of Technology  
Cambridge, Massachusetts 02139

## C O N T E N T S

CONTENTS . . . . .	5
LIST OF FIGURES. . . . .	7
PREFACE. . . . .	9
ACKNOWLEDGEMENT. . . . .	11
ABSTRACT . . . . .	13
CHAPTER 1 INTRODUCTION. . . . .	15
1.1 Background, 10	
1.2 Problem Statement, 10	
1.3 Principles of Our Approach, 11	
CHAPTER 2 DESIGN OF A CROSS-FLOW (BANKI) TURBINE. . . . .	19
2.1 Description, 19	
2.2 Advantages of Bank Turbine, 19	
2.3 Analysis of the Machine, 21	
2.4 Design of the Rotor, 24	
2.5 Losses and Efficiencies, 32	
2.6 Blade Design, 37	
2.7 Sizing of a Cross Flow Turbine, 46	
2.8 Mechanical Design, 51	
2.9 Evaluation of Efficiencies, 57	
2.10 Radial-Inflow Partial-Admission Water Turbine, 58	
CHAPTER 3 DESIGN OF AXIAL-FLOW TURBINES . . . . .	61
3.1 Description, 61	
3.2 Advantages, 61	
3.3 Analysis, 63	
3.4 Design of Blades, 65	
3.5 Sizing of the Machines, 68	
CHAPTER 4 DISCUSSION ON ADVANTAGES OF DIFFERENT TYPES . . . . .	89
4.1 Improvements on Reaction Machine, 91	
4.2 Off-Design Performance, 92	
APPENDIX I TABLE OF PARTS AND WORKING DRAWINGS. . . . .	97
APPENDIX II FRICTION LOSS IN NONCIRCULAR CONDUITS . . . . .	147

APPENDIX III EFFICIENCIES . . . . .	149
APPENDIX IV PERFORMANCE ESTIMATION OF AXIAL-FLOW TURBINES . . . . .	153

CONTENTS

LIST OF FIGURES . . . . .

TABLES . . . . .

ACKNOWLEDGMENT . . . . .

PREFACE . . . . .

CHAPTER I INTRODUCTION . . . . .

1.1 Background . . . . .

1.2 Technical Statement . . . . .

1.3 Philosophy of Our Report . . . . .

CHAPTER 2 DESIGN OF A CROSS-FLOW (BARKER) TURBINE . . . . .

2.1 Description . . . . .

2.2 Advantages of Bark Turbine . . . . .

2.3 Analysis of the Turbine . . . . .

2.4 Design of the Turbine . . . . .

2.5 Losses and Efficiencies . . . . .

2.6 Blade Design . . . . .

2.7 Design of a Cross Flow Turbine . . . . .

2.8 Mechanical Design . . . . .

2.9 Evaluation of Efficiencies . . . . .

2.10 Radial-Inflow Partial-Admission Water Turbine . . . . .

CHAPTER 3 DESIGN OF AXIAL-FLOW TURBINE . . . . .

3.1 Introduction . . . . .

3.2 Design . . . . .

3.3 Analysis . . . . .

3.4 Design of Blades . . . . .

3.5 Design of the Turbine . . . . .

CHAPTER 4 EVALUATION OF PERFORMANCE OF TURBINE TYPES . . . . .

4.1 Performance of Radial-Inflow Turbine . . . . .

4.2 Performance of Axial-Flow Turbine . . . . .

APPENDIX I LIST OF PARTS AND WORKING DRAWINGS . . . . .

APPENDIX II LIST OF SYMBOLS AND UNITS . . . . .

LIST OF FIGURES

<u>NUMBER</u>	<u>TITLE</u>	<u>PAGE</u>
2-1	Cross-Flow (Banki) Water Turbine	20
2-2	Velocity Diagrams of Different Locations in Cross-Flow Turbine	22
2-3	Effect of Blade Outlet Angle on Stalling	26
2-4	Velocity Diagram Terminology	28
2-5	Work Coefficient $\Psi$ vs. Relative Inlet Flow Angle $\beta_1$	31
2-6	Converging Flow Inside the Rotor	35
2-7	Cross-Flow Turbine-Blade Terminology	38
2-8	Ratio of Blade Radius of Curvature R and Rotor Length L over Rotor Outer Diameter vs. Rotor Inner-to-Outer Dia. Ratio m.	44
2-9	Ratio of Radius to Hydraulic Diameter $R/D_h$ , and Deflection Angle of the Blade Passage $\theta_c$ vs. Rotor Inner-to-Outer Dia. Ratio m.	44
2-10	Number of Blades Z vs. Inner-to-Outer Dia. Ratio m.	45
2-11	Radial-Inflow Partial-Admission Water Turbine	59
3-1	Inlet and Outlet Velocity Diagrams of Axial-Flow Turbine Stage	62
3-2	Blade Terminology	66
3-3	Impulse Velocity Diagram	69
3-4	Blade Sections of the Axial-Flow Impulse Turbine	75
3-5	Reaction Velocity Diagram	83

LIST OF FIGURES (Continued)

<u>NUMBER</u>	<u>TITLE</u>	<u>PAGE</u>
3-6	Blade Sections of the Axial-Flow Reaction Turbine	85
4-1	Characteristic Curves of Reaction Machine for Constant Flow Rate	93
4-2	Characteristic Curves of Reaction Machine in Constant Speed	94
APPENDIX II		
1	Loss Factor for Bends (ASCE, J. Hydraulic Div., Nov. 65)	148
2	Friction Factor $f$ vs $Re$ . for Different $e/D$ . (Rohsenow, W.M., and Choi, H.Y., <u>Heat, Mass, and Momentum Transfer</u> , p. 58)	148
APPENDIX III		
1	Scheme of Losses in Water Turbo-Generators	151
APPENDIX IV		
1	Turbine Blade and Velocity Triangle Notation	156
2	Lift Parameter, $F_L$	156
3	Contraction Ratio for Traction Profiles	157
4	Basic Profile Loss	157
5	Trailing Edge Thickness Losses	157
6	Profile Loss Ratio Against Reynolds Number Effect	158
7	Secondary Loss-Aspect Ratio Factor	158
8	Secondary Loss-Basic Loss Factor	158

## PREFACE

This report is one of a series of publications which describe various studies undertaken under the sponsorship of the Technology Adaptation Program at the Massachusetts Institute of Technology.

In 1971, the United States Department of State, through the Agency for International Development, awarded the Massachusetts Institute of Technology a grant. The purpose of this grant was to provide support at M.I.T. for the development, in conjunction with institutions in selected developing countries, of capabilities useful in the adaptation of technologies and problem-solving techniques to the needs of those countries. At M.I.T., the Technology Adaptation Program provides the means by which the long-term objective for which the A.I.D. grant was made, can be achieved.

The purpose of this project was to study alternative water turbines producing 5-kw electric power from an available hydraulic head of 10 m and sufficient amount of flow, and to recommend one for manufacture.

The work consisted of the preliminary design of different types of water turbine which could be used for this application. Then one was selected and designed completely. A complete set of working drawings was produced for the selected type.

Four different types of water turbine were studied: a cross-flow (Banki); two types of axial-flow turbine; and a radial-flow turbine. Each one has some disadvantages. One of the axial-flow turbine (one with rotor blades having 50% degree of reaction) was chosen for detailed design as presenting the optimum combination of simplicity and efficiency.

In the process of making this T.A.P.-supported study, some insight has been gained into how appropriate technologies can be identified and adapted to the needs of developing countries per se, and it is expected that the recommendations developed will serve as a guide to other developing countries for the solution of similar problems which may be encountered there.

Fred Moavenzadeh  
Program Director

## ACKNOWLEDGMENT

This study was sponsored by the M.I.T. Technology Adaptation Program which is funded through a grant from the Agency for International Development, United States Department of State. The views and opinions expressed in this report, however, are those of the author and do not necessarily reflect those of the sponsors.

Mohammad Durali's financial support during the period of the research work has been provided by the Aria Mehr University of Technology, Tehran, Iran.

This project was initiated by the T.A.P. program director, Fred Moavenzadeh, in his discussions with a group at the Universidad de Los Andes led by Francisco Rodriguez and Jorge Zapp.

We are grateful for this support and help.

*David Gordon Wilson*

David Gordon Wilson,  
project supervisor  
department of mechanical engineering



DESIGN OF SMALL WATER TURBINES FOR  
FARMS AND SMALL COMMUNITIES

by

Mohammad Durali

ABSTRACT

The purpose of this project was to study alternative water turbines producing 5-kw electric power from an available hydraulic head of 10 m and sufficient amount of flow, and to recommend one for manufacture.

The work consisted of the preliminary design of different types of water turbine which could be used for this application. Then one was selected and designed completely. A complete set of working drawings was produced for the selected type.

Four different types of water turbine were studied: a cross-flow (Banki); two types of axial-flow turbines; and a radial-flow turbine. Each one has some advantages and some disadvantages. One of the axial-flow turbines (one with rotor blades having 50% degree of reaction) was chosen for detailed design as presenting the optimum combination of simplicity and efficiency.

5 kw electric power for the cases mentioned before. As this machine would be used by farmers who on average have little technical knowledge, one of the major objects is to avoid very complicated structures. Moreover the machine must not need skilled maintenance. Finally the amortized capital cost for using this machine should be less than the total cost of using the transmitted power produced by mains power plants.

Some members of the faculty of engineering of the Universidad de Los Andes in Bogota have worked on this problem. They have developed a half-kw cross-flow turbine. They plan to modify that model for higher power levels. We have reported our work to this group regularly.

The design of small water-turbine units has not previously been carried to a high degree of sophistication. This might be because of their limited applications. For applications like the one we have (i.e. electricity needed in a period of year when there is plenty of water) the design of a cheap machine may be a good solution to energy problems.

### 1.3 PRINCIPLES OF OUR APPROACH

The effort was put into two different approaches to the problem.

a) Designing a machine which can easily be manufactured by any simple workshop having enough facilities to weld, drill and cut steel parts. Consequently, the machine can be built locally in

each farming area. The parts such as bearings, gears, chain, generator etc., can be shipped to each area. In this approach we tried to use materials like angle bars, sheet metal, round bars and so on which do not need much machinery to be used. Casting and other more complicated processes were excluded.

b) Designing a machine which could be manufactured and shipped to farming locations. This approach a kind of process layout is going to be arranged for manufacturing the machine. The production methods like casting and molding, and using plastic parts seems to be more economical.

In both cases a) and b), the design has to be within the area of the industrial capabilities of the country of the user. The next chapter contains the design of a cross-flow turbine based on the "a" assumptions. In the end of Chapter 2 design of a simple rapid inflow turbine is discussed very briefly. Chapter 3 is about the design of 2 modified axial-flow turbines with short blades. The design of the two latter types is based on the assumptions made on the "b" type of approach.

## Chapter 2

### DESIGN OF A CROSS-FLOW (BANKI) TURBINE

#### 2.1 DESCRIPTION

This machine was first designed by Dr. Banki over 60 years ago. Since then some low-power models of this kind have been developed in Europe and have given good performances.

This machine is an atmospheric radial-flow impulse wheel which gets its energy from the kinetic energy of an inward jet of water. The wheel is simply a squirrel-cage-shaped assemblage of curved horizontal blades (Fig. 2-1) fixed between circular end plates to which the shaft is attached. The jet of water coming out of the nozzle passes through the rotor blades twice.

The blades have to be designed to direct the flow inward to the open internal space inside the cage and then to drain it to the tail water outward through another set of blades in another part of the inner circumference.

#### 2.2 ADVANTAGES OF BANKI TURBINE

The cross-flow turbine has significant advantages which make it a suitable solution to our problem. Its simple structure makes it easy to be manufactured. The atmospheric rotor avoids the need for a complicated and well-sealed housing. The bearings have no contact with the flow, as they are out of the housing; they can simply be lubricated and they don't need to be sealed. And finally, when,

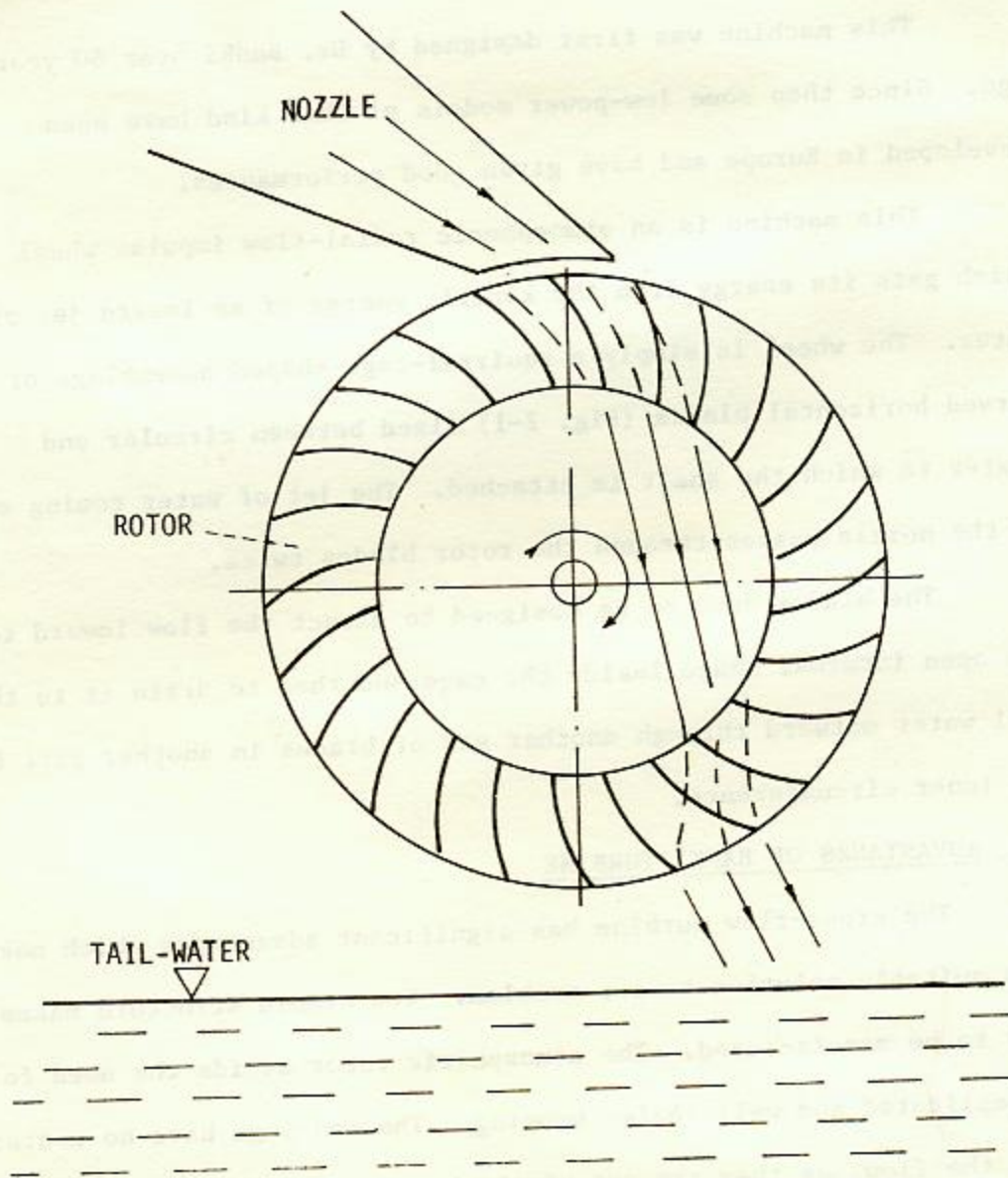


FIG.2-1. CROSS-FLOW (BANKI) WATER TURBINE.

for a constant head and a given power level a simple fixed rotor cross section is obtained, then for higher power levels one can simply use a longer rotor.

### 2.3 ANALYSIS OF THE MACHINE

The most useful relation in design of a turbomachine is the Euler equation,

$$U_i C_{\theta i} - U_o C_{\theta o} = g_c (h_{o_i} - h_{o_o})$$

where  $U$  stands for rotor peripheral speed,  $C_{\theta}$  is the tangential component of absolute velocity of the fluid and  $h_o$  is the stagnation enthalpy. Subscripts  $i$  and  $o$  stand for inlet and outlet of the rotor, respectively (Fig. 2-1).

The rotor normally is designed so that the absolute velocity of the fluid leaving the rotor is in the radial direction, so

$$C_{\theta o} = 0$$

and therefore

$$U_i C_{\theta i} = g_c \Delta h_{i-o}$$

and then the parameter "work coefficient" for the rotor will simply be

$$\psi = \frac{\Delta(UC_{\theta})}{U_i^2} = \frac{C_{\theta i}}{U_i}$$

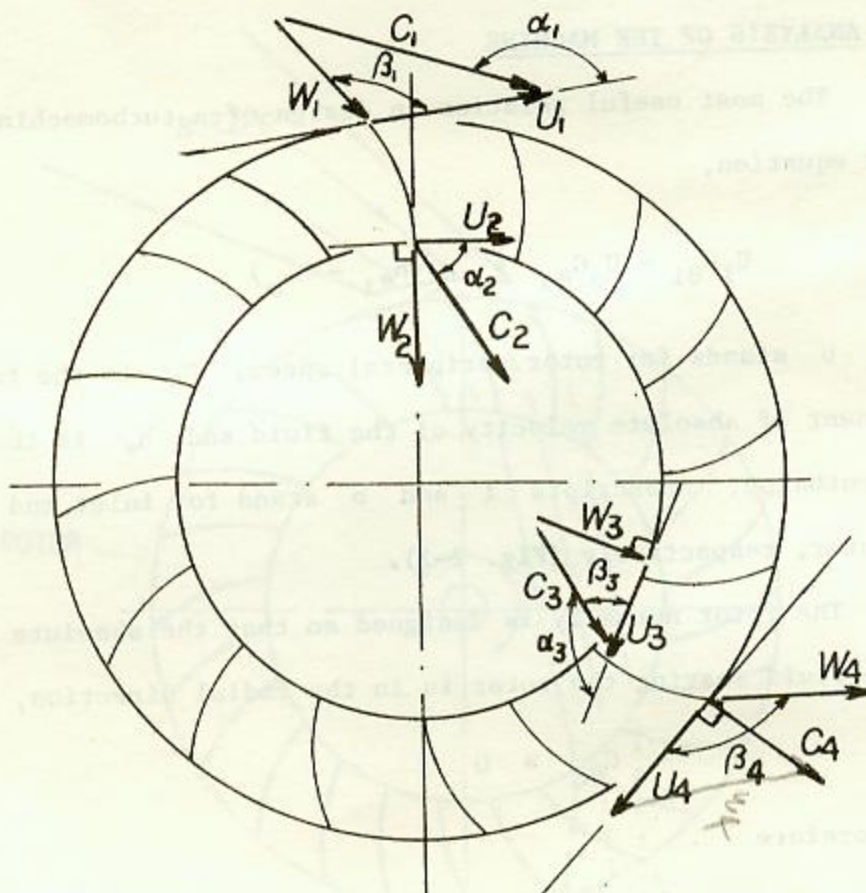


FIG.2-2. VELOCITY DIAGRAMS OF DIFFERENT LOCATIONS IN CROSS-FLOW TURBINE.

From the first law of thermodynamics,

$$\frac{\dot{Q} - \dot{W}}{\dot{m}} = \Delta h_o = \Delta \left( h + \frac{C^2}{2} + zg \right) ,$$

but for water turbines the rate of heat transfer and change in static enthalpy are very small and for small units like the one we are to study the drop in height from inlet to outlet is negligible, so that,

$$\frac{\dot{W}}{\dot{m}} = \Delta h_o = \frac{1}{2} (C_i^2 - C_o^2)$$

using the equations we had before,

$$U_i C_{\theta i} = \frac{1}{2} (C_i^2 - C_o^2) ,$$

$$\Psi U_i^2 = \frac{1}{2} (C_i^2 - C_o^2)$$

or finally

$$U_i^2 = \frac{1}{2\Psi} (C_i^2 - C_o^2) \quad (a)$$

For an impulse machine the value of  $\Psi$  is normally taken equal to 2.0. If the total hydraulic head before the nozzle is  $\Delta H_o$  and  $\eta_N$  be taken as nozzle efficiency (which covers the loss of kinetic energy through the nozzle) then equation (a) can be written as follows,

$$U_i^2 = \frac{1}{2\Psi} (2g \Delta H_o \eta_N - C_o^2) ,$$



or

$$U_1 = \frac{g}{\Psi} \left( \Delta H_o \eta_N - \frac{C_o^2}{2g} \right) \quad (2.1)$$

From Eq. (2.1) we find that for a given hydraulic head, choice of the velocity diagrams enables us to determine the rotor speed and hence rotor dimensions.

#### 2.4 DESIGN OF THE ROTOR

The choice of the blade inlet and outlet angles is the important part of the design. They have to be chosen so that the jet of water transfers useful work to the rotor in both passes through the blades.

Throughout this analysis angles are measured from tangents to the circles and are positive in the direction of rotation. Also we assume that at design point the incidence angle is zero and the deviation angle is very small so that the design will not be affected if we assume the derivation to be zero. From Fig. (2-2) by simple geometry we have for all cases

$$\alpha_2 = \alpha_3 ,$$

This is true for all shaft speeds and flow inlet velocities. But one may question why the inter stage angle of the blades is taken equal to  $90^\circ$  (i.e. the outlet angle of the first "stage" or pass, and the inlet angle of the second stage). The reasoning behind this choice is as follows.

Assume zero deviation angle for the flow leaving the blades in the first pass; therefore, the flow relative velocity angle will be equal to the blade outlet angle. Now suppose that the angle of the blade at the outlet of first pass is bigger than  $90^\circ$  (Fig. 2-3a). As you see there will be negative incidence at the second pass. This time assume  $\beta_2 < 90^\circ$  (Fig. 2-3b). In this case positive incidence will take place. Now as a comparison in Fig. (2-3c) the situation is shown with  $\beta = 90^\circ$ .

Therefore the optimum blade outlet angle has a value around  $90^\circ$ . Now assume  $\delta$  as deviation angle at outlet of the first pass (Fig. 2-3d). If the blade angle is kept equal to  $90^\circ$  then there will be an angle of incidence "i" so that  $i = \delta$  (in the inlet of the second pass). Consequently if the blade's outlet angle is slightly more than  $90^\circ$  (equal to  $90 + \delta/2$ ) then the incidence will be near to zero.

Normally the values of deviation angle are of the order of  $2^\circ$  to  $8^\circ$ . Therefore the optimum value for the blade outlet angle is between  $91^\circ$  to  $94^\circ$ . Obviously taking the blade angle equal to  $90$  would not cause much effect on the performance.

Because the cross-flow turbine rotor works totally at atmospheric pressure there is no static-pressure difference from inlet to outlet of a blade passage. Therefore the flow through a blade passage does not accelerate or diffuse. In fact, blade passages do not fill with water and flow passes through the blade passage as a jet deflecting

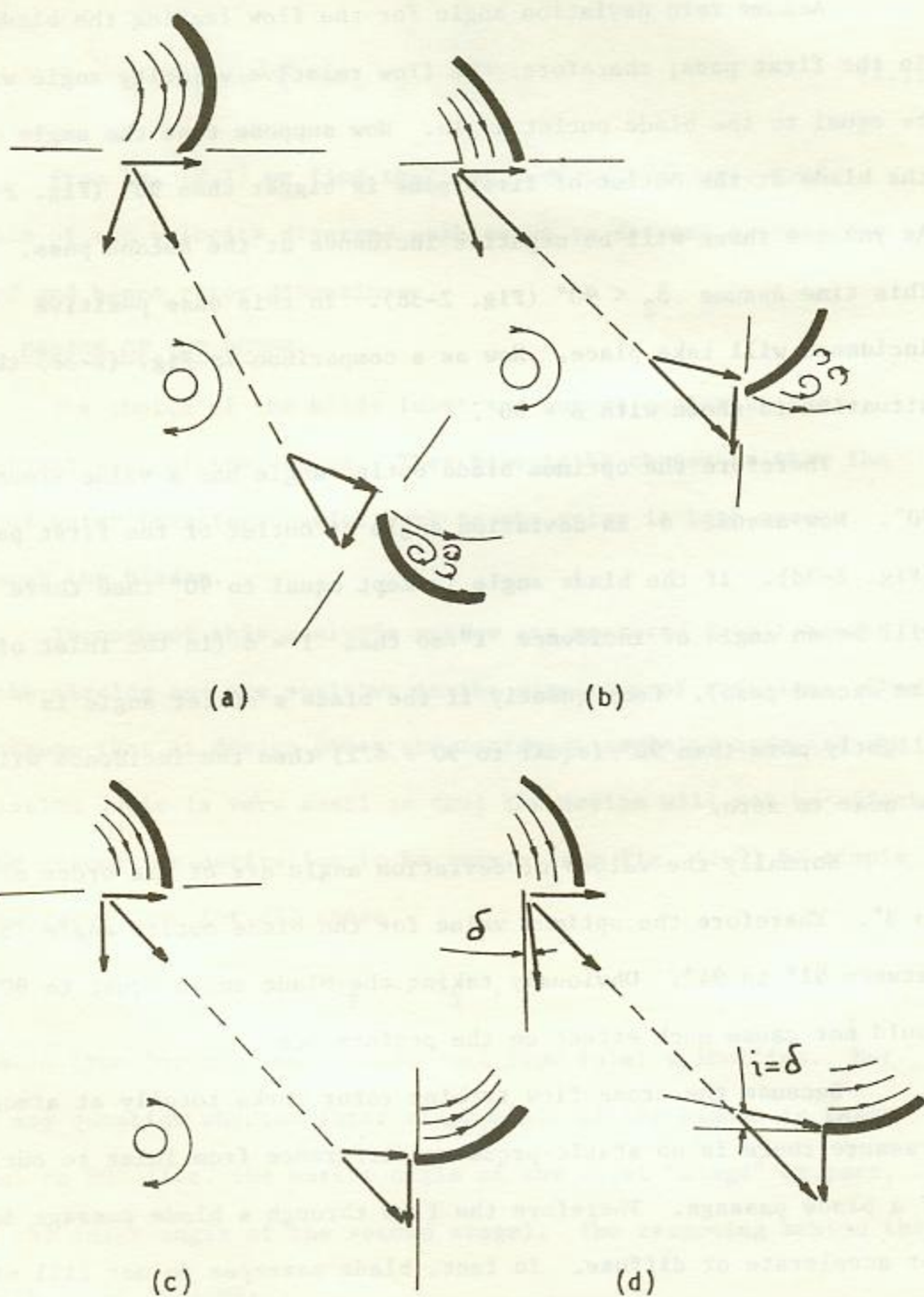


FIG.2-3. EFFECT OF BLADE OUTLET ANGLE ON STALLING.

along the pressure side of the blade. Consequently the flow will have a constant relative velocity through the passage (in the absence of friction) and the maximum flow will be determined by the smaller area of the passage which is at the inner diameter side of the rotor.

The rotor specifications are then as follows (Fig. 2-4): outlet relative velocity angle (first pass)  $\beta_2 = 90^\circ$  so from Fig. (2-4a)  $C_{\theta 2} = U_2$  and the absolute velocity of water leaving the rotor is in radial direction (Fig. 2-4b)  $\alpha_4 = 90^\circ$ .

Let us define

$$x \equiv \frac{C_{\theta 1}}{U_1} ,$$

(Notice that in this particular case  $x$  is equal to the work coefficient.)

and

$$m \equiv \frac{r_2}{r_1}$$

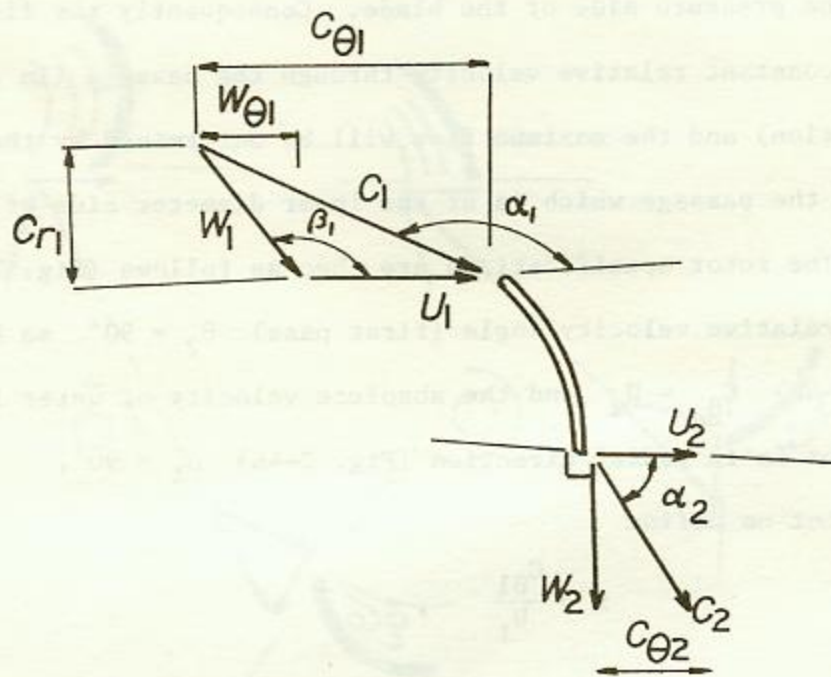
$r_2$  and  $r_1$  are inner and outer radii of the blading respectively, therefore

$$m = \frac{U_2}{U_1} = \frac{U_3}{U_4} .$$

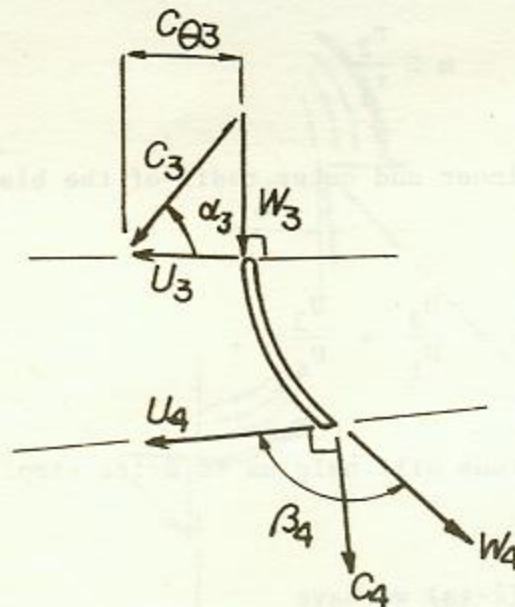
The above definitions will help us to write simpler geometric relations.

From Fig. (2-4a) we have

$$x \equiv \frac{C_{\theta 1}}{U_1} = \frac{C_1 \cos \alpha_1}{U_1} = \frac{-C_1 \cos \alpha_1}{-C_1 \cos \alpha_1 + W_1 \cos \beta_1} \quad (2.2)$$



(a)



(b)

FIG.2-4. VELOCITY DIAGRAM TERMINOLOGY.

Also,

$$C_{r1} = C_1 \sin(\pi - \alpha_1) = W_1 \sin(\pi - \beta_1) \quad (2.3)$$

from (2.2) and (2.3)

$$x = \frac{\tan \beta_1}{(\tan \beta_1 - \tan \alpha_1)}$$

Therefore

$$\beta_1 = \tan^{-1} \left( \left( \frac{x}{x-1} \right) \tan \alpha_1 \right) \quad (2.4)$$

From the outlet velocity triangle (Fig. 2-4a)

$$C_2 = \sqrt{W_2^2 + U_2^2}$$

If we assume no loss of kinetic energy through the blade passage, then the relative velocity of the water has to remain unchanged along the blade passage, so using Eqs. (2.2) and (2.3) we have

$$C_2 = U_1 \sqrt{\left( \frac{x \tan \alpha_1}{\sin \beta_1} \right)^2 + m^2} \quad (2.5)$$

But

$$C_2 = \frac{U_2}{\cos \alpha_2} = \frac{m U_1}{\cos \alpha_2} \quad (2.6)$$

Combining (2.6) and (2.5) we have,

$$\alpha_2 = \cos^{-1} \frac{m}{\sqrt{\left( x \frac{\tan \alpha_1}{\sin \beta_1} \right)^2 + m^2}} \quad (2.7)$$

From Fig. (2-4b) we have;

$$\cos(\pi - \beta_4) = \frac{U_3}{m W_3} = \frac{1}{m \tan \alpha_3} \quad (2.8)$$

but as illustrated before at any condition  $\alpha_3 = \alpha_2$  and if incidence and deviation angles are assumed to be zero then  $\beta_1 = \beta_4$  so from (2.8) we have:

$$\tan \alpha_2 = - \frac{1}{m \cos \beta_1}$$

$$\alpha_2 = \tan^{-1} \frac{1}{m \cos \beta_1} \quad (2.9)$$

Therefore we found two values for  $\alpha_2$ , one by using the first "stage" geometry (Eq. (2.7)) and the other was found by using the second-stage conditions. Putting these two values equal we get a nondimensional relation between the design parameters  $m$ ,  $x$  and  $\alpha_1$ , as follows:

$$\tan^{-1} \left( - \frac{1}{m \cos \beta_1} \right) = \cos^{-1} \frac{m}{\sqrt{\left( -x \frac{\tan \alpha_1}{\sin \beta_1} \right)^2 + m^2}} \quad (2.10)$$

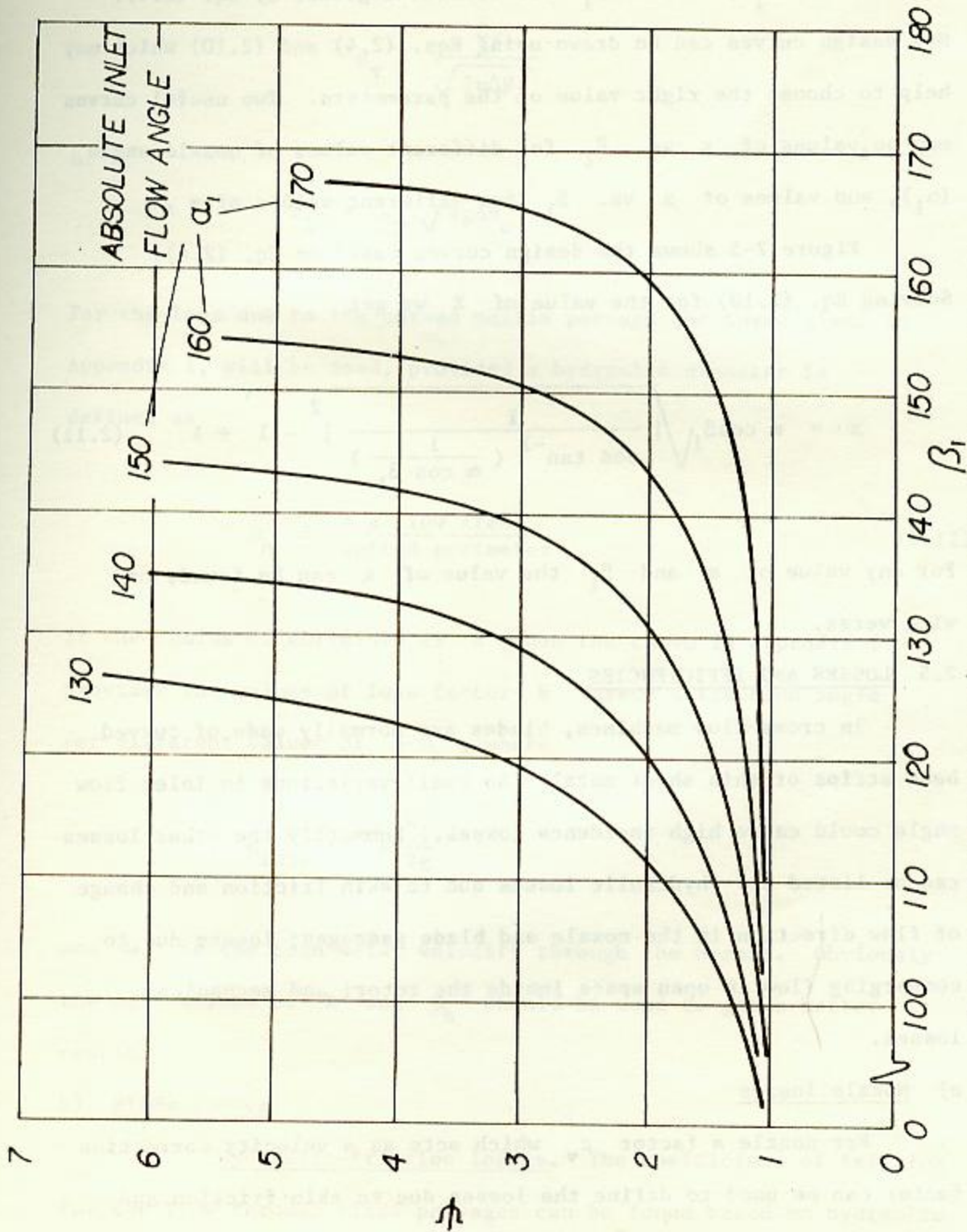


FIG. 2-5. WORK COEFFICIENT  $\psi$  VS. RELATIVE INLET FLOW ANGLE  $\beta_1$ .



Notice that  $\alpha_1$ ,  $x$  and  $\beta_1$  are related together by Eq. (2.4). Now design curves can be drawn using Eqs. (2.4) and (2.10) which may help to choose the right value of the parameters. Two useful curves may be, values of  $x$  vs.  $\beta_1$  for different values of nozzle angle ( $\alpha_1$ ), and values of  $x$  vs.  $\beta_1$  for different values of  $m$ .

Figure 2-5 shows the design curves based on Eq. (2.4).

Solving Eq. (2.10) for the value of  $X$  we get

$$x = m \cos \beta_1 \sqrt{\left[ \frac{1}{\cos \tan^{-1} \left( \frac{1}{m \cos \beta_1} \right)} \right]^2 - 1} + 1 \quad (2.11)$$

For any value of  $m$  and  $\beta_1$  the value of  $x$  can be found, or vice versa.

## 2.5 LOSSES AND EFFICIENCIES

In cross-flow machines, blades are normally made of curved bent strips of thin sheet metal. So small variations in inlet flow angle could cause high incidence losses. Summarily the other losses can be listed as: hydraulic losses due to skin friction and change of flow direction in the nozzle and blade passages; losses due to converging flow in open space inside the rotor; and mechanical losses.

### a) Nozzle losses

For nozzle a factor  $c_v$  which acts as a velocity correction factor can be used to define the losses due to skin friction and converging flow, so

$$c_v \equiv \frac{c_1}{\sqrt{2g\Delta H_o}}$$

or

$$c_1 = c_v \sqrt{2g\Delta H_o}$$

For the loss due to the curved nozzle passage the curve given in Appendix I, will be used, provided a hydraulic diameter is defined as

$$D_h \equiv \frac{4 \times \text{flow area}}{\text{wetted perimeter}} \quad (2.12)$$

If the radius of curvature is  $R$  then the curve in Appendix I provides the values of loss factor  $k$  versus deflection angle for different values of  $R/D_h$ , where

$$H_{\text{Loss}} = K \frac{W_1^2}{2g}$$

and  $W_1$  is the mean water velocity through the nozzle. Obviously the mean values of  $R$  and  $D_h$  should be used to get a better result.

#### b) Blade losses

1) Hydraulic-friction losses. The coefficient of friction for the flow through blade passages can be found based on hydraulic diameter, and using the curve given in Appendix I. So

$$h_{\text{Loss}} = f_h \frac{L}{D_h} \times \frac{W^2}{2g},$$

subscript h stands for values evaluated on basis of hydraulic diameter. "L" is the length of the blade passage and W is the relative flow velocity.

II) Losses due to flow direction change. In this case we can use the curve given in Appendix I, as for the nozzle.

c) Losses within the rotor

As seen in Fig. 2-6, the direction of actual velocity leaving different blades converges to one point. This effect will cause a change in flow direction entering the second set of blades.

As seen in Fig. 2-6 from simple geometry, the maximum incidence angle " $\gamma$ " caused by this effect is half of the admission angle " $\theta$ ". It is assumed that the central stream line remains undeflected. Also the bigger the admission angle is, the closer the right-hand side jets will get to the inner surface of the rotor and that will cause negative work on the second pass. Therefore the angle of admission has to be kept as small as possible. A reasonable range of magnitude for admission angle is between  $20^\circ$  to  $40^\circ$ . For these values of admission angle the loss due to this effect is very small.

d) Efficiencies

Normally the overall efficiency for a water turbine is defined as;

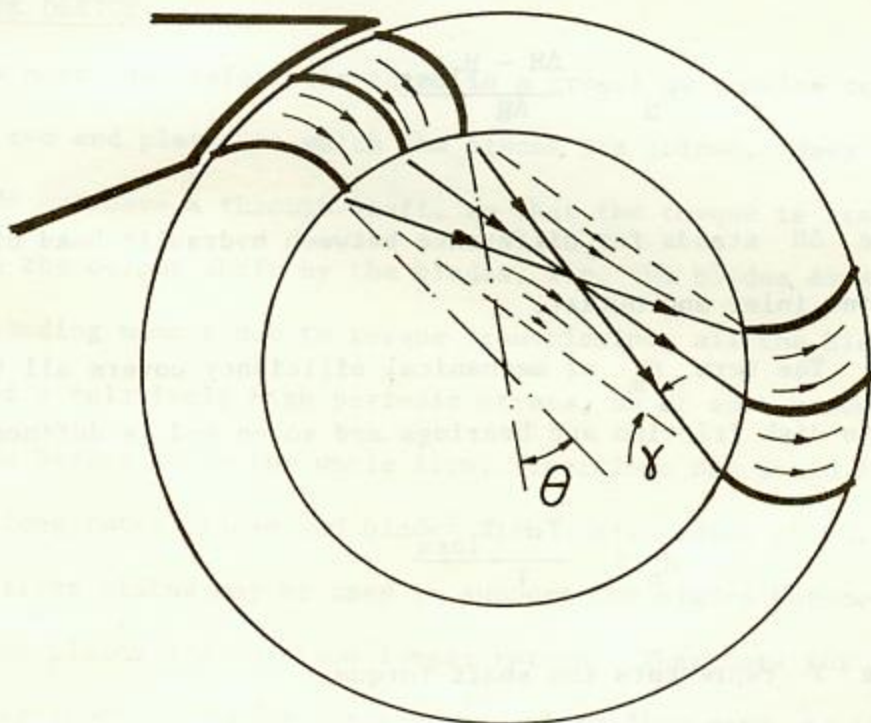


FIG.2-6. CONVERGING FLOW INSIDE THE ROTOR.

$$\eta \equiv \eta_h \times \eta_m \times \eta_Q$$

where  $\eta_h$  is the hydraulic efficiency of the turbine, and covers all the hydraulic losses across the blading. (See also Appendix II).

$$\eta_h \equiv \frac{\Delta H - H_{\text{loss}}}{\Delta H}$$

where  $\Delta H$  stands for difference between hydraulic head of the turbine inlet and outlet.

The term  $\eta_m$  or mechanical efficiency covers all the losses due to disk friction and bearings and so on and is defined as;

$$\eta_m \equiv \frac{T - T_{\text{loss}}}{T}$$

where  $T$  represents the shaft torque.

Finally  $\eta_Q$  is the volumetric efficiency which covers the leakages and the flow which passes the turbine without giving any power

$$\eta_Q \equiv \frac{Q - Q_{\text{lk}}}{Q}$$

where  $Q$  is the volume flow rate.

The important part of the evaluation of the efficiency of a turbine is to find the hydraulic efficiency. This term is very

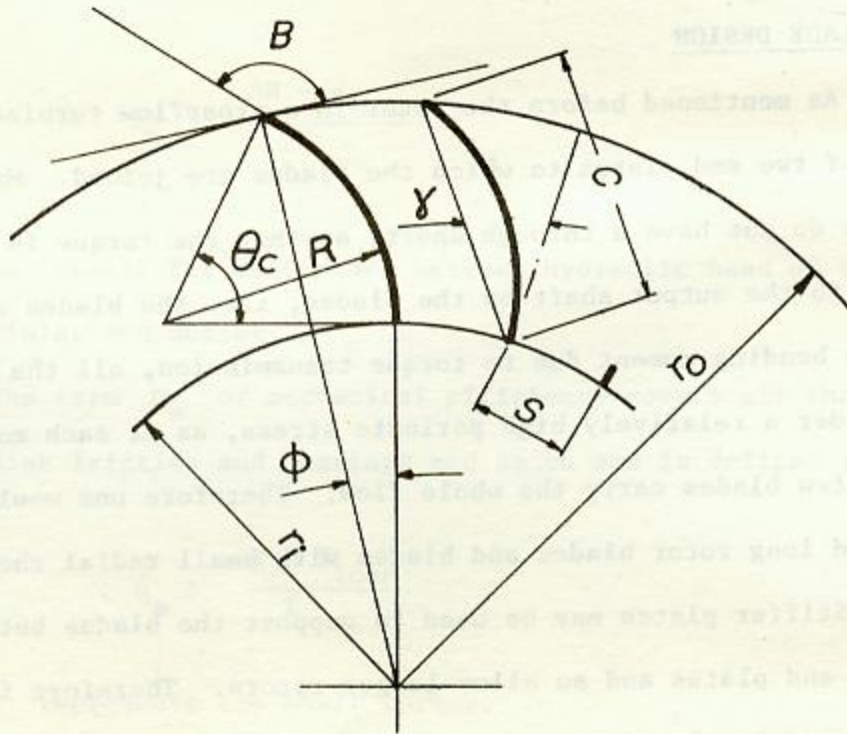
sensitive to the blade profile and flow angles (see Appendix III). In order to get the hydraulic efficiency of the crossflow turbine using Eq. (2.15), one has to write all the losses mentioned in the last section in terms of hydraulic head.

## 2.6 BLADE DESIGN

As mentioned before the rotor in a crossflow turbine consists of two end plates to which the blades are joined. Many designs do not have a through shaft, so that the torque is transmitted to the output shaft by the blades, i.e. the blades experience all the bending moment due to torque transmission, all the blades come under a relatively high periodic stress, as at each moment only a few blades carry the whole flow. Therefore one would like to avoid long rotor blades and blades with small radial chord.

Stiffer plates may be used to support the blades between the two end plates and so allow longer rotors. Therefore for a given power level and hence a specified volume flow rate, if the rotor can be reinforced with stiffer plates one can go for smaller rotor diameter and longer rotors and hence higher shaft speed. The cost for these apparent advantages is that of the higher complexity.

For the type of design we have chosen, we will only be concerned with rotors having no stiffer plates. Also the blade profiles will be segments of a circle. Therefore the blades can be cut out of thin-wall tubes, or made of strips of thin sheet



$Z \equiv$  number of blades

$d_i \equiv$  inner dia.

$d_o \equiv$  outer dia.

$L \equiv$  length of rotor

FIG.2-7. CROSS-FLOW TURBINE-BLADE TERMINOLOGY.

metal rolled around a pipe. The most important parameter to be specified is the ratio of inner to outer diameter of the rotor "m" which affects most of the other rotor parameters, such as length, number of blades, etc., effect of m on other blade design parameters can be found using Eqs. (2.13a) to (2.13f) which relate these parameters. (See Fig. 2-7 for blade notation.)

$$\gamma - \frac{\theta_c}{2} = 0 \quad (2.13a)$$

$$2\gamma - \phi = B - \frac{\pi}{2} \quad (2.13b)$$

$$c \sin \gamma = \frac{d_o}{2} \sin \phi \quad (2.13c)$$

$$R = \frac{c}{2 \sin(\theta_c/2)} \quad (2.13d)$$

$$c \cos \gamma + d_o \sin \phi/2 = \frac{d_o - d_i}{2} \quad (2.13e)$$

$$\sigma = \frac{c}{d_i \sin \pi/Z} \quad (2.13f)$$

The solidity  $\sigma$  is defined as the ratio of the blade chord to the spacing of the blades on the inner-diameter side of the rotor.

It will be easier to work with the nondimensional forms of Eqs. (2.13a) to (2.13f). Let's define



$$\lambda \equiv \frac{c}{d_o} \quad \text{and} \quad \zeta \equiv \frac{R}{d_o}$$

then,

$$\gamma = \theta_c / 2 \quad (2.14a)$$

$$2\gamma - \phi = B - \frac{\pi}{2} \quad (2.14b)$$

$$2\lambda \sin \gamma = \sin \phi \quad (2.14c)$$

$$\zeta = \frac{\lambda}{2 \sin \gamma} \quad (2.14d)$$

$$\lambda \cos \gamma + \sin \phi / 2 = \frac{1}{2} (1-m) \quad (2.14e)$$

$$\sigma = \frac{\lambda}{m \sin \pi / Z} \quad (2.14f)$$

As discussed in the last section the hydraulic loss through the blade passage is a function of the ratio of the radius of curvature of the blade camberline (centerline) over the hydraulic diameter of the passage and the deflection angle of the blade. Figure 2-8 shows the variation of the ratio of the rotor length and the blade curvature ratios over the rotor outer diameter versus values of rotor inner-to-outer diameter ratio. These curves show that shorter and more curved blades result from using bigger values of  $m$ .

As mentioned in Section 2.5 the loss through the blade passage is a function of the ratio  $R/D_h$  and  $\theta_c$ , where  $D_h$  is the passage hydraulic diameter and  $\theta_c$  is the blade deflection angle. Bigger values of  $R/D_h$  and smaller values of  $\theta_c$  give us less loss. Both these parameters can be found in terms of geometrical parameters introduced in Eqs. (2.13) and (2.14), as follows:

as defined 
$$D_h = \frac{4 \times \text{flow}}{\text{wetted perimeter}}$$

but as pointed out before, flow through the blade passage is the deflection of a jet of water along pressure side of the blade and so the jet thickness is fairly constant. Consequently the hydraulic diameter of the blade passage can be determined by the inner-diameter side of the rotor. By the aid of Fig. 2-7 we then have

$$D_h = \frac{4 \times (L \times s)}{L + 2s}$$

The reason for defining the wetted perimeter as  $(L + 2s)$  is that the flow does not fill the passage fully. Only the blade's pressure side and side walls guide the flow. If  $W_1$  is the relative velocity of water through the passage and  $\alpha$  is the rotor admission angle then at the inner-diameter side of the rotor we have:

$$Q = W_1 A = W_1 L \frac{\alpha}{360} \pi d_i$$

but as  $m \equiv d_i/d_o$ , then

$$L = \frac{Q}{\frac{\alpha}{360} \pi W_1 m d_o}$$

Defining  $\sigma \equiv c/s$  and  $\lambda = c/d_o$  (Eq. (2.14) therefore,

$$S = \frac{c}{\sigma} = \frac{c}{d_o} \frac{d_o}{\sigma} = \frac{\lambda d_o}{\sigma}$$

Substituting these into the relation for  $D_h$  we have:

$$D_h = \frac{\frac{4Q}{\frac{\alpha}{360} \pi m W_1 d_o} \times \frac{d_o \lambda}{\sigma}}{\frac{Q}{\frac{\alpha}{360} \pi m W_1 d_o} + \frac{2 d_o \lambda}{\sigma}}$$

Dividing both the denominator and the numerator by  $d_o$

and naming

$$C' \equiv \frac{Q}{\frac{\alpha}{360} \pi d_o^2 W_1}$$

then we have

$$D_h = \frac{4 \frac{C'}{m} \times \frac{\lambda}{\sigma} d_o}{\frac{C'}{m} + 2 \frac{\lambda}{\sigma}}$$

Also from Eqs. (2.14) we have the definition of

$$\zeta \equiv \frac{R}{d_o} ,$$

or

$$R = \zeta d_o ,$$

Therefore

$$\frac{R}{D_h} = \frac{\zeta \left( \frac{C'}{m} + \frac{2\lambda}{\sigma} \right)}{4 \frac{C'}{m} \times \frac{\lambda}{\sigma}} ,$$

or

$$\frac{R}{D_h} = \frac{\zeta (C'\sigma + 2\lambda m)}{4C' \lambda}$$

The parameter  $c'$  will be a constant value for homologous units of this kind (turbines having similarity in geometry and velocity diagrams). Figure 2-9 shows the variation of  $\theta_c$  versus  $m$  and the variation of  $R/D_h$  versus  $m$  for different values of solidity. From Fig. 2-9 we find that the maximum value of  $R/D_h$  happens at values of  $m$  closer to unity as solidity increases. With reference to Fig. I-1 (Appendix I) we find that the loss factor for the range of deflection angle we have (between  $41^\circ$  to  $58^\circ$ ) does not change much with variations of  $\theta_c$  but is strongly a function of  $R/D_h$ , especially for lower values of  $R/D_h$  (values from 1 to about 5). Consequently for a chosen value of solidity  $\sigma$ , the maximum value of  $R/D_h$  seems to lead to the efficient passage.

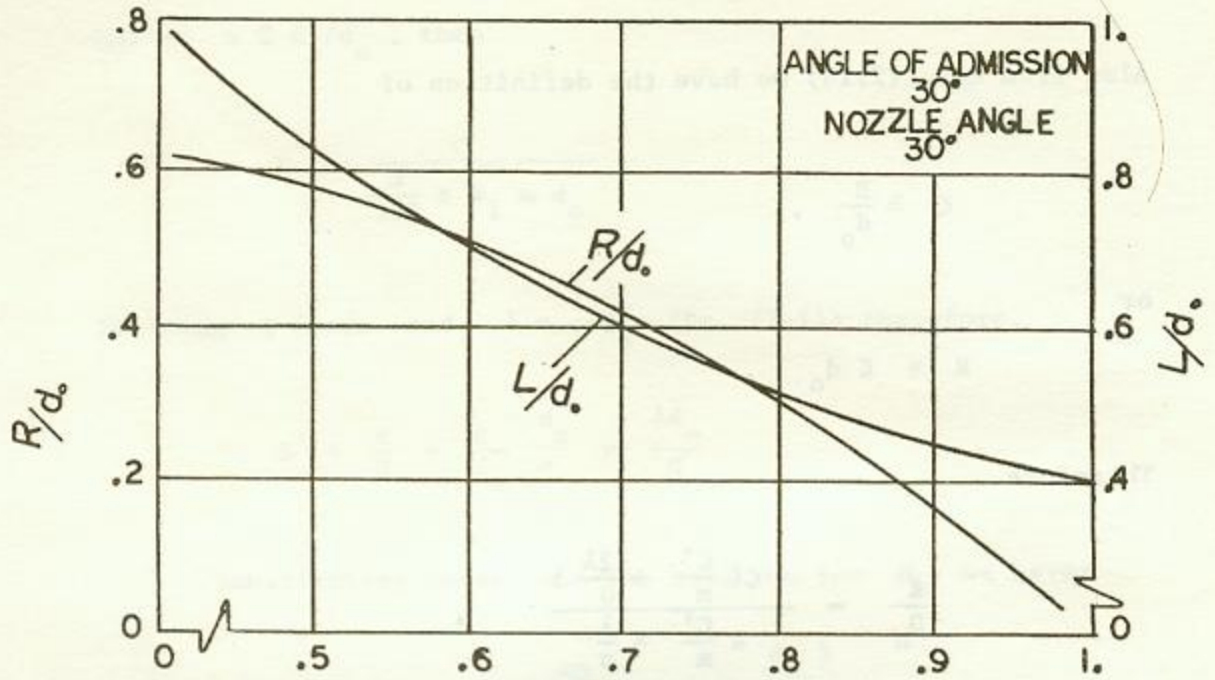


FIG.2-8. RATIO OF BLADE RADIUS OF CURVATURE  $R$  AND ROTOR LENGTH  $L$  OVER ROTOR OUTER DIAMETER VS. ROTOR INNER-TO-OUTER DIA. RATIO  $m$ .

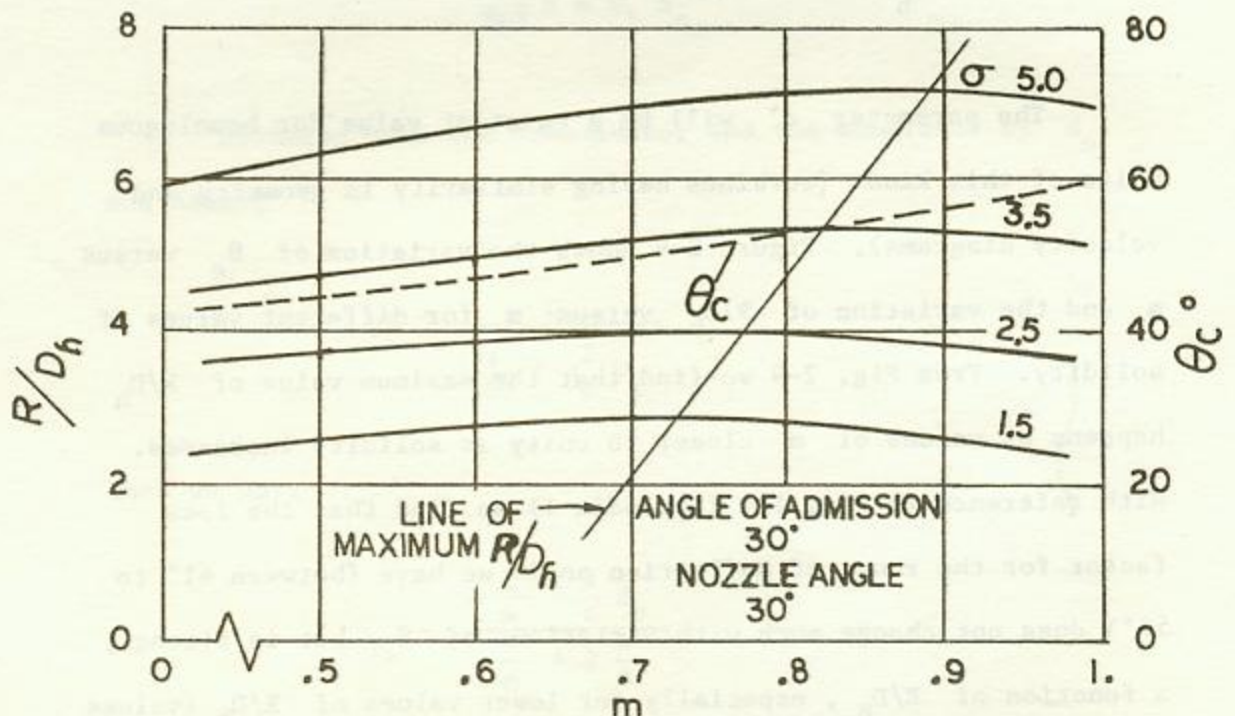


FIG.2-9. RATIO OF RADIUS TO HYDRAULIC DIAMETER  $R/D_h$ , AND DEFLECTION ANGLE OF THE BLADE PASSAGE  $\theta_c$  VS. ROTOR INNER-TO-OUTER DIA. RATIO  $m$ .

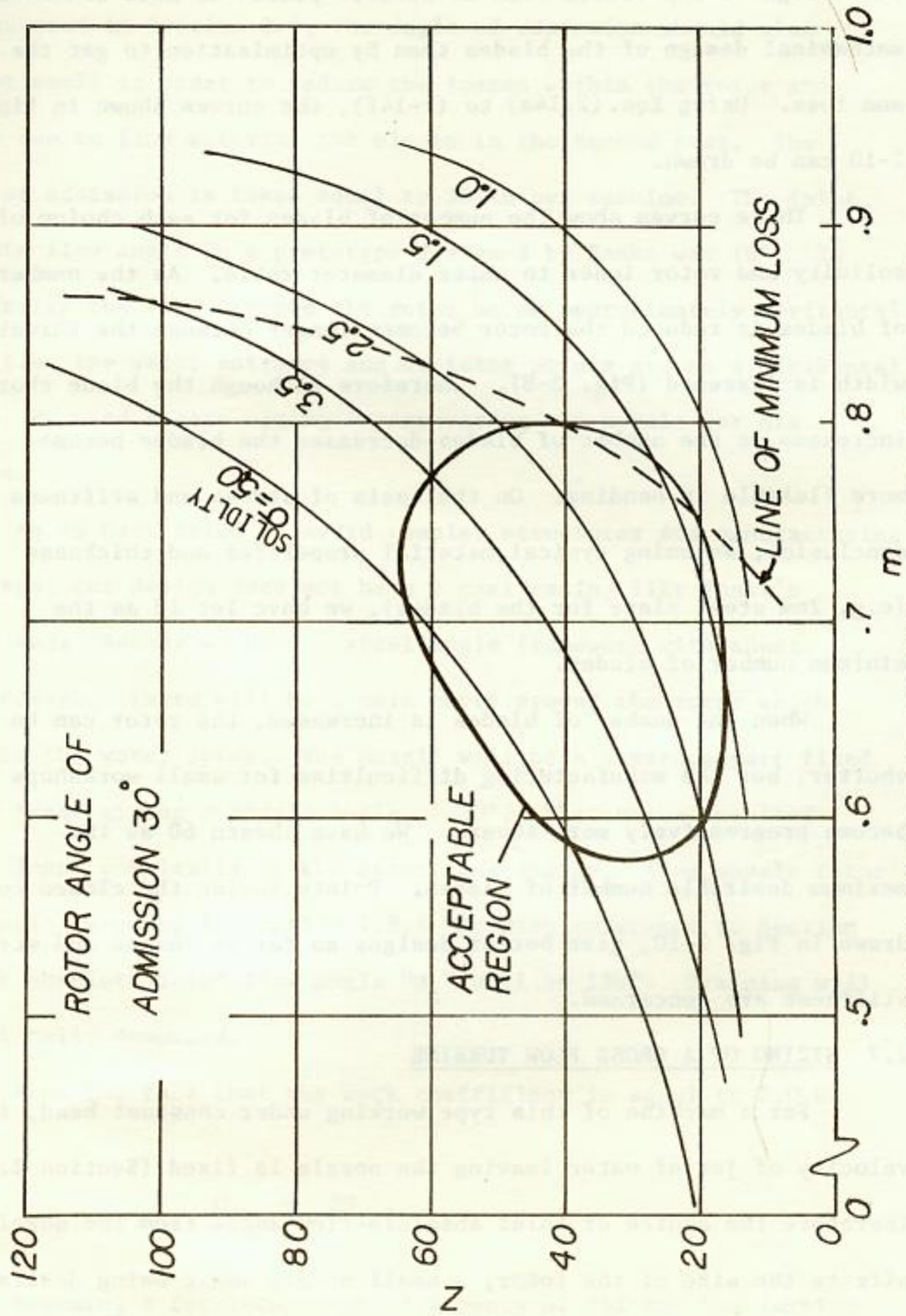


FIG.2-10. NUMBER OF BLADES  $Z$  VS. INNER-TO-OUTER DIA. RATIO  $m$ .

The design of the rotors with no stiffer plates is more dominated by mechanical design of the blades than by optimization to get the minimum loss. Using Eqs. (2.14a) to (2.14f), the curves shown in Fig. 2-10 can be drawn.

These curves show the number of blades for each choice of solidity and rotor inner to outer diameter ratio. As the number of blades is reduced the rotor becomes longer because the throat width is lessened (Fig. 2-8). Therefore although the blade chord increases as the number of blades decreases the blades become more flexible in bending. On the basis of stress and stiffness conclusion, assuming typical material properties and thickness (e.g. 2mm steel plate for the blades), we have let 18 as the minimum number of blades.

When the number of blades is increased, the rotor can be shorter, but the manufacturing difficulties for small workshops become progressively more severe. We have chosen 60 as the maximum desirable number of blades. Points inside the closed curve drawn in Fig. 2-10, give better designs as far as losses and structural stiffness are concerned.

## 2.7 SIZING OF A CROSS FLOW TURBINE

For a machine of this type working under constant head, the velocity of jet of water leaving the nozzle is fixed (Section 2.4). Therefore the choice of inlet absolute flow angle from the nozzle affects the size of the rotor, a small nozzle angle being desirable.

As discussed in Section 2.5, the angle of admission should also be kept small in order to reduce the losses within the rotor and losses due to flow entering the blades in the second pass. The angle of admission is taken equal to 30 in our machine. The inlet absolute flow angle in a prototype designed by Banki was 16°. In that design the flow crosses the rotor on an approximately horizontal line (i.e. the water entrance and draining points are on a horizontal line). He used a cast casing incorporating the nozzle for his turbine.

As we have tried to avoid complex structures and manufacturing processes, our design does not have a cast casing like Banki's design had. Rather we used a steel angle framework with sheet metal covers; there will be a main cover around the rotor which confines the water spray. The nozzle will be a separate part fixed to the frame giving a nozzle angle of 30°. That value resulted in the least complexity of the structural design. (See nozzle rotor combination drawing in Section 2.8.) So with reference to Section 2.4 the absolute inlet flow angle " $\alpha_1$ " will be 150°. Draining will be vertically downward.

From the fact that the work coefficient is equal to 2.0 we have

$$C_{\theta 1} = 2U_1 .$$

Assuming a total-to-total efficiency of 75% for the turbine (nozzle and rotor), from Eq. (2.1) we get,



$$\Delta(UC_{\theta}) = 69.20 \text{ m}^2/\text{s}^2$$

then

$$U_1 = 5.88 \text{ m/s}$$

$$C_1 = 13.88 \text{ m/s}$$

$$W_1 = 9.00 \text{ m/s} .$$

The choice of shaft speed depends on how large the rotor outer diameter can be and what are the speed limitations for the bearings. As we were to use wooden bearings the sliding velocity between shaft and bearing bore limited us to a shaft speed of 300 rpm. This speed is lower than desirable, because a high gear up ratio is needed to reach the shaft speed to 1800 rpm (generator speed). In future design studies it would be justifiable to specify bearings to run at high speeds.

Therefore specifying  $N = 300 \text{ rpm}$  we get

$$d_o = 0.3743 \text{ m} .$$

We would like to join the blades to the side plates by rivets (see general arrangement drawing and nozzle-rotor combination drawing in Section 2.8). Therefore we would like to have the least possible number of blades in order to get sufficient space for riveting the bent ends of the blades to the side plates. Using Fig. 2-10 in the last section we get  $m = 0.6$  and 24 blades.

Now using Eqs. (2-13a) to (2-13f) we get the following results and blade parameters. First from the velocity diagram (zero incidence) we get

$$B = 130^{\circ} 53'$$

and then

$$\theta_c = 52^{\circ} 58'$$

$$\gamma = 26^{\circ} 29'$$

$$R = 0.0956 \text{ m}$$

$$S = 0.0293 \text{ m}$$

$$C = 0.0843 \text{ m}$$

we have previously chosen,

$$Z = 24$$

$$m = 0.6$$

The inner diameter of the rotor then will be

$$d_i = 0.2246 \text{ m} .$$

If 20% extra power is specified to cover the mechanical losses and the losses in the generator then the output shaft power has to be 6 Kw. The volume flow rate required will be

$$Q = \frac{W}{\Delta(U C_{\theta})} = 0.0867 \text{ m}^3/\text{s}$$

The length of the rotor then will be

$$L = \frac{Q}{\frac{\alpha}{360} \pi d_1 W_1} = 0.164 \text{ m}$$

$\alpha$  being the admission angle.

Once more recalling the velocity triangles shown in Fig. 2-4, we can write the following relation

$$\Delta(U C_\theta)_{\text{total}} = \Delta(U C_\theta)_{\text{1st pass}} + \Delta(U C_\theta)_{\text{2nd pass}}$$

or

$$\Delta(U C_\theta) = (U_1 C_{\theta_1} - U_2 C_{\theta_2}) + (U_3 C_{\theta_3} - U_4 C_{\theta_4})$$

but as we specified,

$$U_2 = U_3, \quad U_1 = U_4, \quad C_{\theta_2} = C_{\theta_3} = U_2$$

$$C_{\theta_1} = 2U_1, \quad C_{\theta_4} = 0 \quad \text{and} \quad \Delta(U C_\theta)_{\text{total}} = 2U_1^2$$

Therefore

$$\begin{aligned} \Delta(U C_\theta)_{\text{1st pass}} &= 2U_1^2 - U_2^2 = 2U_1^2 - m^2 U_1^2 = \\ &2U_1^2 \left(1 - \frac{m^2}{2}\right) \end{aligned}$$

and

$$\Delta(U C_\theta)_{\text{2nd pass}} = U_2^2 = m^2 U_1^2$$

The above relations show that for a value of  $m = 0.6$ , the energy transferred to the rotor in first pass is 82% of the total energy and only 18% of the total energy is received by the second pass. This means that as hydraulic losses within the rotor and the entrance losses in the second pass do not affect the performance of the turbine very much.

## 2.8 MECHANICAL DESIGN

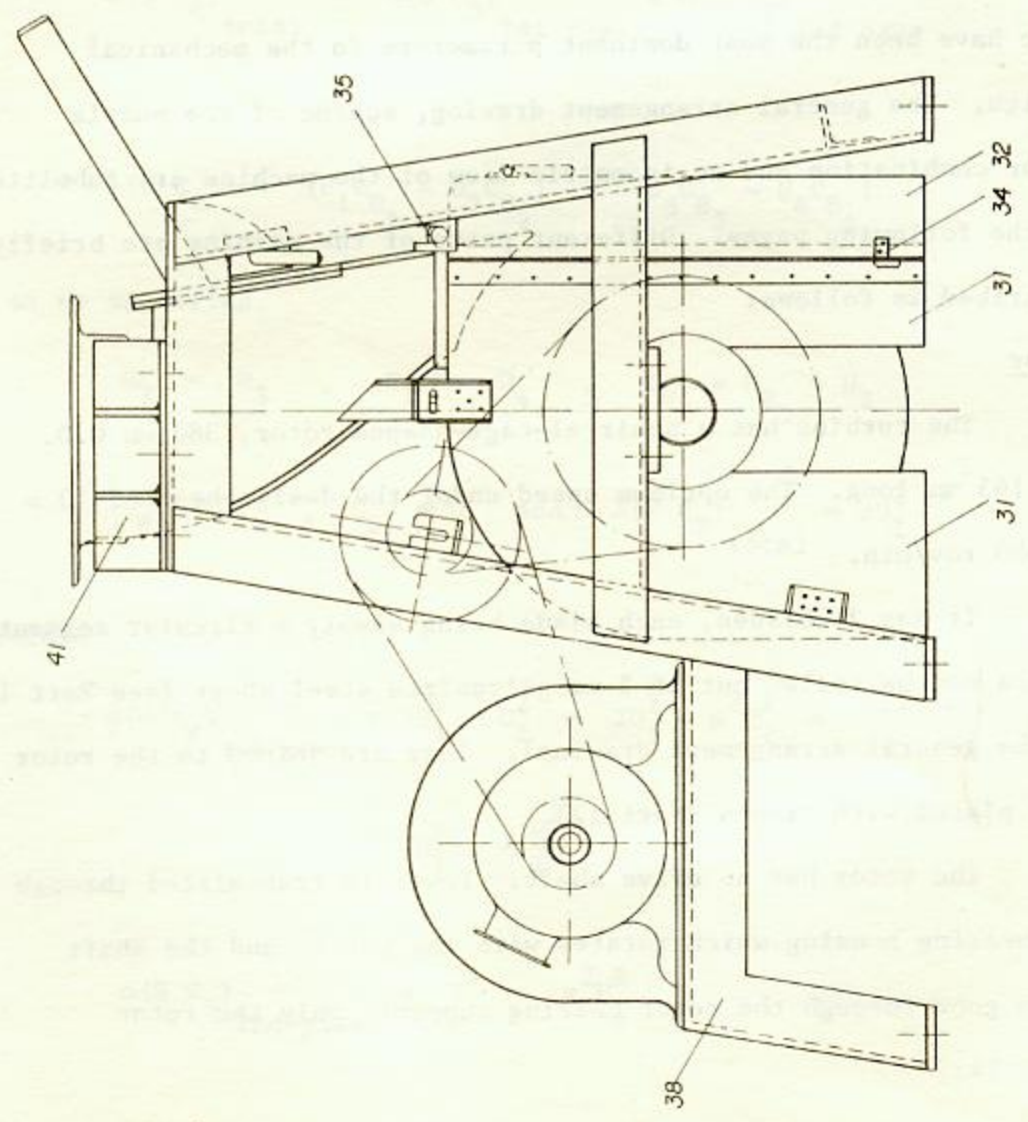
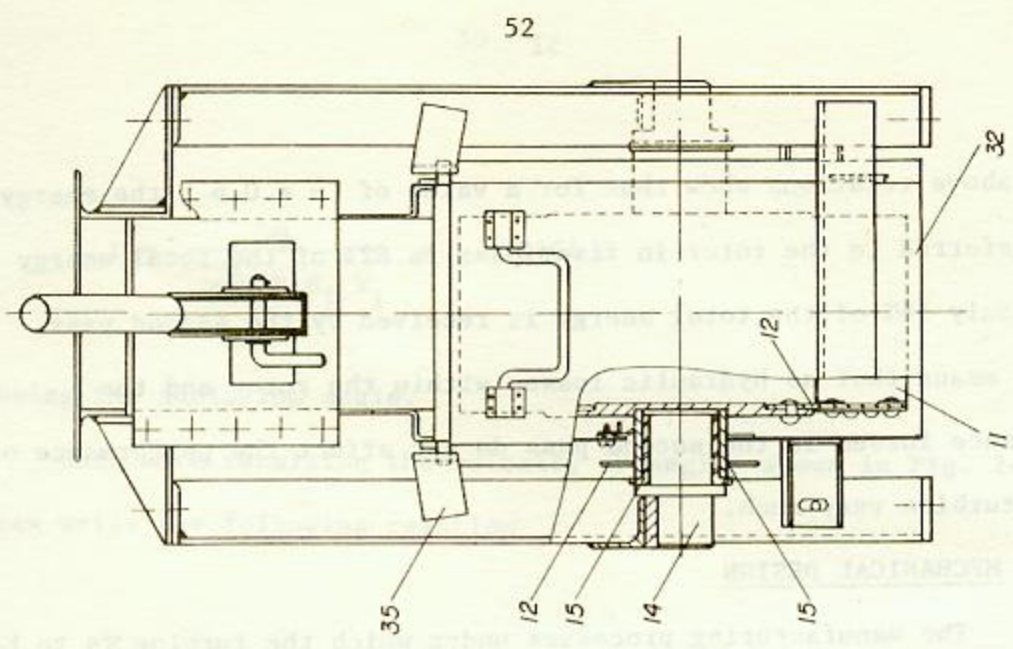
The manufacturing processes under which the turbine is to be made have been the most dominant parameters in the mechanical design. The general arrangement drawing, scheme of the nozzle rotor combination and an isometric view of the machine are submitted in the following pages. Different parts of the machine are briefly described as follows:

### Rotor

The turbine has a squirrel-cage-shaped rotor, 380 mm O.D. and 165 mm long. The optimum speed under the design head of 10 m is 300 rev/min.

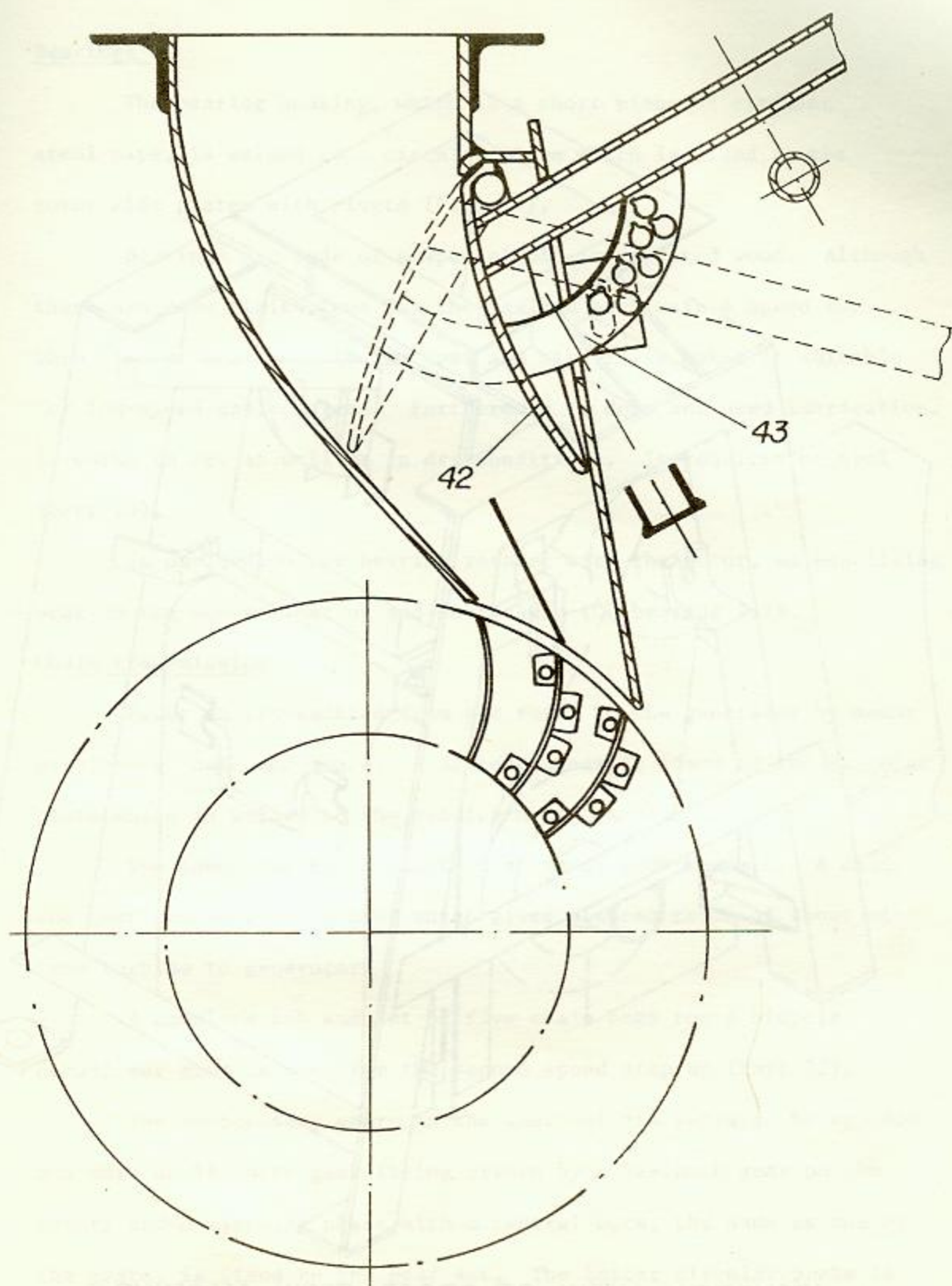
It has 24 blades, each blade being simply a circular segment. Blades can be rolled out of 2 mm galvanized steel sheet (see Part 11 on the general arrangement drawing). They are joined to the rotor side plates with rivets (Part 12).

The rotor has no drive shaft. Power is transmitted through the bearing housing which rotates with the rotor, and the shaft which goes through the rotor bearing supports only the rotor (Part 14).

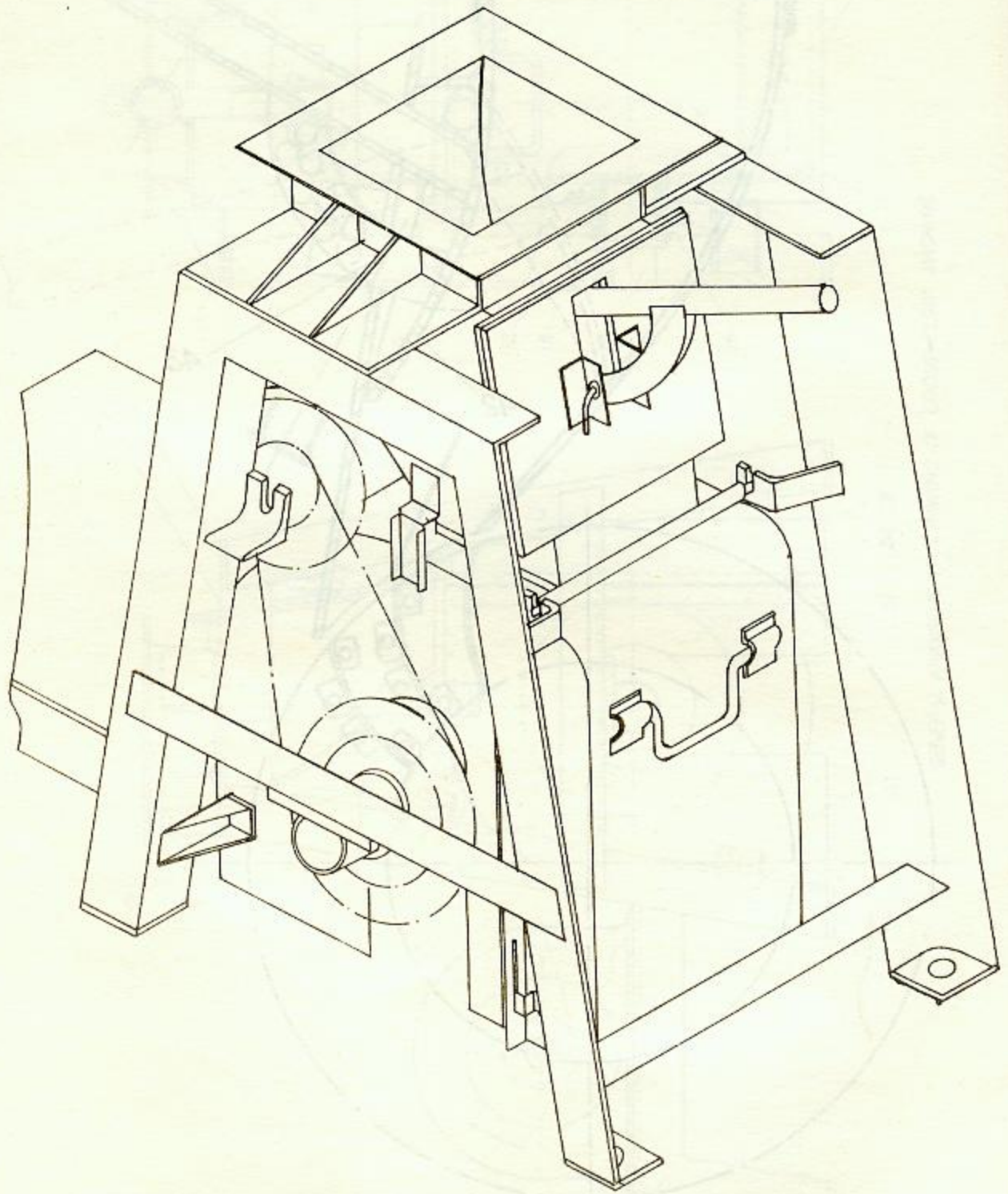


52

GENERAL ARRANGEMENT DRAWING OF CROSS-FLOW MACHINE



NOZZLE-ROTOR COMBINATION OF  
CROSS-FLOW TURBINE



ISOMETRIC VIEW OF CROSS-FLOW MACHINE

### Bearings

The bearing housing, which is a short piece of circular steel pipe, is welded to a circular plate which is fixed to the rotor side plates with rivets (Part 13).

Bearings are made of a special oil-impregnated wood. Although there are some limitations for the maximum permissible speed for this kind of bearing, its low cost and simplicity makes it suitable for low-speed applications. Furthermore it does not need lubrication. It works in wet as well as in dry conditions. It requires no seal (Part 15).

In our design the bearing rotates with the rotor, so equalizing wear on the wooden bearing and increasing the bearing life.

### Chain transmission

Power is transmitted from the rotor to the generator by means of bicycle chain and gears. A 52-tooth gear is fixed to the circular plate which is welded to the bearing housing (Part 21).

The generator has a constant speed of 1800 rev/min. A chain and gear combination is used which gives a speed ratio of about six from turbine to generator.

A complete hub and set of five chain cogs for a bicycle derailleur gear is used for the second speed step up (Part 22).

The unnecessary gears in the gear set are replaced by spacers and only an 18-tooth gear (being driven by a 52-tooth gear on the rotor) and a circular plate with a central bore, the same as one of the gears, is fixed to the gear set. The latter circular plate is



be fixed with a 36-tooth gear being used for the second speed-up step (Part 23). The last gear has 17-teeth and must be fixed to the generator shaft. For the power level we have in this machine a good lubrication condition should be provided for the chain.

The two-step transmission in this turbine makes it difficult to incorporate an oil bath around the chain. As you will see in Chapter 4 this machine would not be selected as the final choice, so we did not do further improvements on its transmission system. In order to increase the life of the chain and sprockets, we recommend that two chains in parallel be used. Therefore two sprockets should be installed side by side on each shaft.

#### Housing

The housing is completely made of thin galvanized sheet steel. It has a fixed section which covers most of the rotor (Part 31), and a removable door (Part 32), placed in the back of the turbine, for servicing. It has a lifting handle and is fastened to the fixed section with two simple latches (Parts 34 and 35).

#### Frame

The frame is totally made of angles, welded together. The generator mounting is a steel plate welded to short legs and its size may vary when using different generators (Part 38).

#### Nozzle

The nozzle is completely made of steel plates, welded together (Part 41). The flow can be changed and set on different valves for different output powers. This is possible by changing the angle of

flap (Part 42). The semi-circular channel (Part 43) which is welded to the flap has holes for different settings.

Warning: never change the flow while the turbine is in operation

As the system works under a relatively high head, a change of flow while the turbine is working can cause "water-hammer" in the piping which can result in serious damage.

To avoid this there has to be a gate valve before the nozzle. The flow must be slowly reduced almost to the shut-off position before changing the flap position. After setting, the valve must be opened gently.

The possibility of installing a surge-tank as a shock absorber has not been studied, because it would increase the size and the cost of the turbine.

## 2.9 EVALUATION OF EFFICIENCIES

Knowing the size of different parts of the turbine the hydraulic efficiency of the turbine can be found. Following the method given in the last sections we get:

$$\eta_h = 76\%$$

This efficiency is the total-to-total efficiency and is very close to our prediction, so the design is acceptable. Taking the effect of the energy loss by drain flow into account we get,

$$\eta_{t-s} = 60\%$$

If a mechanical efficiency of 94% and a generator efficiency of 90% is assumed then

$$\eta_{t-sm} = 56.5\%$$

and

$$\eta_{t-su} = 51\%$$

(See Appendix II.)

## 2.10 RADIAL-INFLOW PARTIAL-ADMISSION WATER TURBINE

### Description

This type of turbine is a potential alternative to the cross-flow and axial types.

The turbine simply consists of a spiral-shaped distributor with rectangular cross section which distributes the flow in two opposite portions of its inner circumference, each one being an arc of 80°. The rotor blades are rolled out of sheet metal and are fastened at one end only, around the circumference of the turbine disk as cantilevers. The flow enters the rotor with a swirling radially inward motion, passes through the blades while still in the radial plane, and subsequently is deflected to leave the rotor in the axial direction.

### Flow Control

This type as described gives the possibility of controlling the volume flow to the rotor under constant head. Therefore the velocity diagrams would keep their design-point geometry and consequently the turbine would work at its design-point efficiency through the whole range of power.

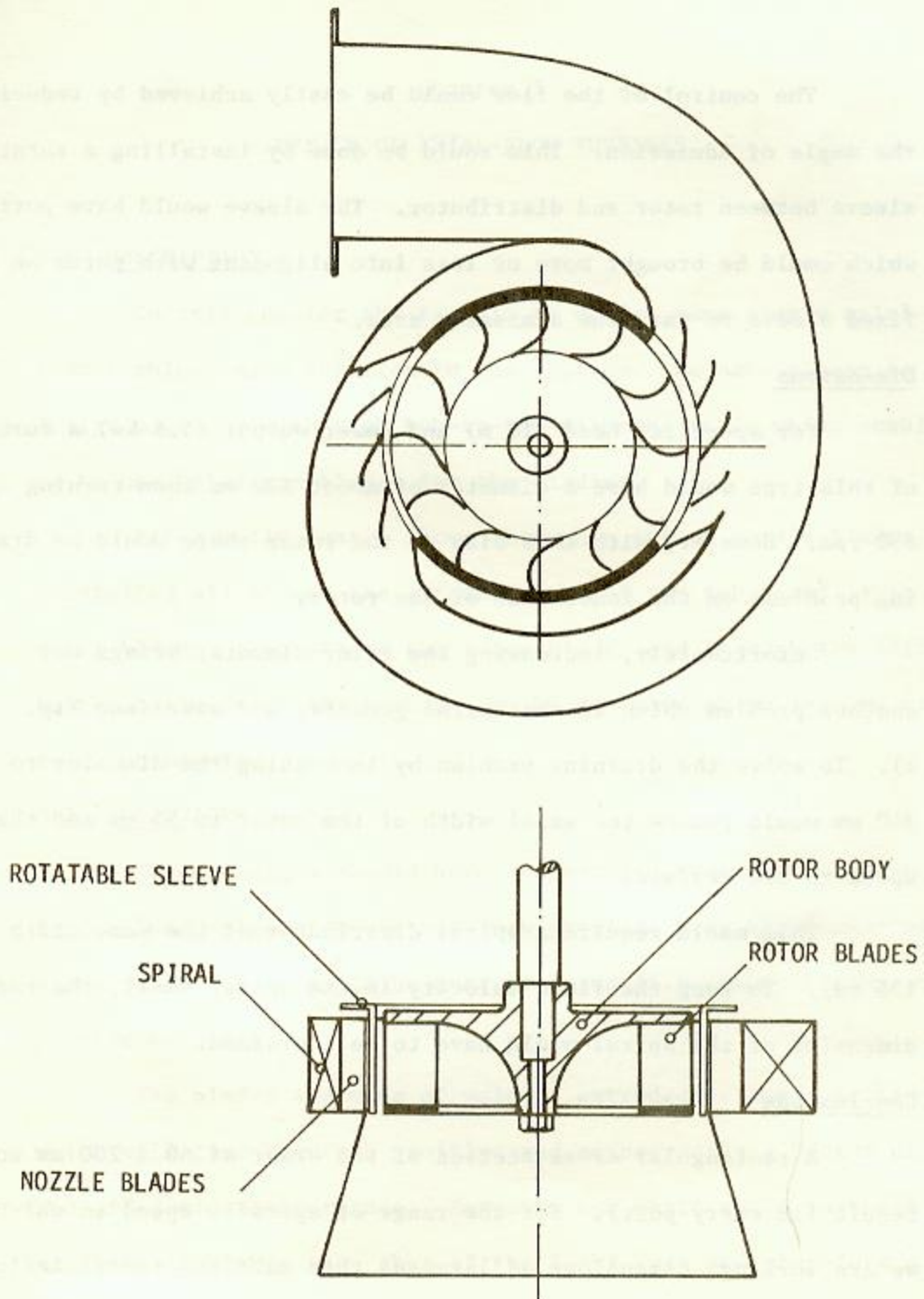


FIG.2-11. RADIAL-INFLOW PARTIAL-ADMISSION WATER TURBINE.

The control of the flow could be easily achieved by reducing the angle of admission. This could be done by installing a rotatable sleeve between rotor and distributor. The sleeve would have ports which could be brought more or less into alignment with ports on a fixed sleeve to vary the admission area.

### Dimensions

For specified head (10 m) and power output (5.5 kw) a turbine of this type would have a diameter of about 220 mm when turning at 450 rpm. However, with this size of the rotor there would be draining problems on the inner side of the rotor.

Unfortunately, increasing the rotor diameter brings out another problem which is the spiral geometry and size (see Fig. 2). To solve the draining problem by increasing the diameter to 340 mm would reduce the axial width of the rotor to 55 mm and the speed to 300 rev/min.

This would require a spiral distributor of the same width (55 mm). To keep the fluid velocity in the spiral small, the radial dimension of the spiral would have to be increased.

### Conclusions

A rectangular cross section of the order of 60 x 200 mm would result (in entry port). For the range of specific speed in which we are working, dimensions as large as this make the radial inflow turbine unattractive. We have not taken the design further.

## Chapter 3

### DESIGN OF AXIAL-FLOW TURBINES

#### 3.1 DESCRIPTION

In this chapter the task is to design some simple axial-flow turbines as a solution to the problem. We have chosen to design machines with high hub-to-tip-diameter ratio which enables us to use untwisted blades for the blading.

Principally, water flows through a set of nozzle blades (installed all around the circumference of the hub disk), into the rotor blades, then passes the rotor blades and through the diffuser to the tailwater. The turbine can be designed as an impulse or a reaction machine.

#### 3.2 ADVANTAGES

These designs should have comparable advantages with the Banki type. The design of these machines provides easy manufacturing processes if they are to be mass produced (i.e. sand casting and plastic molding).

The blades are made of molded, extruded or cast plastic which will give accurate profiles and consequently a better design and off-design performance. Moreover the shaft speed in these machines is higher than that of the Banki type and therefore a simpler transmission and a lower gear-up ratio will be needed. These machines can also be used as a drive motor to drive other machines besides the generator.

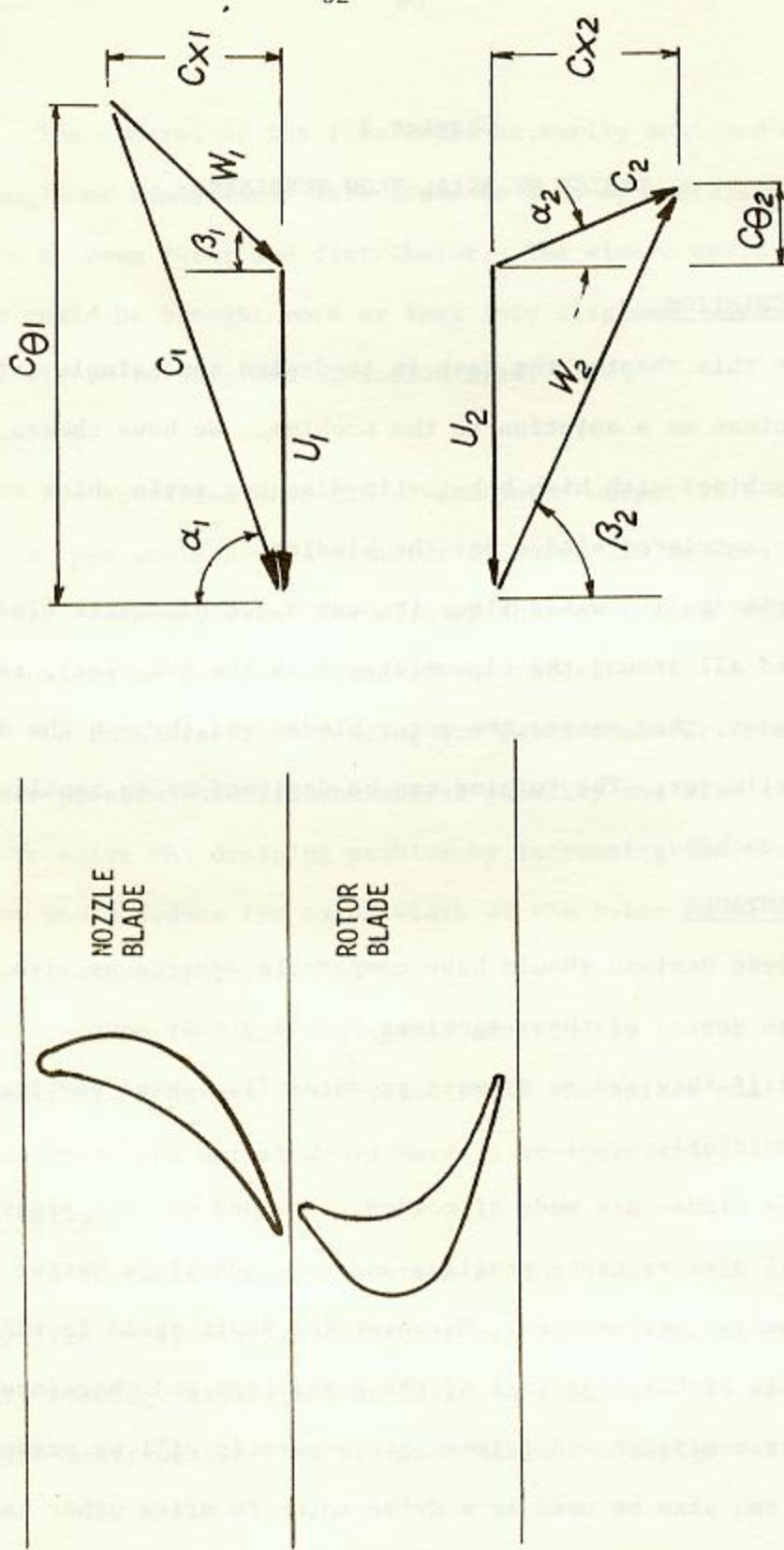


FIG. 3-1. INLET AND OUTLET VELOCITY DIAGRAMS OF AXIAL-FLOW TURBINE STAGE.

### 3.3 ANALYSIS

Similar to the analysis shown for the cross-flow turbine, we can write Euler's equation to relate different velocity-triangle specifications together (Fig. 3-1).

$$h_{01} - h_{02} = U_1 C_{\theta 1} - U_2 C_{\theta 2} \quad (3.1)$$

But if  $\Delta H_o$  is the total hydraulic head difference across the rotor then

$$h_{01} - h_{02} = \eta_{tt} \Delta H_o g \quad (3.2)$$

where  $\eta_{tt}$  is the total-to-total efficiency of the turbine (see Appendix II).

The three parameters: flow coefficient, work coefficient and reaction which specify the type of the velocity diagram and blading are defined respectively as follows:

$$\phi \equiv \frac{C_x}{U} \quad (3.3a)$$

$$\psi \equiv \frac{U_1 C_{\theta 1} - U_2 C_{\theta 2}}{U_m^2} \quad (3.3b)$$

$$R \equiv 1 - \frac{C_{\theta 1} + C_{\theta 2}}{2U} \quad (3.3c)$$



The analysis is done for the mean diameter, for the usual case where  $C_x$  remains constant from inlet to the nozzles to outlet of the rotor. Now for each design a velocity triangle can be chosen, hence values of  $\psi$ ,  $\phi$  and  $R$  can be specified.

A good approach to the design of different machines of this type with different degrees of reaction is to keep the inlet flow angle to the rotor " $\alpha_1$ " constant and to vary the two other parameters (i.e.  $R$  and  $\psi$ ).

From (3.2) and (3.3b) we have

$$U = \frac{\eta_{tt} g \Delta H_o}{\psi} \quad (3.4)$$

Now, choice of shaft speed gives us the mean diameter

$$d_m = \frac{60 U}{\pi (\text{RPM})} \quad (3.5a)$$

and

$$d_m = \frac{dt + dh}{2} \quad (3.5b)$$

and mass flow rate will be

$$\dot{m} = \frac{W}{\Delta(U C_\theta)} \quad (3.6)$$

where  $W$  is the output power of the turbine.

The annulus area then will be

$$A_a = \frac{\dot{m}}{\rho C_x} \quad (3.7)$$

where  $\rho$  is the density. Also we know that in terms of hub and tip diameters the annulus area will be

$$A_a = \frac{\pi}{4} (d_t^2 - d_h^2) \quad (3.8)$$

As mentioned before we try to keep the ratio of hub to tip diameter high enough, to be able to use untwisted blades. A reasonable value for this ratio is around 0.8.

Now, a choice of velocity triangle gives us the value of  $\Delta(U C_\theta)$  and hence from Eq. (3.4), (3.6) and (3.7) the values of  $U, A_a$  are found. Then the shaft speed can be determined and using Eq. (3.5a) gives us the value of mean diameter. Then using Eqs. (3.5b) and (3.8) we can find  $d_h$  and  $d_t$ .

If the ratio of  $d_h/d_t$  is not acceptable a new shaft speed has to be chosen to optimize the  $d_h/d_t$  ratio.

### 3.4 DESIGN OF BLADES

Figure 3-2 shows the terminology used in this design procedure. To find blade angles from flow angles we may use the information and curves given in Reference (2). The following two relations approximate the curves given in Ref. (2) with a good

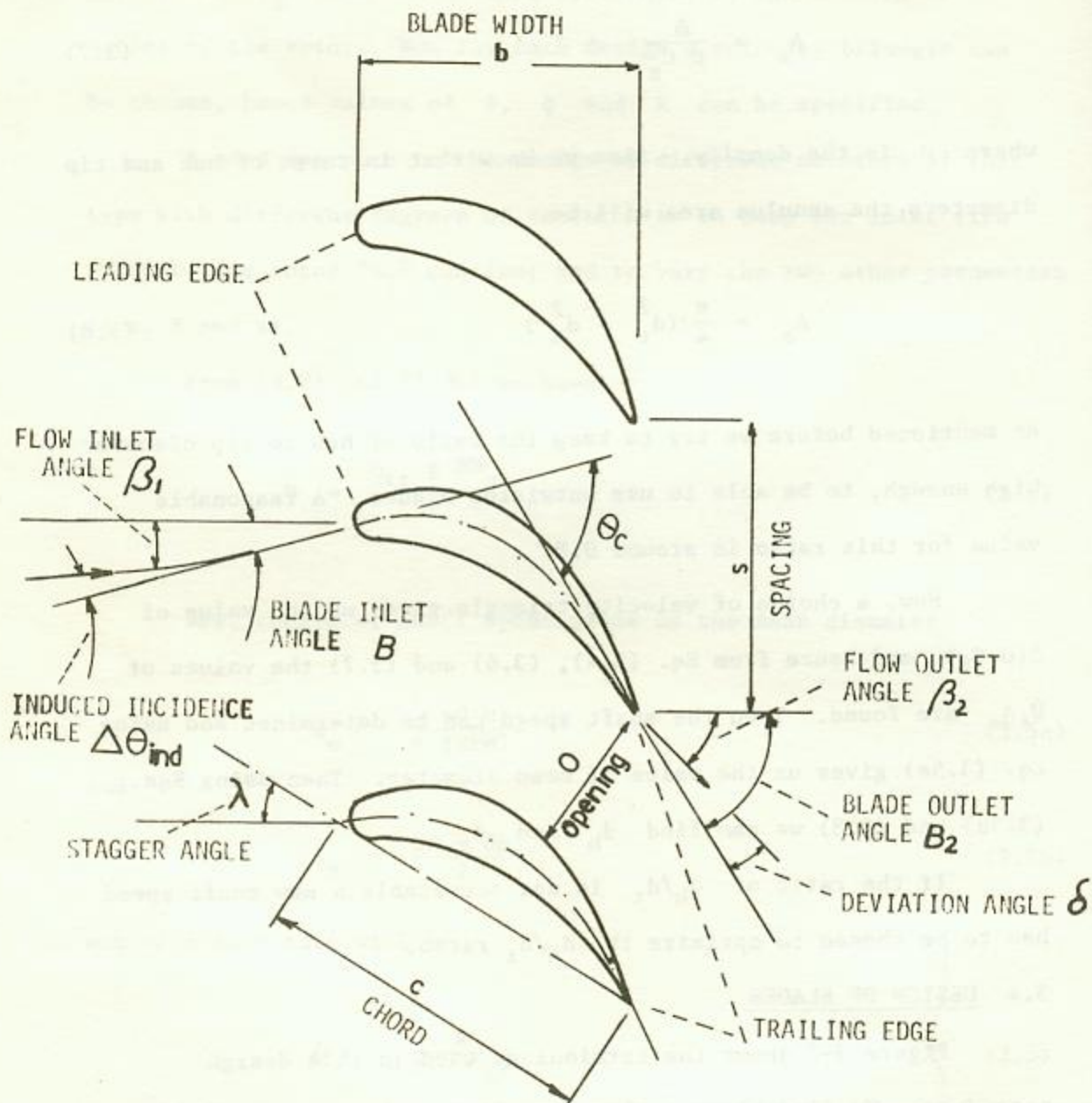


FIG.3-2. BLADE TERMINOLOGY.

accuracy, for incidence and deviation angles.

$$\frac{\Delta \theta_{\text{ind}}}{\alpha_1} = 0.25 \left( \frac{70^\circ}{\alpha_1} - 1 \right) (2.6 - \sigma) \quad (3.9)$$

and

$$\frac{\delta}{\theta_c} = \frac{0.08 + \left( \frac{60-\lambda}{300} \right)^2}{c/s} \quad (3.10)$$

Please see Fig. 3-2 for information on parameters used in above formulae. These two formulae are useful in preliminary design.

In Eq. (3.10),  $\theta_c$  or blade turning angle is equal to

$$\theta_c = \beta_1 + \Delta\theta_{\text{ind}} + \beta_2 + \delta$$

so the blade angles will be

$$B_1 = \beta_1 + \Delta\theta_{\text{ind}}$$

$$B_2 = \beta_2 + \delta$$

Suggested values for leading and trailing edge radii are

$$r_e = (0.03 \text{ to } 0.05)C$$

$$r_t = (0.02 \text{ to } 0.01)C$$

The design procedure for the blades is to choose a stagger angle " $\lambda$ " and an optimum value for solidity  $\sigma$ . The optimum solidity can be estimated by the Zweifel criterion for the value of width-to-chord ratio;

$$\frac{b}{s} = 2.5 \cos^2 \alpha_2 (\operatorname{tg} \alpha_1 + \operatorname{tg} \alpha_2) \quad (3.11)$$

also from Fig. 3-2,

$$\frac{b}{c} = \cos \lambda \quad (3.12)$$

from Eqs. (3.12) and (3.11) we find  $\sigma$ ,

$$\sigma = \frac{c}{s} .$$

In steam and gas turbines the dimensions of the blades and the number of the blades are normally determined by choosing a reasonable value for chord as far as vibration and stresses are concerned. In our case, as blades are short, a good choice for the number of the blades which gives us a reasonable blade passage seems to be a good approach.

Then finding the dimensions of the blades we can find the blade shapes by trying different curves for the blade profile.

### 3.5 SIZING OF THE MACHINES

Single-stage axial-flow turbines are normally named on the

basis of their velocity triangles. Two possible and most common types of velocity triangle are: impulse and 50%-reaction.

The design procedure in each case is to guess a value of total-to-total efficiency for the turbine. Then the machine will be designed with respect to the estimated efficiency. Finally for the designed machine the efficiency will be calculated using the method given in Appendix III. The design can then be optimized.

In order to get 5Kw. electrical power from the generator the turbine itself will be designed for 10% extra power. So the specifications of the turbine are 5.5 Kw. output power and 10 m. hydraulic head.

a) Design of an impulse machine

Assumptions are a total-to-total efficiency of 0.80 and velocity-diagram specifications of: work coefficient of 20 (implicit in an impulse machine), and flow coefficient of 0.8 (which gives an acceptable nozzle angle). Also we will specify that the absolute velocity leaving the rotor is to be in the axial direction, to minimize leaving losses therefore we have,

$$\Delta H_0 = H_{01} - H_{02} = 10 - \frac{C_2^2}{2g}$$

from Fig. 3-3 we have,

$$\phi \equiv \frac{C_x}{U} = \frac{C_2}{U}$$

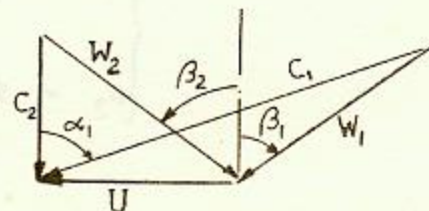


Fig. 3.3. IMPULSE VELOCITY DIAGRAM

Substituting the last two relations into Eqr. (3.4) and rearranging for U we have:

$$U = \frac{\eta g H_{o1}}{\psi + \frac{\phi^2}{2} \eta}$$

applying numerical values we have (at mean diameter);

$$U = 5.90 \text{ m/s}$$

so

$$\Delta(UC_\theta) = \psi U^2 = 69.75 \text{ m}^2/\text{s}^2$$

Then from Eq. (3.6) the volume-flow rate is

$$Q = 0.0791 \text{ m}^3/\text{s} .$$

Then from the velocity diagram

$$\begin{cases} \alpha_1 = 68.2^\circ \\ \alpha_2 = 0^\circ \end{cases}$$

and

$$\begin{cases} \beta_1 = 51.34^\circ \\ \beta_2 = 51.34^\circ \end{cases}$$

and

$$C_1 = 13.26 \text{ m/s}$$

$$W_1 = W_2 = 7.38 \text{ m/s}$$

$$C_2 = 3.54 \text{ m/s}$$

The choice of the shaft speed has to be done with regard to the following considerations: a) the value of hub-to-tip diameter ratio should be around 0.8; and b) a combination of two standard available sprockets can be found which gives us 1800 rev/min on the generator shaft. The minimum number of teeth for a 1/2"-pitch sprocket spinning at 1800 rev/min is 24 teeth. This value is recommended by almost all manufacturers. Therefore the value of shaft speed gotten by specifying the hub-to-tip diameter ratio should lead to an available number for sprocket teeth.

With regard to the above discussion a shaft speed of 540 rev/min gives 80 teeth for the big sprocket. The dimensions of the rotor then will be

$$d_m = 0.2087 \text{ m}$$

$$A_a = 0.0168 \text{ m}^2$$



and

$$d_t = 0.2347 \text{ m}$$

$$d_h = 0.1827 \text{ m}$$

$$\text{blade height} = 0.0260 \text{ m}$$

The ratio of hub-to-tip diameter ratio is then 0.78 which is in an acceptable range.

Blade design. Nozzle and rotor blades should be designed separately for this machine as they have different flow inlet and outlet angles.

First for nozzle blades: by looking through curves and information given in Ref. (2) for different blade profiles, for cases having the same deflection and inlet angle, an optimum solidity of 1.5 and a stagger angle of  $45^\circ$  are suggested. (We tried several profiles with other staggers but this value gave the best-looking profile.)

From Eqs. (3.9) and (3.10) we have:

$$\Delta\theta_{\text{ind}} = 19.25^\circ$$

$$\delta = 5.09^\circ$$

The blade angles are then

$$\begin{cases} B_1 = 19.25^\circ \\ B_2 = 72.29^\circ \end{cases} .$$

To choose the number of the blades we have to specify the spacing. From the above specifications we have

$$\frac{b}{c} = \cos 45 = 0.71$$

$$\frac{c}{s} = 1.5$$

(See Fig. 3-2).)

In this case a different number of blades were tried. Finally 15 blades seemed to be a good number as it gives a reasonable cross-sectional area for the blades (as we want to use plastic blades, we prefer to have blades with bigger chordal length and hence more cross-sectional area).

With the above specification nozzle blade sizes are as follows:

$$s_m = 0.0434 \text{ m}$$

$$C = 0.0651 \text{ m}$$

$$b = 0.0462 \text{ m}$$

$$r_t = 0.0025 \text{ m}$$

$$r_\ell = 0.0005 \text{ m}$$

In the same way calculations for the rotor blades were done. The results are tabulated in Table 3-1. Also see Fig. 3-4 for blade sections.

	$\beta_1^\circ$	$\beta_2^\circ$	Z	$\sigma$	$\lambda^\circ$	$\Delta\theta_{ind}^\circ$	$\delta^\circ$	$B_1^\circ$	$B_2^\circ$	S	C	b	$r_\ell$	$r_t$	0
NOZZLE BLADES	0.0	68.2	15	1.5	45	19.25	5.09	19.25	73.29	43.4	65.1	46.2	2.5	0.5	12.4
ROTOR BLADES	51.3	51.3	16	1.5	30	5.13	6.27	56.34	57.57	40.7	61.6	53.35	2.5	0.5	21.8

TABLE 3-1: IMPULSE TURBINE BLADING DIMENSIONS (DIMENSIONS IN MM)

Evolution of axial-flow impulse turbines. With respect to the method given in Appendix III and information we got about the blades the value of each flow parameter can be found in

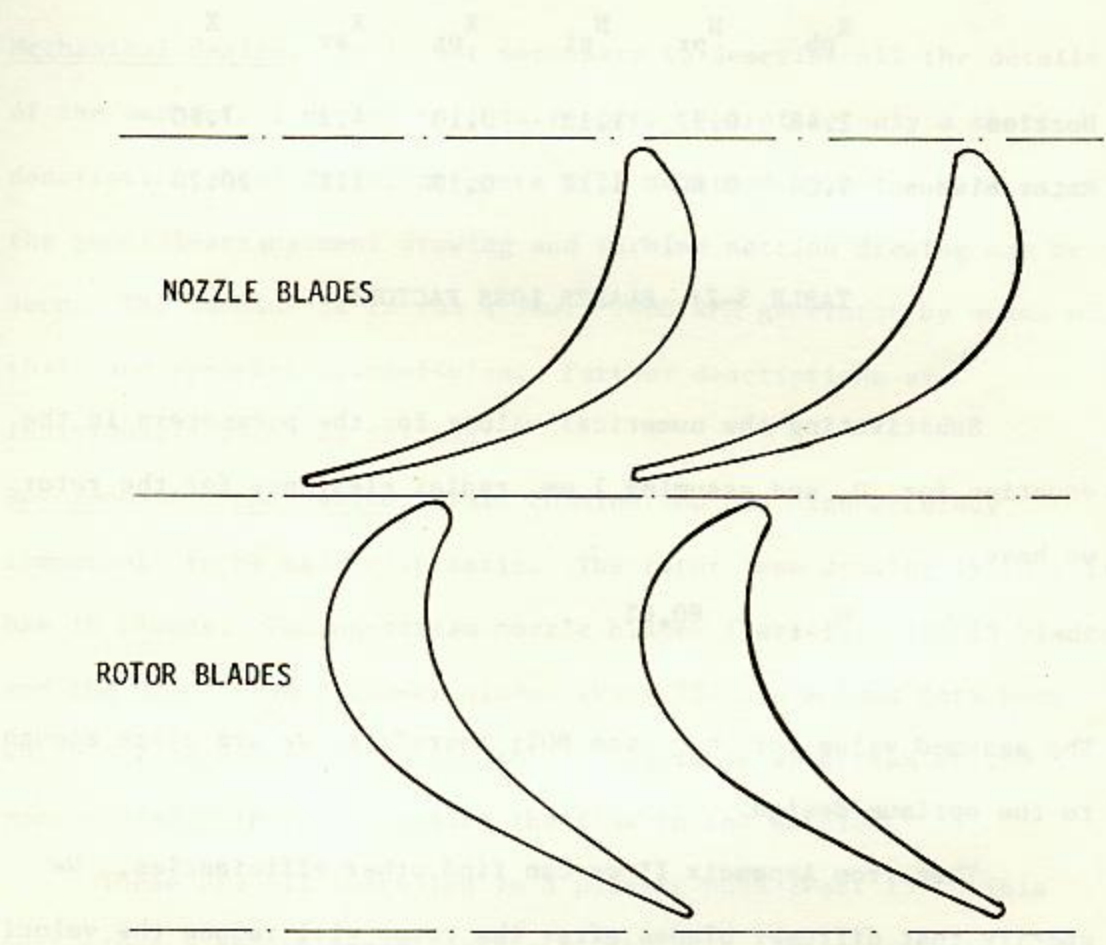


FIG. 3-4. BLADE SECTIONS OF THE AXIAL-FLOW IMPULSE TURBINE.

Evaluation of efficiencies. With respect to the method given in Appendix III and information we got about the blades the value of each loss parameter can be found.

	$X_{pb}$	$N_{pr}$	$N_{pt}$	$X_{pt}$	$X_{ar}$	$X$
Nozzles	2.48	0.97	1.13	0.10	4.2	7.20
Rotor blades	9.04	0.80	1.12	0.10	1.2	20.20

TABLE 3-2: BLADES LOSS FACTORS

Substituting the numerical values for the parameters in the equation for  $\eta$  and assuming 1 mm. radial clearance for the rotor we have,

$$\eta_{t-t} = 80.6\%$$

The assumed value for  $\eta_{tt}$  was 80%; therefore, we are close enough to the optimum design.

Then from Appendix II we can find other efficiencies. We specify that diffuser blades after the rotor will reduce the velocity of the flow down to .75 of its value when it leaves the rotor so,

$$\eta_{t-s} = 75\%$$

if mechanical efficiency is 95% and generator efficiency equal to 90% then the machine and the unit efficiencies will be;

$$\eta_{t-sm} = 71.0\%$$

$$\eta_{t-sU} = 64.1\%$$

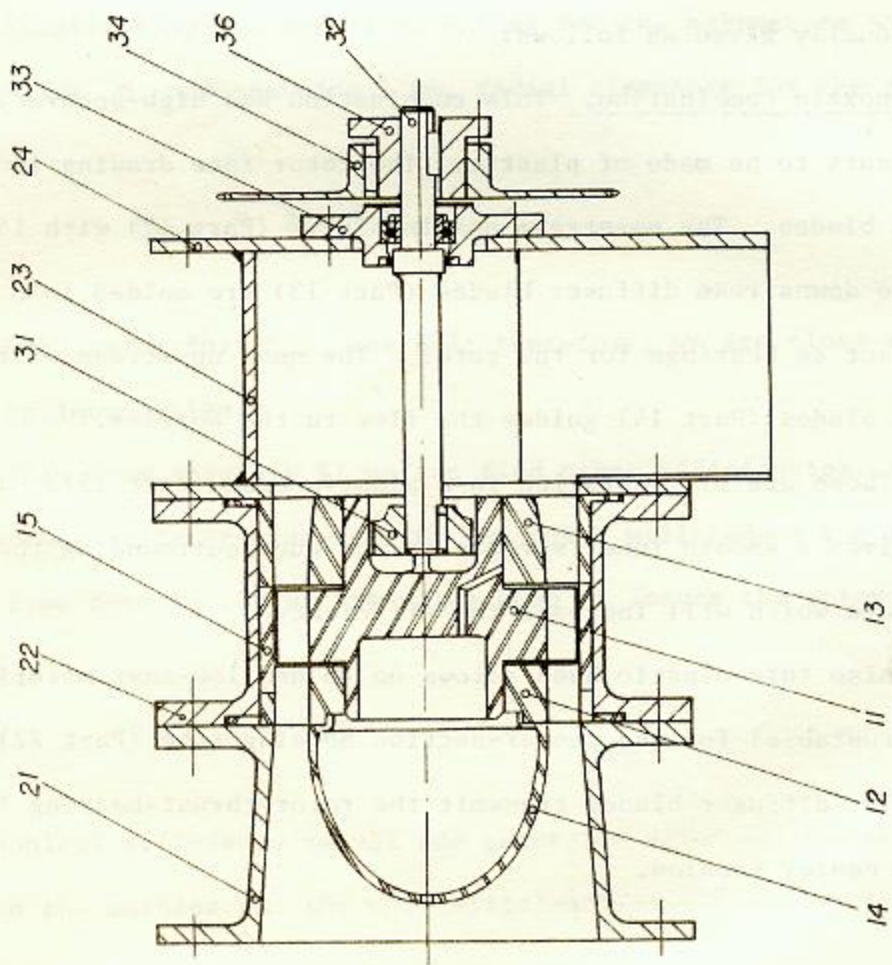
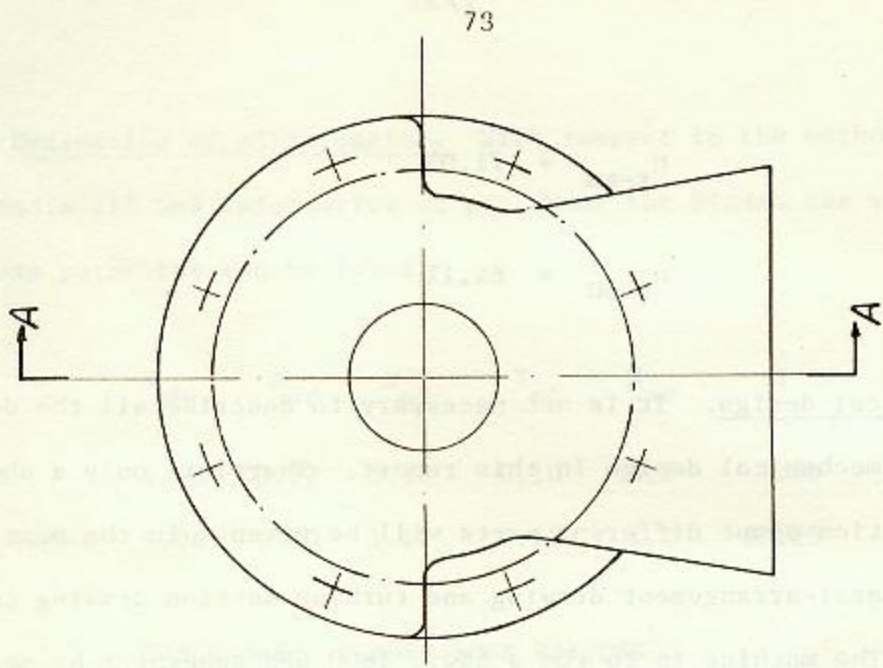
Mechanical design. It is not necessary to describe all the details of the mechanical design in this report. Therefore only a short description about different parts will be given. In the next pages the general-arrangement drawing and turbine section drawing can be seen. The machine is to run a 5Kw., 1800 RPM generator by means of chain and sprocket transmission. Further descriptions are individually given as follows:

Rotor-nozzle combination. This combination has high-accuracy components to be made of plastic. The rotor (see drawing 1, Part 11) has 16 blades. The up-stream nozzle blades (Part 12) with 15 blades, and the downstream diffuser blades (Part 13) are molded into hubs which act as bearings for the rotor. The nose up-stream of the nozzle blades (Part 14) guides the flow to the nozzles.

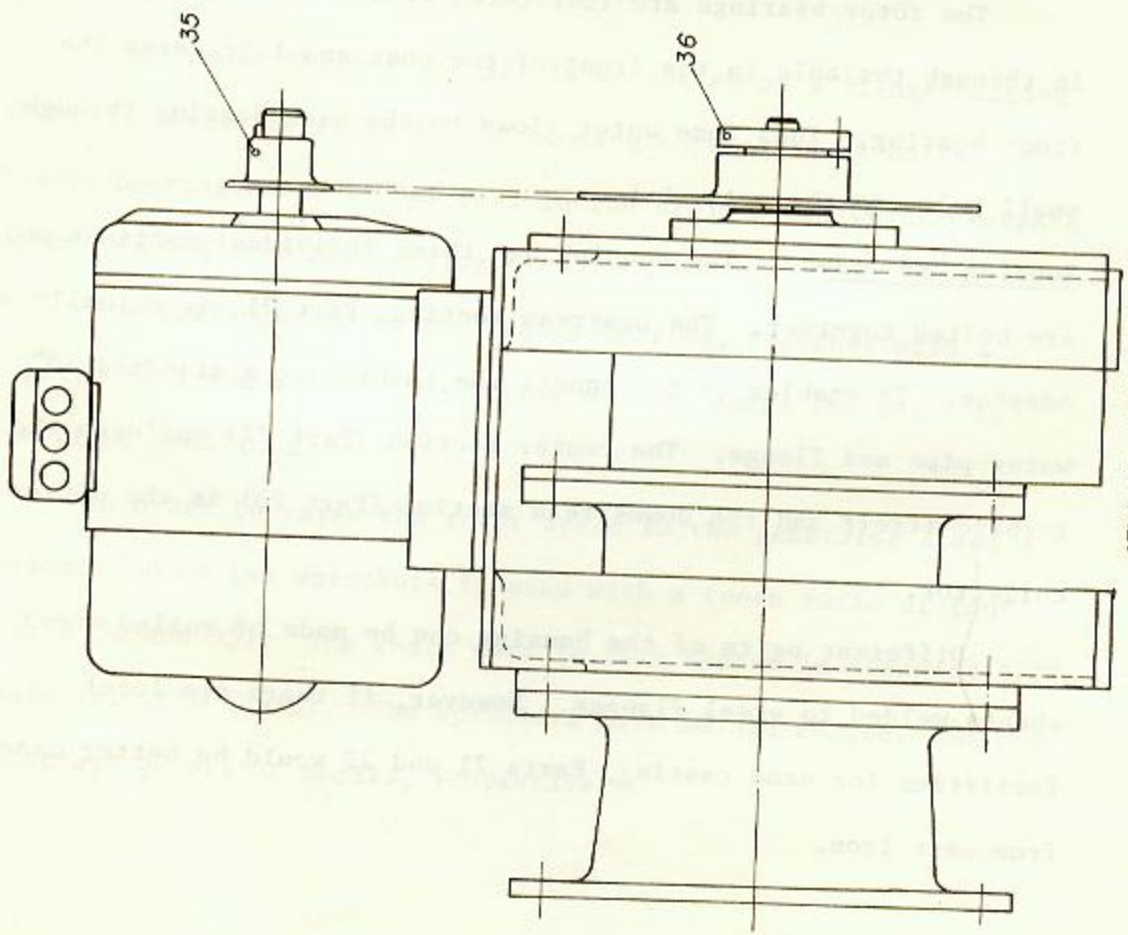
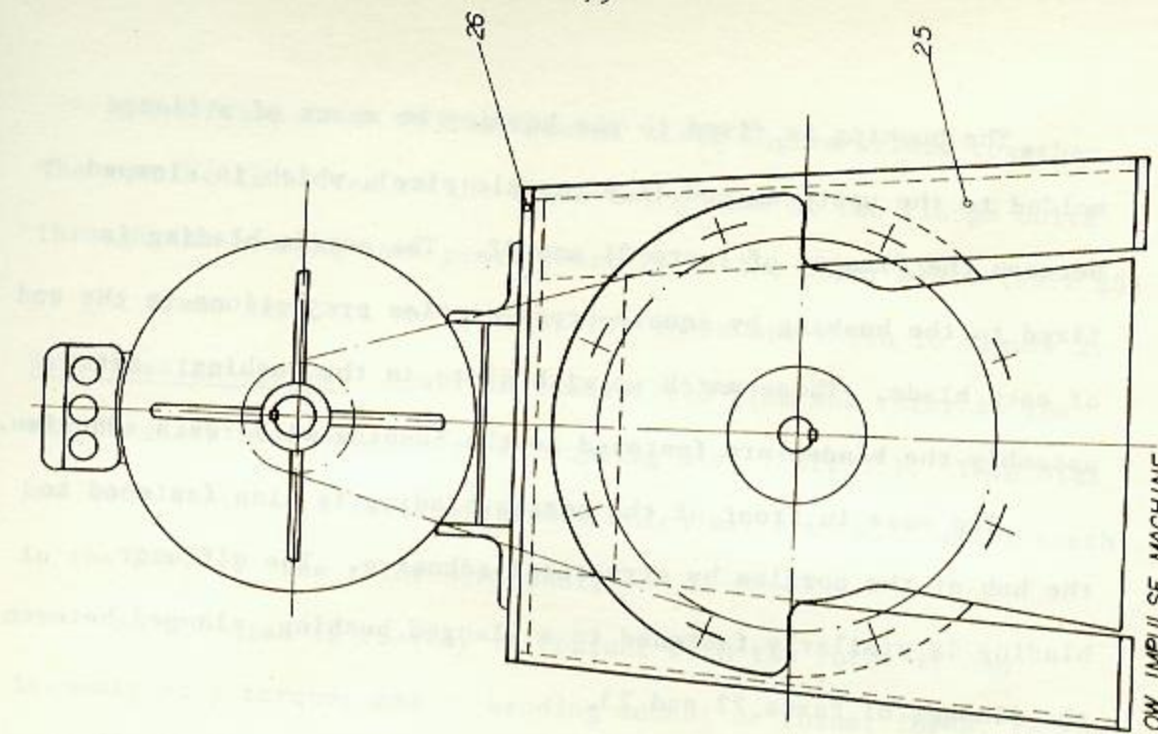
These are all installed in a plastic bush (Part 15). This bush gives a smooth inner surface to the duct surrounding the rotor, a feature which will increase the efficiency.

Also this plastic bush allows us to use low-cost materials (even rustable) for the center-section housing tube (Part 22).

The diffuser blades transmit the rotor-thrust-bearing force to the center section.



SEC. A-A  
AXIAL FLOW IMPULSE MACHINE CROSS SECTION



GENERAL ARRANGEMENT DRAWING OF AXIAL FLOW IMPULSE MACHINE



The bushing is fixed to the housing by means of a flange molded to the upstream end (i.e. nozzle size), which is clamped between the flanges of Parts 21 and 22. The nozzle blading is fixed to the bushing by square-cross-section projections in the end of each blade. These match up with slots in the bushing. After assembly the blades are fastened to the bushing with resin adhesive.

The nose in front of the nozzle blading is also fastened to the hub of the nozzles by structural adhesive. The diffuser blading is similarly fastened to a flanged bushing, clamped between the flanges of Parts 22 and 23.

The rotor bearings are lubricated with water. Water flows in through the hole in the front of the nose and lubricates the front bearing. Then some water flows to the back bearing through small holes in the rotor hub.

Housing and frame. The housing has three individual sections which are bolted together. The upstream section, Part 21, is actually an adaptor. It enables us to connect the turbine to a standard 10" water pipe and flange. The center section (Part 22) encloses the turbine itself and the downstream section (Part 23) is the outlet collector.

Different parts of the housing can be made of rolled steel sheets welded to steel flanges. However, if there are local facilities for sand casting, Parts 21 and 22 would be better made from cast iron.

The frame (Part 25) is made of steel angles welded together. The turbine is bolted to the frame using some of the flange bolts through the housing back plate (Part 24). The upper plate (Part 26) of the frame supports the generator. These are shown in Figure 2.

Transmission system. Power is transmitted from the rotor to the output shaft by the means of a coupling disk (Part 31). This disk has four slots on its circumference which match up with small teeth in the bore of the rotor stub shaft.

As the disk is loosely in contact with the rotor it can transmit only torque, and no bending moment or thrust force, to the output shaft.

The output shaft (Part 32) is supported by a flange bearing (Part 33) which is fixed to the housing back plate by bolts. The flange bearing has a rubber seal in the drain side, which prevents water leaking into the bearing.

The ball bearing in the flange bearing, together with a tapered bush and a nut with locking washer, keeps the shaft in the right position.

In order to raise the rotor speed to the generator speed a combination of two sprockets is used with a tooth ratio of four (Parts 34 and 35). The chain used in this system is standard 1/2" chain (bicycle chain). The sprockets have 80 and 24 teeth on the rotor and generator shafts, respectively.

We do not recommend the use of standard bicycle sprockets in this case. To transmit five kw at a speed of 1800 RPM would be loading them up to their maximum strength and would leave no safety margin.

To fix the larger sprocket to the rotor shaft a split taper bushing (Part 36) is used. This is done to avoid any need for hammering or pressing on the shaft.

Using the unit in powers lower than five kw

To run the turbine at a power level less than five kw, the flow to the turbine has to be reduced by the means of a valve installed at least a meter before the turbine inlet. Obviously the turbine will work at its best efficiency when it is run fully loaded.

Different possibilities for controlling the output power by installing some kind of mechanism were studied, but all cases result in a significant increase in size and complexity. I feel that users would not find these possibilities attractive.

b) Design of a reaction machine

This section is concerned with design of a 50% reaction axial turbine. The principles of the calculations are exactly the same as for the impulse machine. Therefore only the assumptions and tabulated results will be presented. In fact the structure of both turbines are also the same, so to avoid repeating the mechanical drawing of this machine it is not submitted as it is quite similar

to impulse machine. But a short description of the differences is given in the following paragraphs.

The significance of the 50% reaction machine is that its rotor and nozzle blades will have the same cross section. We specify a work coefficient of one, and absolute flow angle to the rotor to be the same for both impulse and reaction turbines. The absolute flow leaving the rotor will then be in the axial direction. The first

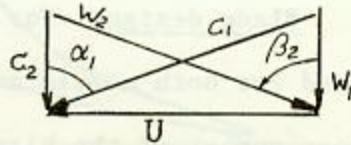


FIG. 3-5: REACTION VELOCITY DIAGRAM

guess for the total-to-total efficiency is 85%. The result of the velocity diagram calculation is:

$$\begin{cases} \alpha_1 = \beta_2 = 68.2^\circ \\ \alpha_2 = \beta_1 = 0.0^\circ \end{cases}$$

$$U = 8.84 \text{ m/s}$$

$$\Delta(Uc\theta) = 78.08 \text{ m}^2/\text{s}^2 \text{ or J/Kg}$$

$$Q = 0.0704 \text{ m}^3/\text{s}$$

$$\begin{cases} C_1 = W_2 = 9.52 \text{ m/s} \\ C_2 = C_x = W_1 = 3.54 \text{ m/s} \end{cases}$$

A suitable shaft speed for above results which can give an acceptable  $d_h/d_t$  is 720 RPM. Therefore;

$$d_m = 0.2345 \text{ m}$$

$$d_t = 0.2615$$

$$d_h = 0.2075 \text{ m}$$

$$\text{blade height} = 0.027$$

$$d_h/d_t = 0.79$$

Blade design. For simplicity the rotor-blade section will be used for both nozzle and rotor blading. But because of differences between number of the blades for the nozzle and the rotor, the solidity of bladings will be different. For preliminary design let's select a stagger of  $45^\circ$ , 15 blades for nozzle and 16 blades for the rotor. From the Zweifel criterion (Eq. (3.11)) for rotor blades we have

$$\frac{b}{s} = 0.86$$

also

$$\frac{b}{c} = \cos \lambda = 0.71$$

Then blade dimensions will be as follows (Table 3-3):

	Z	S	b	c	$\Delta\theta_{in}^\circ$	$\delta$	$\theta_c$	$B_1$	$B_2$	$r_e$	$r_t$
NOZZLE BLADES	15	48.76	39.3	55.3	20.0	6.4	94.6	20	74.6	2.5	0.5
ROTOR BLADES	16	45.76	39.3	55.3	20.0	6.4	94.6	20	74.6	2.5	0.5

TABLE 3-3: REACTION-TURBINE BLADE DIMENSIONS.

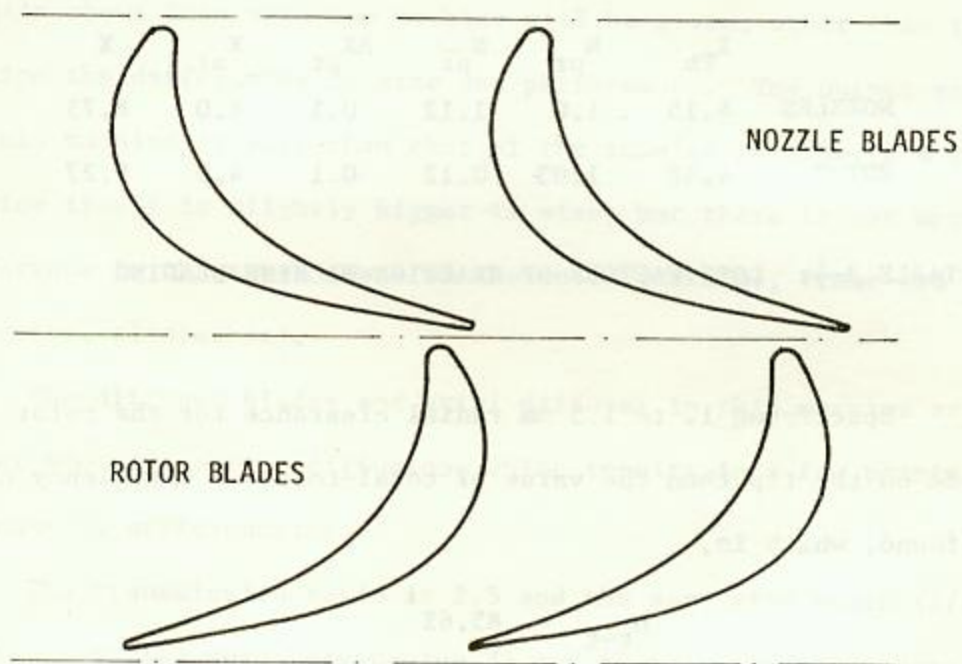


FIG.3-6. BLADE SECTIONS OF THE AXIAL-FLOW REACTION TURBINE.

The blade cross-sections are shown in Fig. 3-5.

Evaluation of efficiencies. Using the method given in Appendix III, the values of different loss coefficients are as given in Table 3-4:

	$X_{pb}$	$N_{pr}$	$N_{pt}$	$\Delta X_{pt}$	$X_{ar}$	$X$
NOZZLES	4.15	1.0	1.12	0.1	4.0	8.75
ROTOR	4.48	1.03	0.12	0.1	4.0	9.27

TABLE 3-4: LOSS FACTORS OF REACTION-MACHINE BLADING

Specifying 1. to 1.5 mm radial clearance for the rotor blade on the tip then the value of total-to-total efficiency can be found, which is,

$$\eta_{t-t} = 85.6\%$$

For preliminary design this is close enough to the first guess, so that the design is acceptable.

If we specify that diffuser blades will diffuse the flow to half of its absolute velocity when leaving the rotor, then the total-to-static efficiency will be,

$$\eta_{t-s} = 83.6\%$$

If 95% mechanical efficiency and 90% generator efficiency are assumed as before then the machine and the unit efficiencies are,

$$\eta_{t-sm} = 79.4\% \quad , \quad \eta_{t-su} = 71.5\%$$

Mechanical design. The general mechanical design on both impulse and reaction machines are the same. Therefore no further details about this reaction machine will be given, other than to mention the differences in size and performance. The output speed of this machine is more than that of the impulse turbine, and the turbine itself is slightly bigger in size, but there is not much difference in the total sizes of the units (turbine, frame and generator, altogether).

The diffuser blades and axial diffuser in this machine are longer and give better diffusion, which results in a few points increase in efficiency.

The transmission ratio is 2.5 and the same size chain (1/2") is used with two sprockets having 24 and 60 teeth on the generator and rotor shafts, respectively.



## Chapter 4

### DISCUSSION ON ADVANTAGES OF DIFFERENT TYPES

As seen in the last chapters, each of the studied prototypes had individually some advantages and some disadvantages. Looking at the problem from the view of a developing country, the price of the turbine, the manufacturing processes under which the turbine is going to be made and the type of maintenance and service needed are important parameters in the choice of the best machine.

All machines are designed not to need skilled maintenance. Therefore cost and manufacturing requirements have to be discussed. The crossflow turbine gives both possibilities of being manufactured locally in farming areas and/or being manufactured in industrial areas and shipped to farms. But axial-flow turbines should be made centrally and shipped to farms. The type of processes under which the cross-flow turbine could be made are mostly intermediate processes such as sheet-metals fabrications, but the axial-flow turbines have parts which need more sophisticated processes (i.e. plastic molding, and casting, etc.). To satisfy the goals of the Technology Adaptation Program it might be preferred to choose processes which provide improvements in industry in the developing countries. In that case encouraging industries such as plastic molders may be of great importance.

The amount of labor which has to be put into making each cross-flow turbine is much higher than what has to be done for the

axial-flow type. The axial-flow machines would probably be cheaper because of automation and their smaller size when produced in large numbers.

Comparison of the structures of the turbines shows that, the high speed of the reaction machine is an advantage over the impulse and cross flow machines, as it provides a lower gear up ratio to the electrical generator, so that a simpler transmission and lower forces in chain and sprockets are entailed.

For the kind of generator speed we have chosen the chain must work in an oil bath and be well lubricated, otherwise it will not last long even for the axial flow reaction machine. Therefore the low speed of cross-flow turbine and its two-step transmission makes it unattractive, because a far more expensive transmission becomes necessary.

A big portion of the price of each of the units is the generator cost. The rest of the construction cost seems likely to be similar for all units for small scale production. For large scale production the cross flow will be much more costly than the axial types. This is because the material cost for the axial flow machines is small but initial investments for molds and dies are required.

Finally the efficiencies of the machines differ. While there is often surplus water flow available a high efficiency machine requiring a lower water flow will therefore require less costly pipes, channels, valves and so forth.

The following table shows the efficiencies of the different machines.

	<u>Cross-Flow Turbine</u>	<u>Axial-Flow Impulse Turbine</u>	<u>Axial-Flow Reaction Turbine</u>
t-t	76%	80%	85%
t-s	60%	75%	83.5%
t-sm	56.5%	71%	79.5%
t-su	51%	64%	71.5%

Key:

- t-t  $\equiv$  total-to-total efficiency of turbine blading
- t-s  $\equiv$  total-to-static efficiency of turbine blading
- t-sm  $\equiv$  total-to-static efficiency of machine (shaft power)
- t-su  $\equiv$  total-to-static efficiency of unit (electrical power)

Based on all considerations we chose the reaction machine as the best solution to the problem.

#### 4.1 IMPROVEMENTS ON REACTION MACHINE

The preliminary design shown in the last chapter has some questionable features. Here we try to improve on that design as much as possible. Following are some items which it seems necessary to cover.

By looking at the general-arrangement drawing submitted in this chapter (DRN. No. AF301), the difference between the rotor-nozzle combinations in two schemes can be seen.

This improved design provides less hydrostatic force on the rotor. The atmospheric pressure is bypassed through the rotor central hole to the other side of the rotor, hence equalizing the pressure on the two sides of the rotor and reducing the axial force on the rotor. The sliding surfaces between the rotor and diffuser hubs are covered with thin stainless-steel sheets which reduce the friction and give a long life. (For the high pressure and velocity on sliding surfaces even the best kinds of plastic can not last and they melt.) Lubrication of these surfaces is possible by the aid of holes in the rotor hub and grooves on the plates. The lubricant water is supplied from upstream through the holes in the stator hub.

The front adaptor in the improved machine is changed. The new adapter enables us to connect the turbine to 8" diameter piping. The smaller tube and valve size reduces the cost.

The oil bath in the back of the turbine provides good lubricating conditions for the chain and sprockets, and hence increases the transmission system's life.

The blade profiles are also changed. The new blades have a settling angle of  $38^\circ$  and their shapes are also optimized for the best performance.

#### 4.2 Off-Design Performance

The type of flow control we recommend for the machine is to use a gate valve installed one m. ahead of the machine. The basic assumption is that the turbine is going to be run under fairly steady

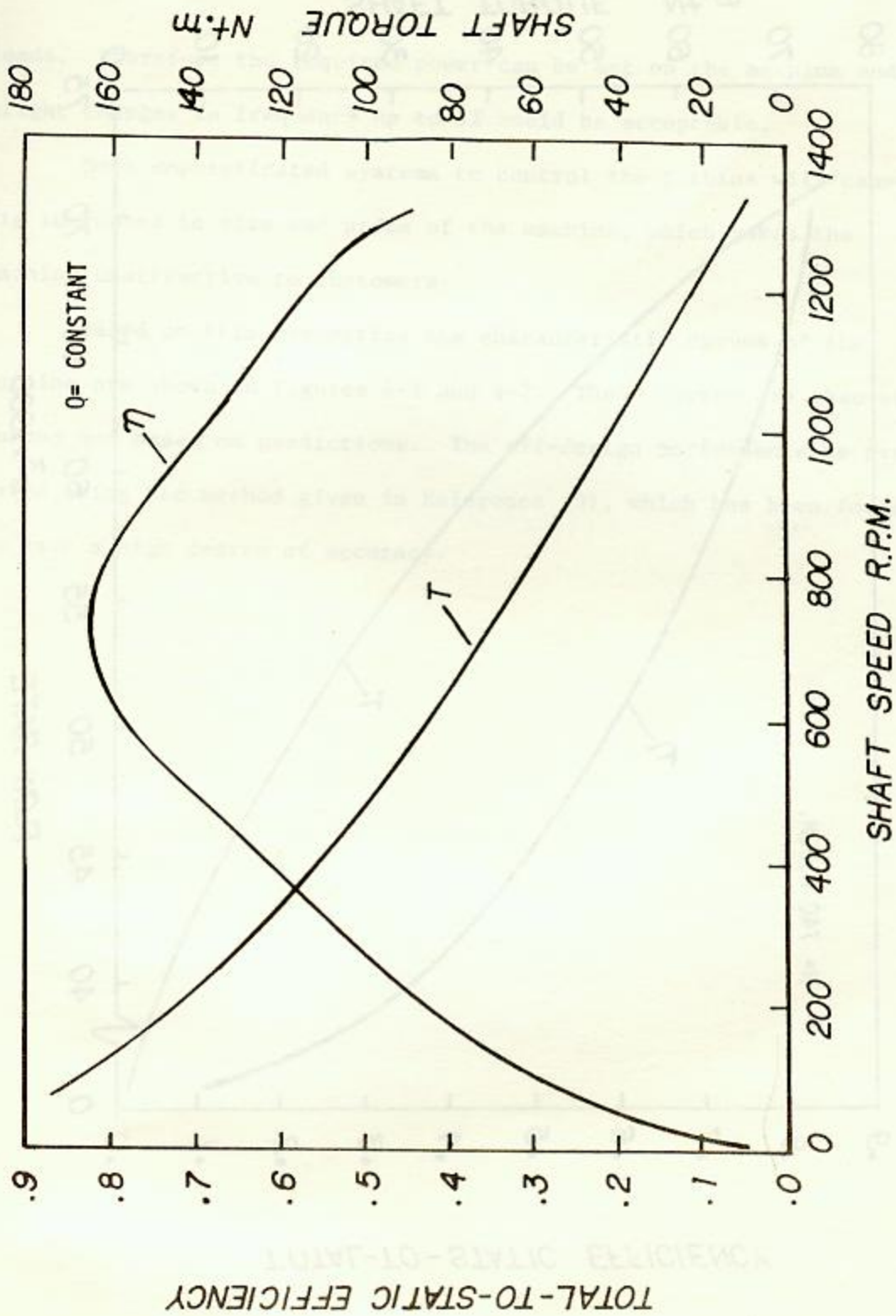


FIG. 4-1. CHARACTERISTIC CURVES OF REACTION MACHINE FOR CONSTANT FLOW RATE.

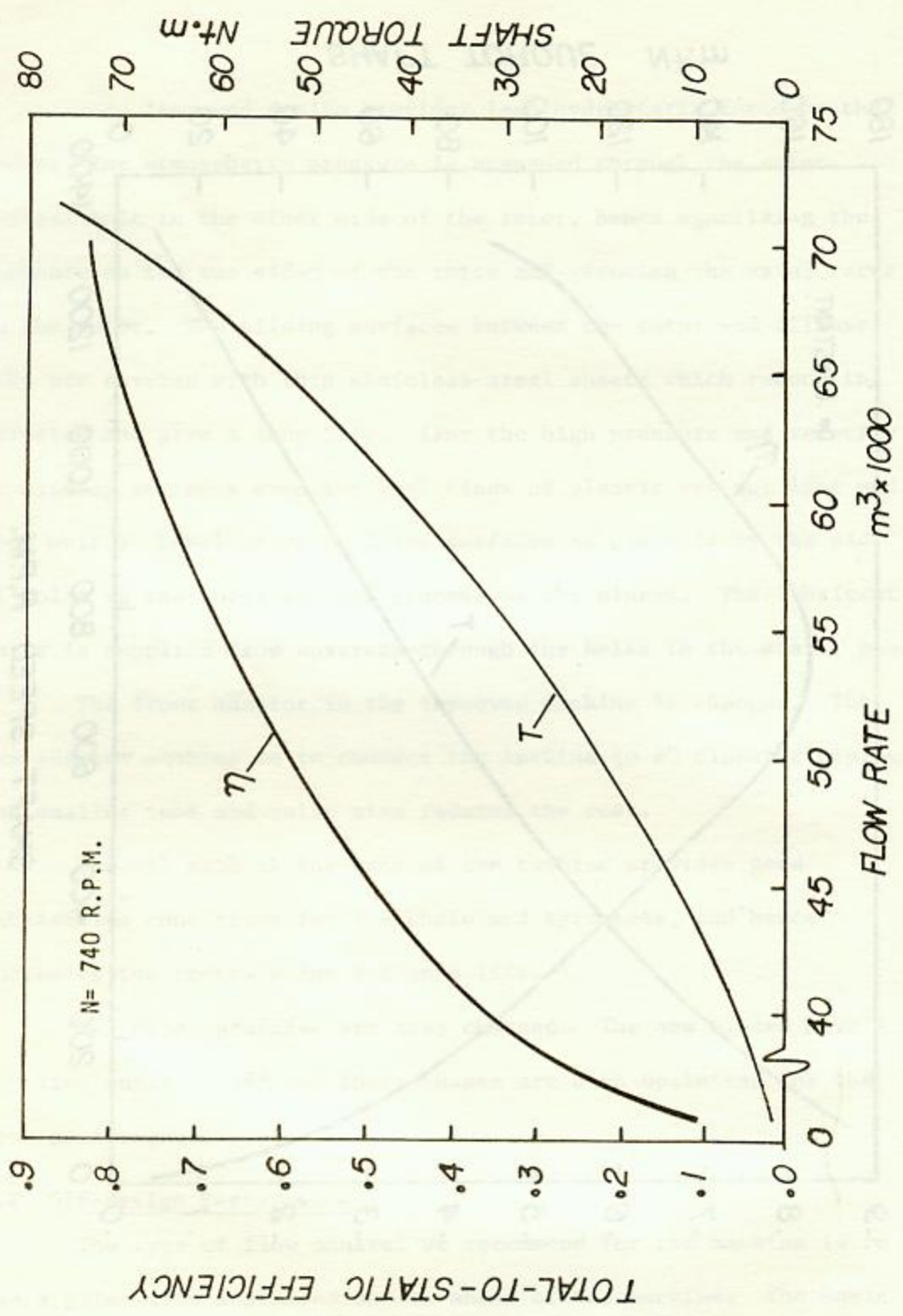


FIG.4-2. CHARACTERISTIC CURVES OF REACTION MACHINE IN CONSTANT SPEED.

loads. Therefore the required power can be set on the machine and slight changes in frequency up to 5% would be acceptable.

More sophisticated systems to control the turbine will cause big increases in size and price of the machine, which makes the machine unattractive to customers.

Based on this assumption the characteristic curves of the turbine are shown in Figures 4-1 and 4-2. These curves are theoretical curves and based on predictions. The off-design performance is predicted using the method given in Reference (3), which has been found to have a high degree of accuracy.

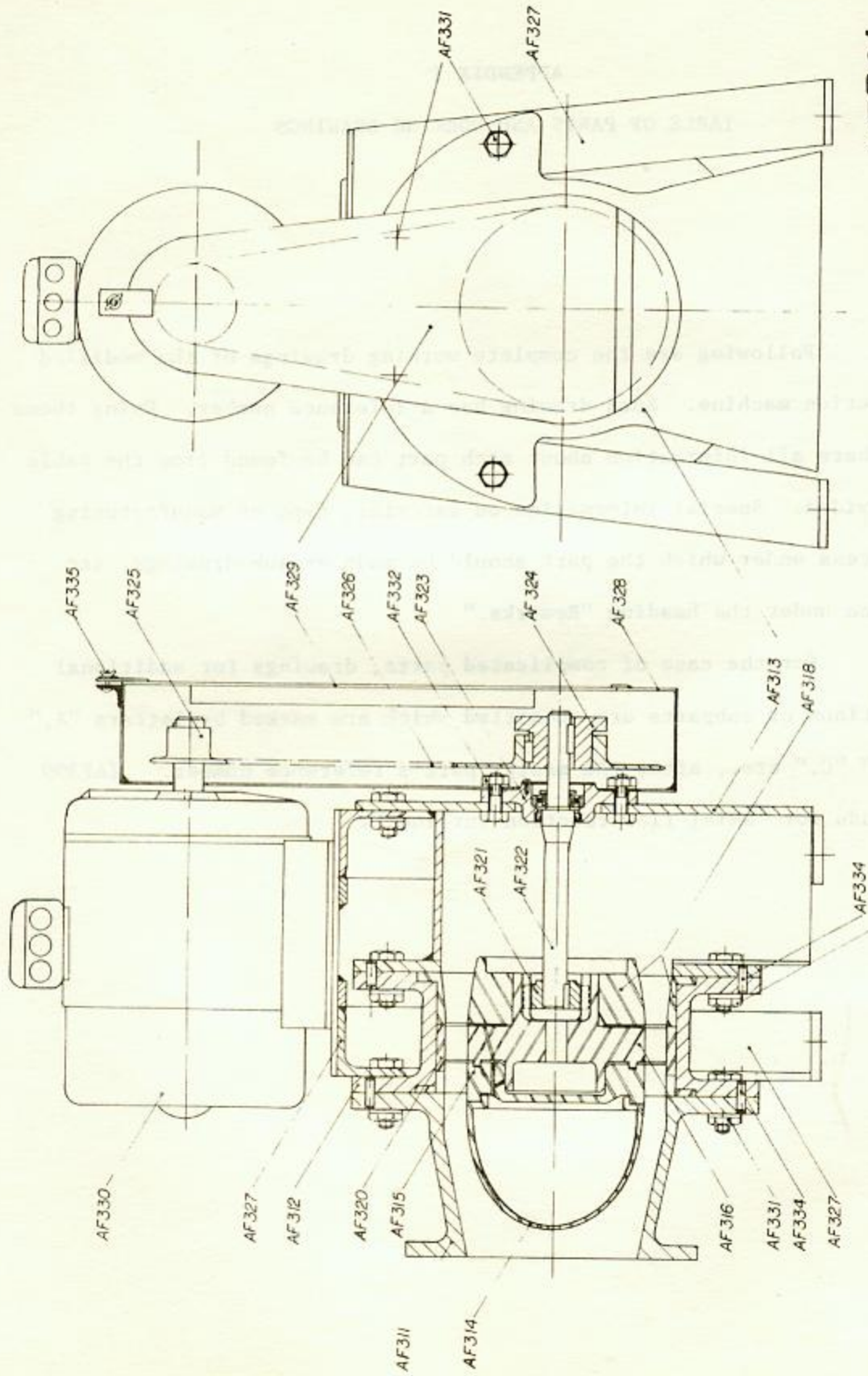
APPENDIX I

TABLE OF PARTS AND WORKING DRAWINGS

Following are the complete working drawings of the modified reaction machine. Each drawing has a reference number. Using these numbers all information about each part can be found from the table provided. Special information on material, type of manufacturing process under which the part should be made, or sub-drawings, are given under the heading "Remarks."

For the case of complicated parts, drawings for additional sections or subparts are submitted which are marked by letters "A," "B," "C," etc., after the master part's reference number. (AF300 stands for 'axial-flow reaction turbine.')





AF301

GENERAL ARRANGEMENT OF MODIFIED REACTION TURBINE

TABLE OF PARTS AND  
LIST OF DRAWINGS OF REACTION TURBINE COMPONENTS

PART NUMBER	NAME OF PART	NUMBER REQ'D	MATERIAL	REMARKS
AF311	FRONT ADAPTOR	1	CAST IRON	
AF312	MIDDLE SECTION	1	CAST IRON	HOLES OF FLANGES SHOULD BE ALIGNED
AF313	DRAIN CHUTE	1	STEEL	SEE SUBDRAWINGS
AF313A	BACK PLATE	1	10MM PLATE	
AF313B	FRONT FLANGE	1	15MM PLATE	
AF313C	CURVED PLATE	1	8MM PLATE	
AF313D	SIDE PLATE	2	5MM PLATE	
AF313E	FRONT PLATE	1	5MM PLATE	

... continued

TABLE OF PARTS AND  
LIST OF DRAWINGS OF REACTION TURBINE COMPONENTS (Continued)

PART NUMBER	NAME OF PART	NUMBER REQ'D	MATERIAL	REMARKS
AF314 (1) AF314 (2)	NOSE	1		SEE ADJACENT TABLE FOR PROFILE COORDINATES
AF315A AF315B AF315C AF315D	STATOR BLADING	1		SEE AF317 FOR BLADES PROFILE.
AF316A AF316B AF316C	ROTOR BLADING	1	GLASS-FIBER-REINFORCED POLYESTER THERMOSET POLYESTER RESINS 30% GLASS BY WT.	THE 1.5MM STAINLESS-STEEL SHEET SHOULD BE JOINED TO SLIDING SURFACE BY METAL-BONDING EPOXY.
AF317	NOZZLE AND ROTOR BLADE SECTION			SEE ADJACENT TABLE FOR BLADE PROFILE.
AF318A AF318B	DIFFUSER BLADING	1	GLASS-FIBER REINFORCED POLYESTER THERMOSET POLYESTER RESINS 30% GLASS BY WT.	THE 1.5MM STAINLESS STEEL SHEET SHOULD BE JOINED TO SLIDING SURFACE BY METAL-BONDING EPOXY.
AF319	DIFFUSER-BLADE SECTION			SEE ADJACENT TABLE FOR BLADE PROFILE.
AF320	BUSH	1	GLASS-FIBER REINFORCED POLYESTER THERMOSET, POLYESTER RESINS 30% GLASS BY WT.	...continued

TABLE OF PARTS AND  
LIST OF DRAWINGS OF REACTION TURBINE COMPONENTS (Continued)

PART NUMBER	NAME OF PART	NUMBER REQ'D	MATERIAL	REMARKS
AF321A	SLOTTED DISK	1	ALUMINUM	
AF321B	KEY	2	HARD STEEL	
AF322	SHAFT	1	STAINLESS STEEL	
	<u>HUB ASSEMBLY</u>			
AF323A	HUB HOUSING	1	CAST STEEL	
AF323B	FRONT CAP	1	1.5MM STEEL SHEET	
AF323C	BALL BEARING	1	M.R.C. BEARING 206-SX ADAPTER AND NUT G-Y	EQUIVALENT STANDARD PARTS WITH THE SAME SIZE CAN ALSO BE USED.
AF323D	SEAL	1	GARLOCK 78 <sub>x</sub> 0542 COMP NO. 26448-05 DES. GRP. D	
AF323E*	(3/16"×32)×5/16" BOLT	3		ROUND HEAD

...continued

\*no drawing; standard component

TABLE OF PARTS AND  
LIST OF DRAWINGS OF REACTION TURBINE COMPONENTS (Continued)

PART NUMBER	NAME OF PART	NUMBER REQ'D	MATERIAL	REMARKS
AF324	BIG SPROCKET	1	BROWNING 40P60 TYPE 4 BUSHING P1	NO. OF TEETH 60 PITCH 1/2" PITCH CIRCLE DIA. 9.554" FOR TYPE 40 CHAIN
AF325	SMALL SPROCKET	1	BROWNING 4024	NO. OF TEETH 24 PITCH 1/2" PITCH DIA. CIRCLE 3.831" FOR TYPE 40 CHAIN
AF326 *	CHAIN	1	BROWNING NO. 40	1/2" PITCH NO. 40 A.S.R.C.

...continued

\*no drawing; standard component

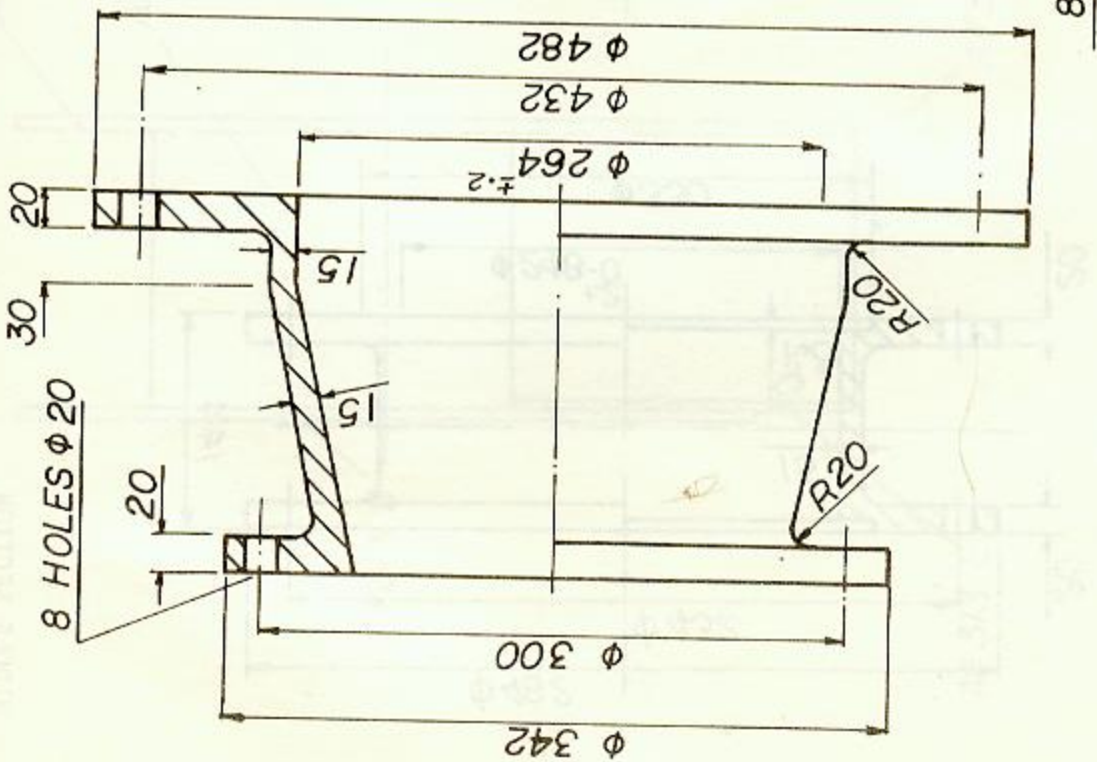
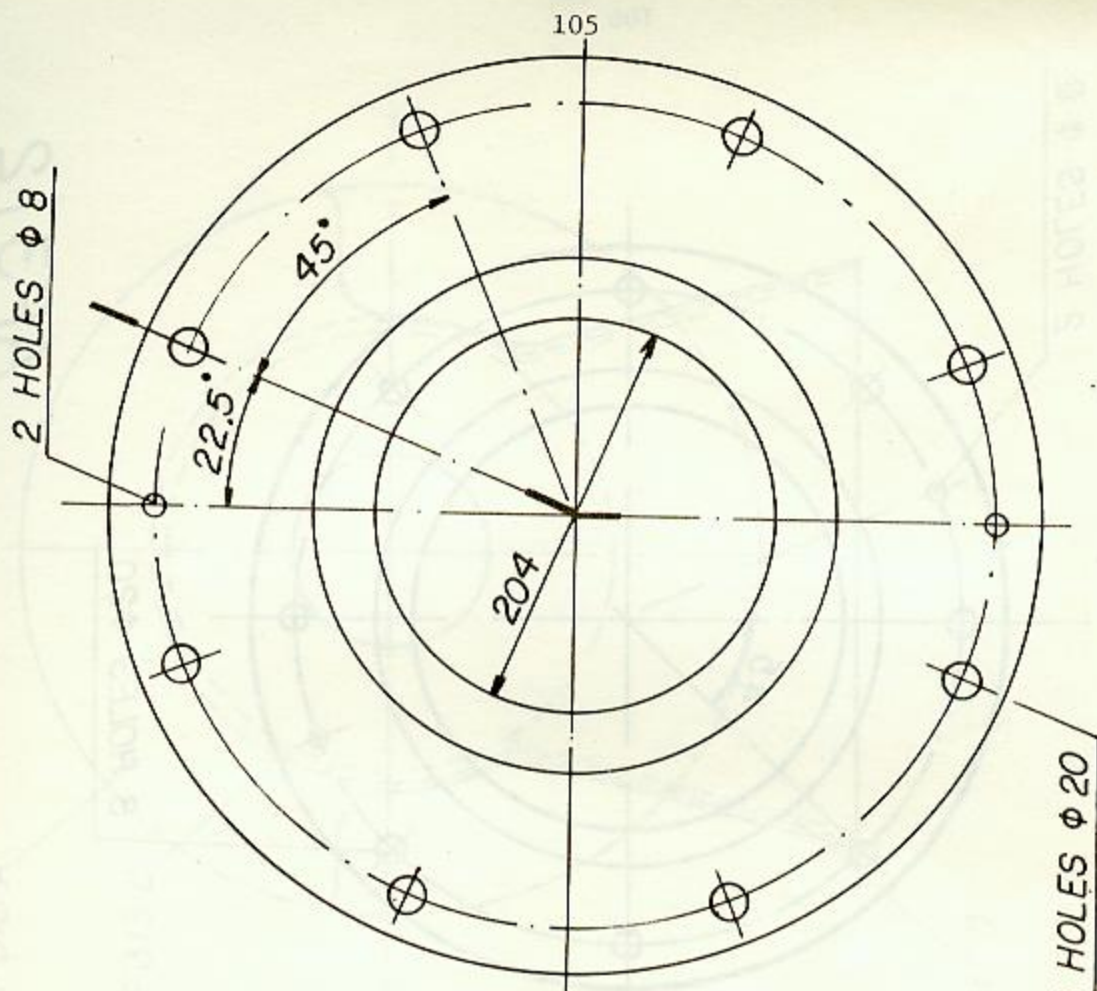
TABLE OF PARTS AND  
LIST OF DRAWINGS OF REACTION TURBINE COMPONENTS (Continued)

PART NUMBER	NAME OF PART	NUMBER REQ'D	MATERIAL	REMARKS
AF327	FRAME	1	STEEL	
AF327A	SIDE ANGLES	2 + 2	80×80×8 L	2 OFF AS DRAWN
AF327B	TOP ANGLE	2	80×80×8 L	OPPOSITE HAND
AF327C	TOP PLATE	1	80MM PLATE	
AF327D	BAR	2	40×8 FLATBAR	
AF327E	FOUNDATION PLATE	4	10MM PLATE	
AF328	OIL BATH	1	2 AND 3MM STEEL SHEETS	SEAMWELDED
AF329	OIL-BATH COVER	1	2MM STEEL SHEET	...continued

TABLE OF PARTS AND  
LIST OF DRAWINGS OF REACTION TURBINE COMPONENTS (Continued)

PART NUMBER	NAME OF PART	NUMBER REQ'D	MATERIAL	REMARKS
AF330 *	GENERATOR	1	WINCO INC. SERIES 5KS4G-3	4 POLE, 5KW, 115/230 VOLTS 21.7 AMP. 60 CYCLE 1800 R.P.M. 1 PH.
AF331A *	(5/8"x12) x 2 1/2" BOLT	20		
AF331B *	5/8"x12 NUT	20		HEXAGON HEADED
AF331C *	5/8" LOCK WASHER	20		
AF332A *	(1/2"x12) 1-1/2" BOLT	4		
AF332B *	1/2"x12 NUT	4		HEXAGON HEADED
AF332C *	1/2" LOCK WASHER	4		
AF333A *	(9/16"x12) x 2" BOLT	4		
AF333B *	(9/16"x12) x NUT	4		
AF333C *	9/16" PLAIN WASHER	4		
AF333D *	9/16" LOCK WASHER	4		
AF334 *	ALIGNMENT-PIN	4	HARD STEEL	
AF335A *	(3/8"x16) 2" BOLT	1		HEXAGON HEADED
AF335B *	3/8" PLAIN WASHER	2		
AF335C *	(3/8"x16) WING NUT	1		...End

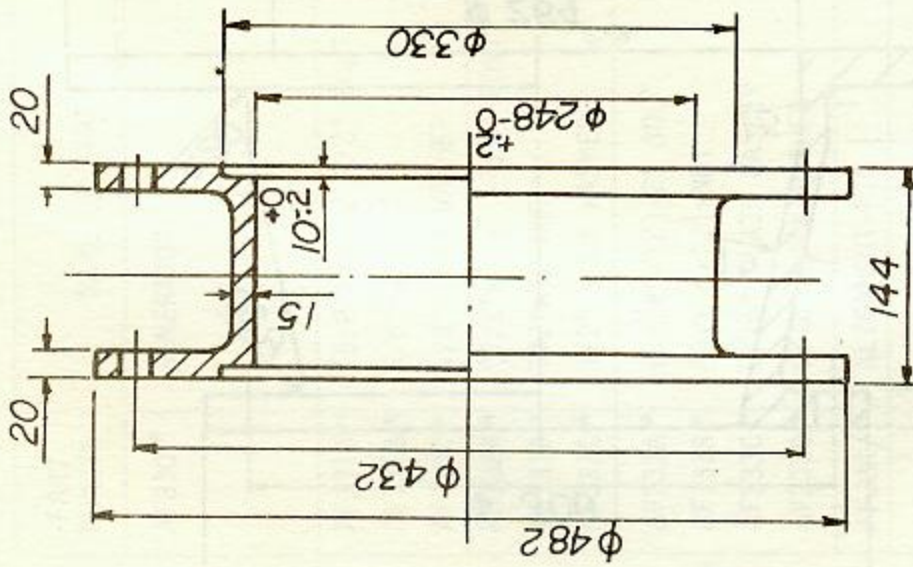
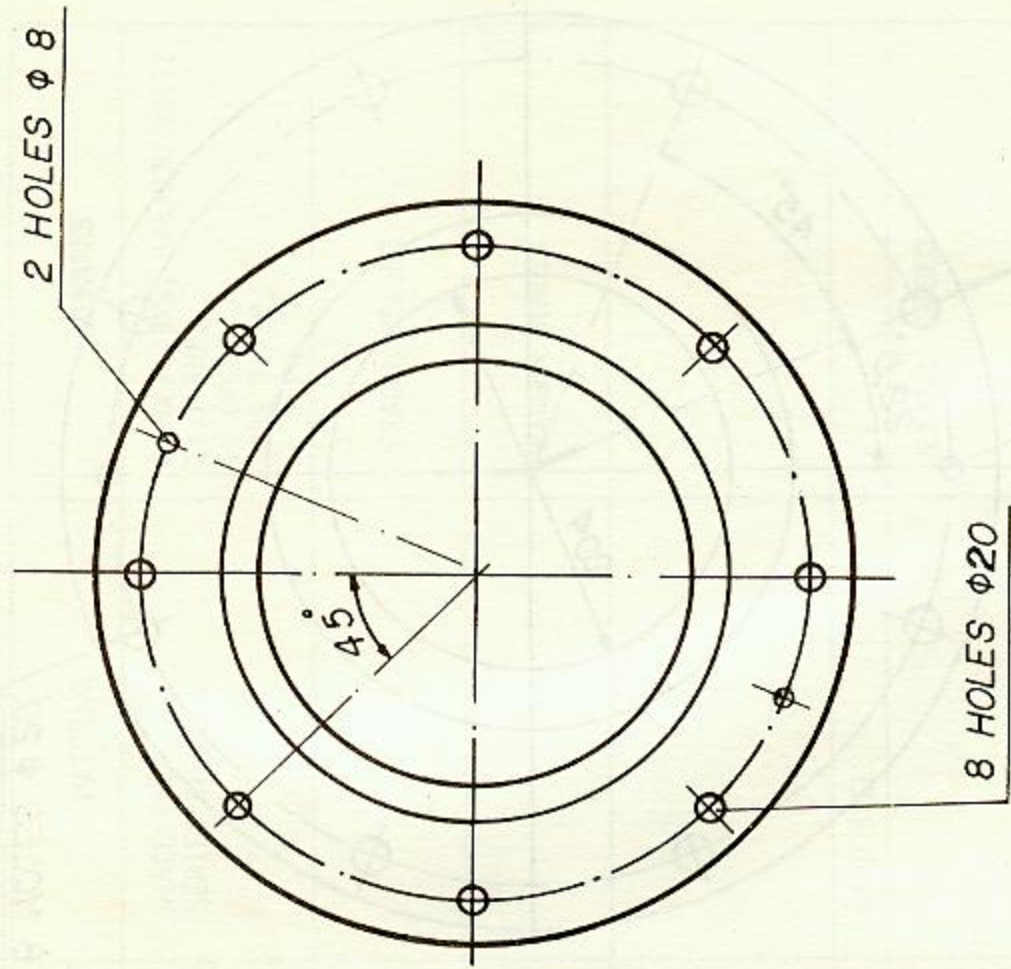
\*no drawing; standard component



AF311

FRONT ADAPTOR



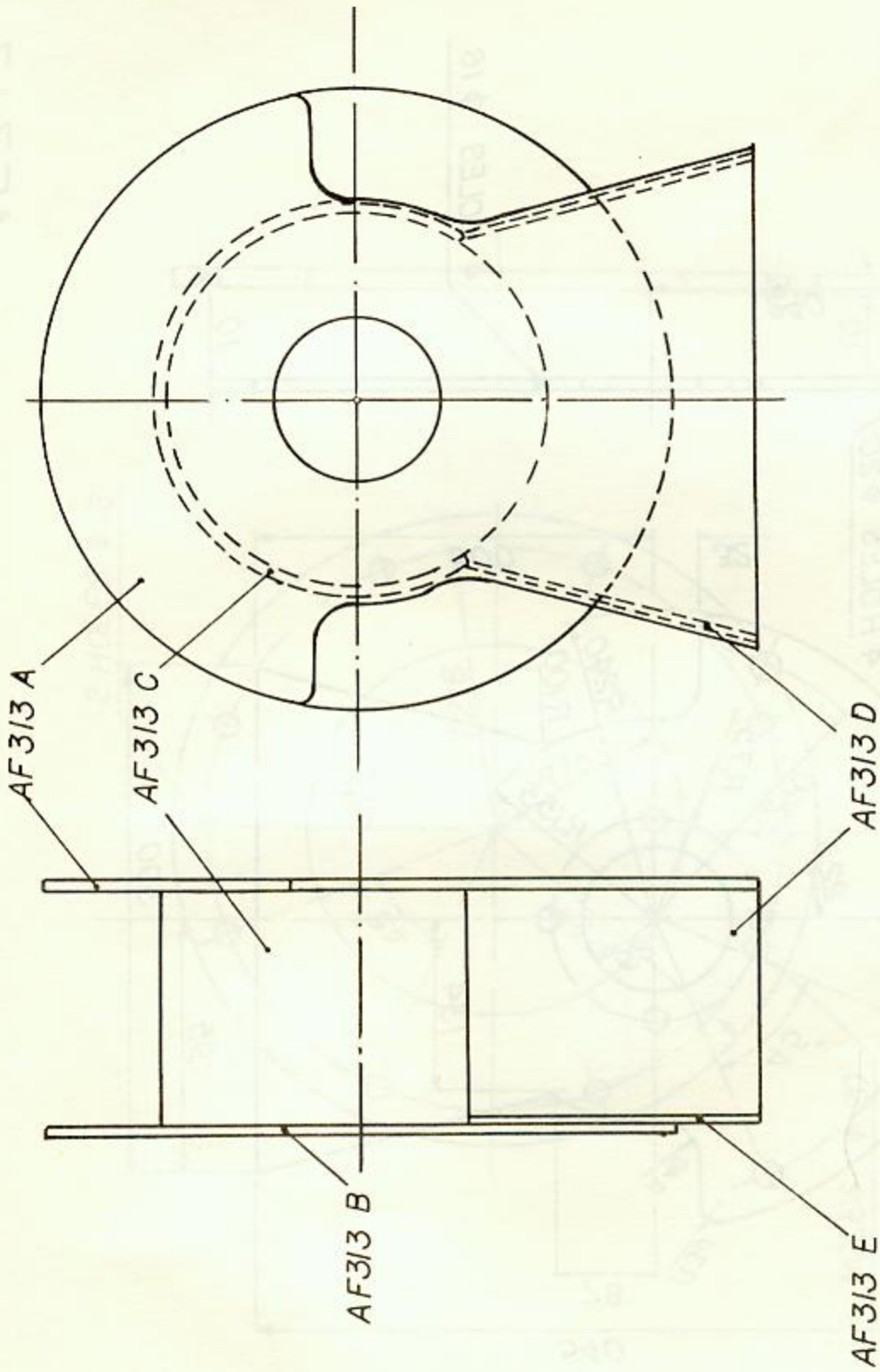


AF312

MIDDLE SECTION

AF313 A

AF313 B

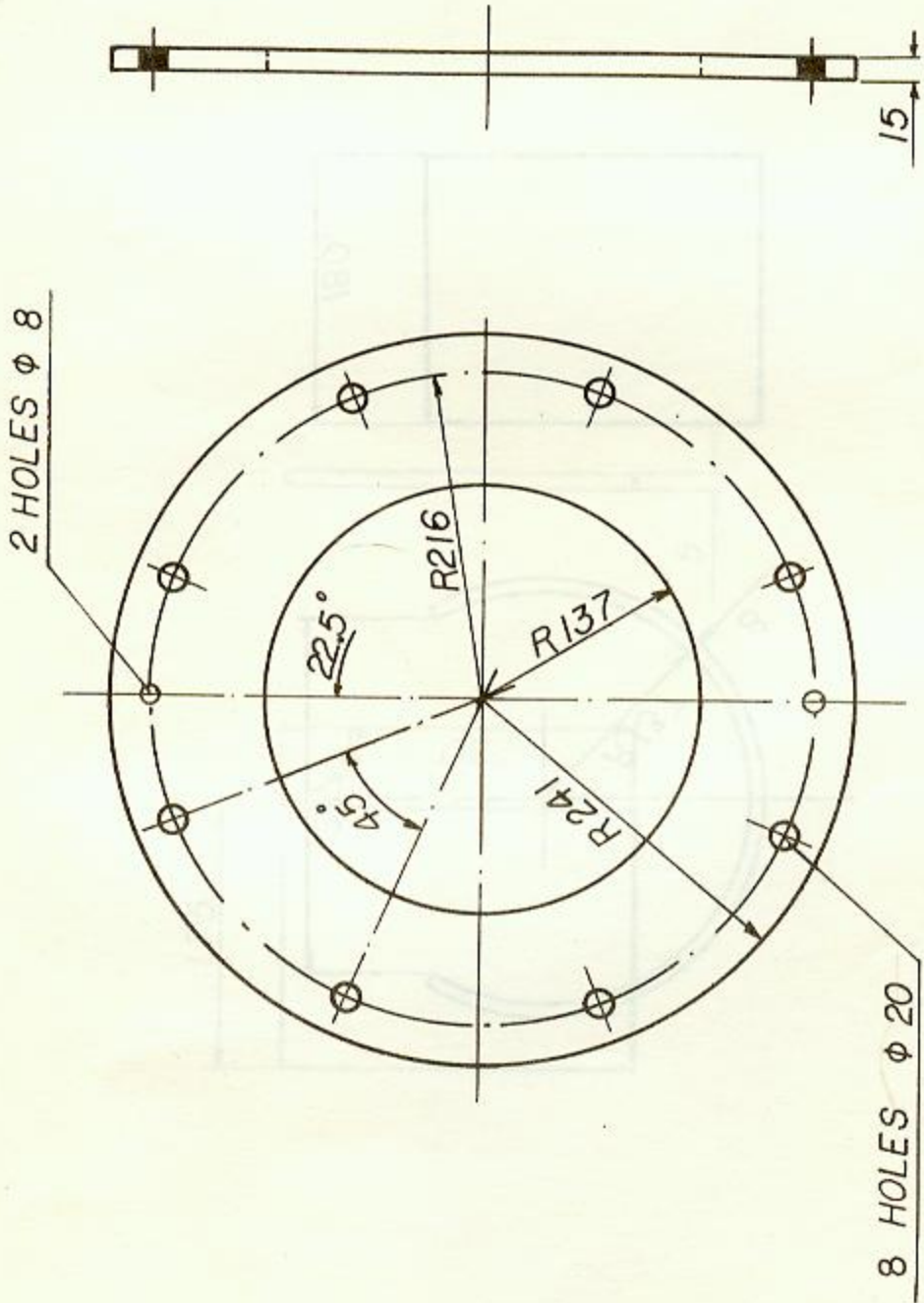


AF313

DRAIN CHUTE

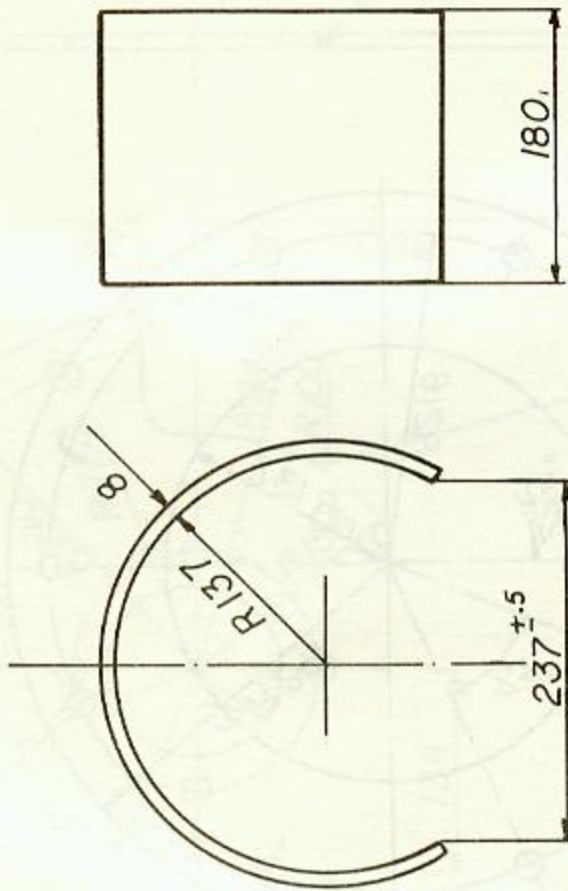


AF313 C



AF313 B

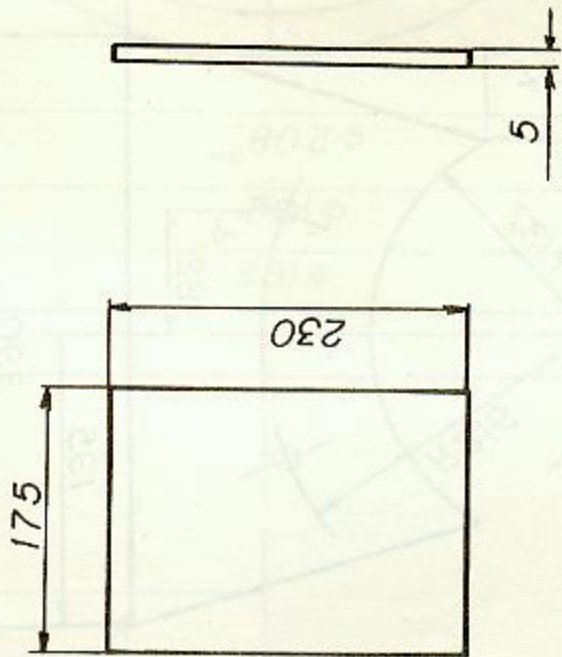
FRONT FLANGE



AF313 C

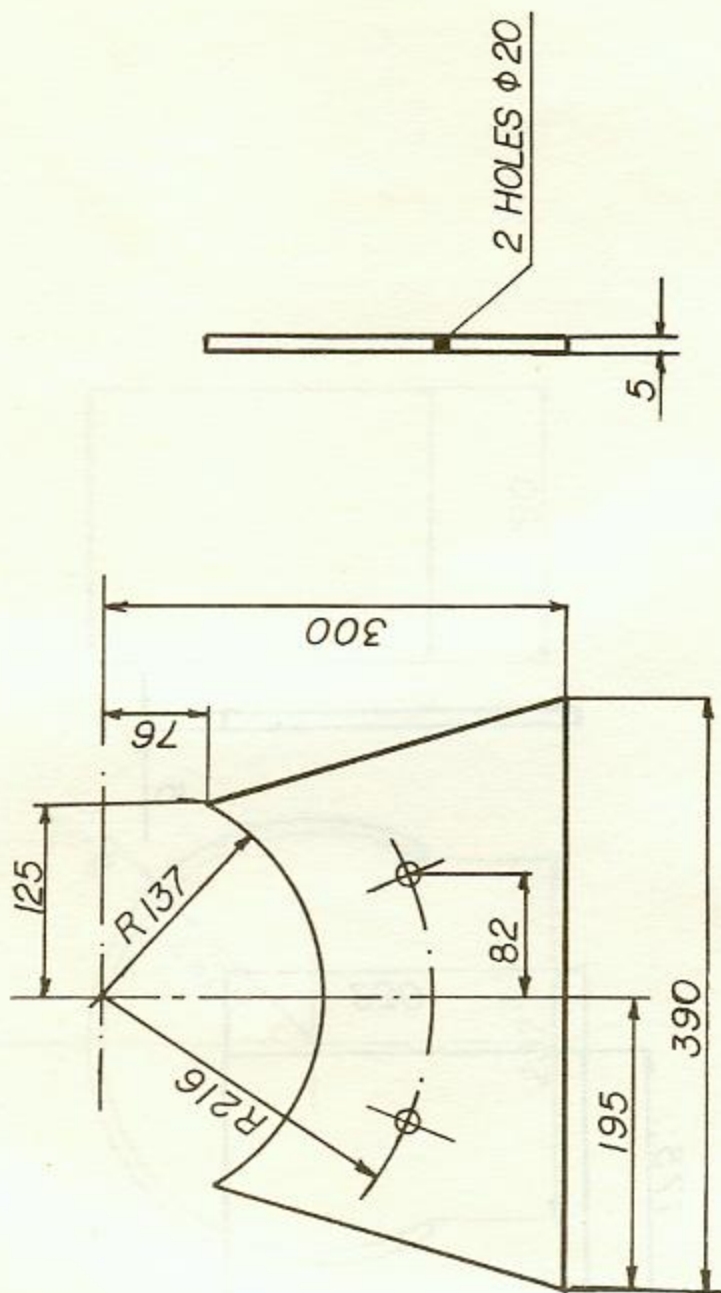
CURVED PLATE

AF313 E



SIDE PLATE

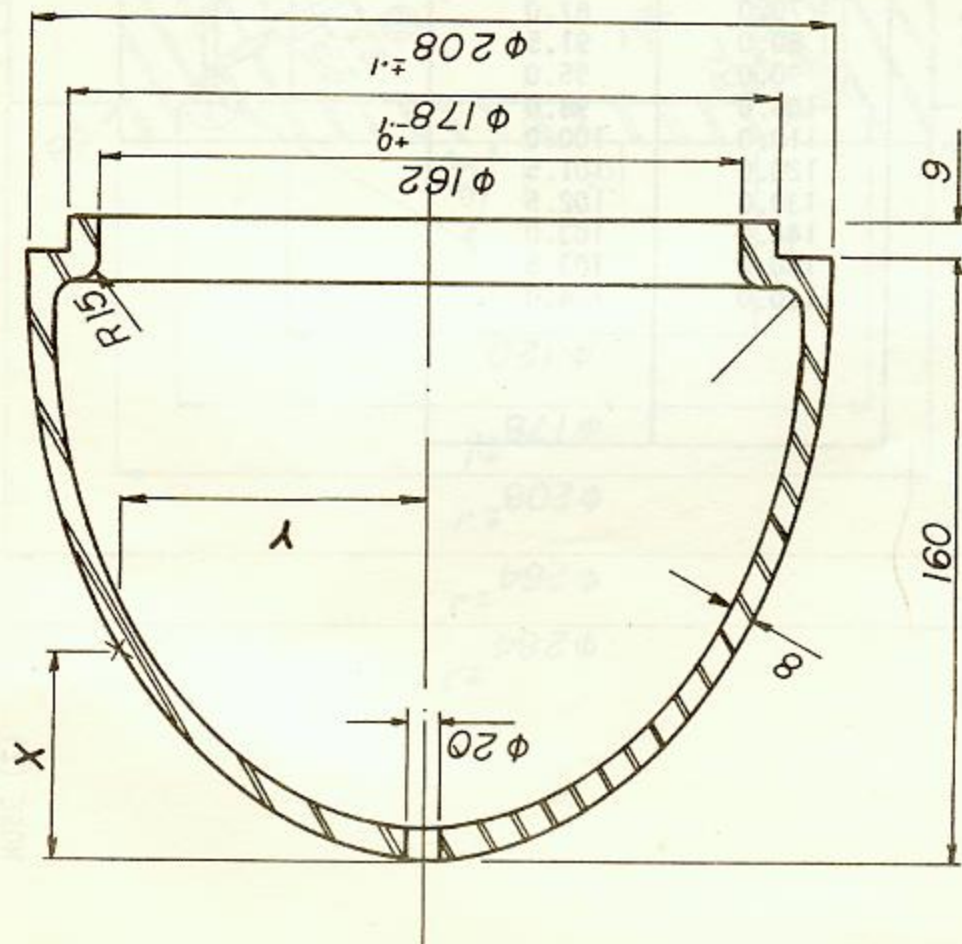
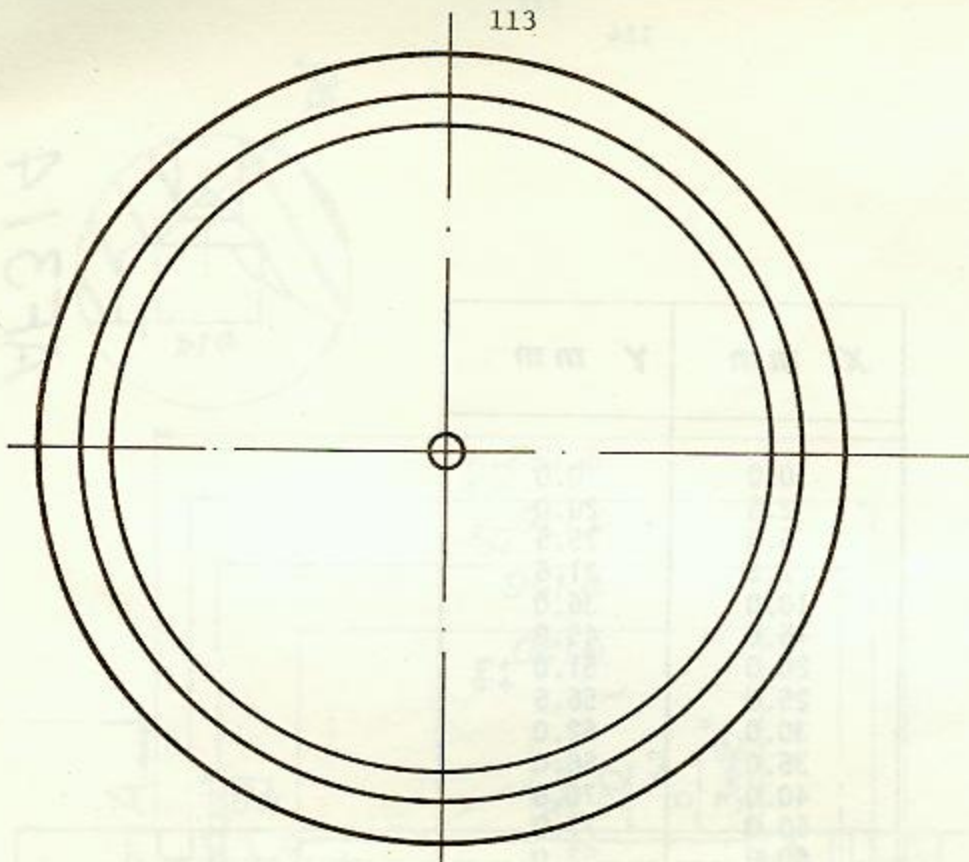
AF313 D



FRONT PLATE

AF313 E

AF313 D



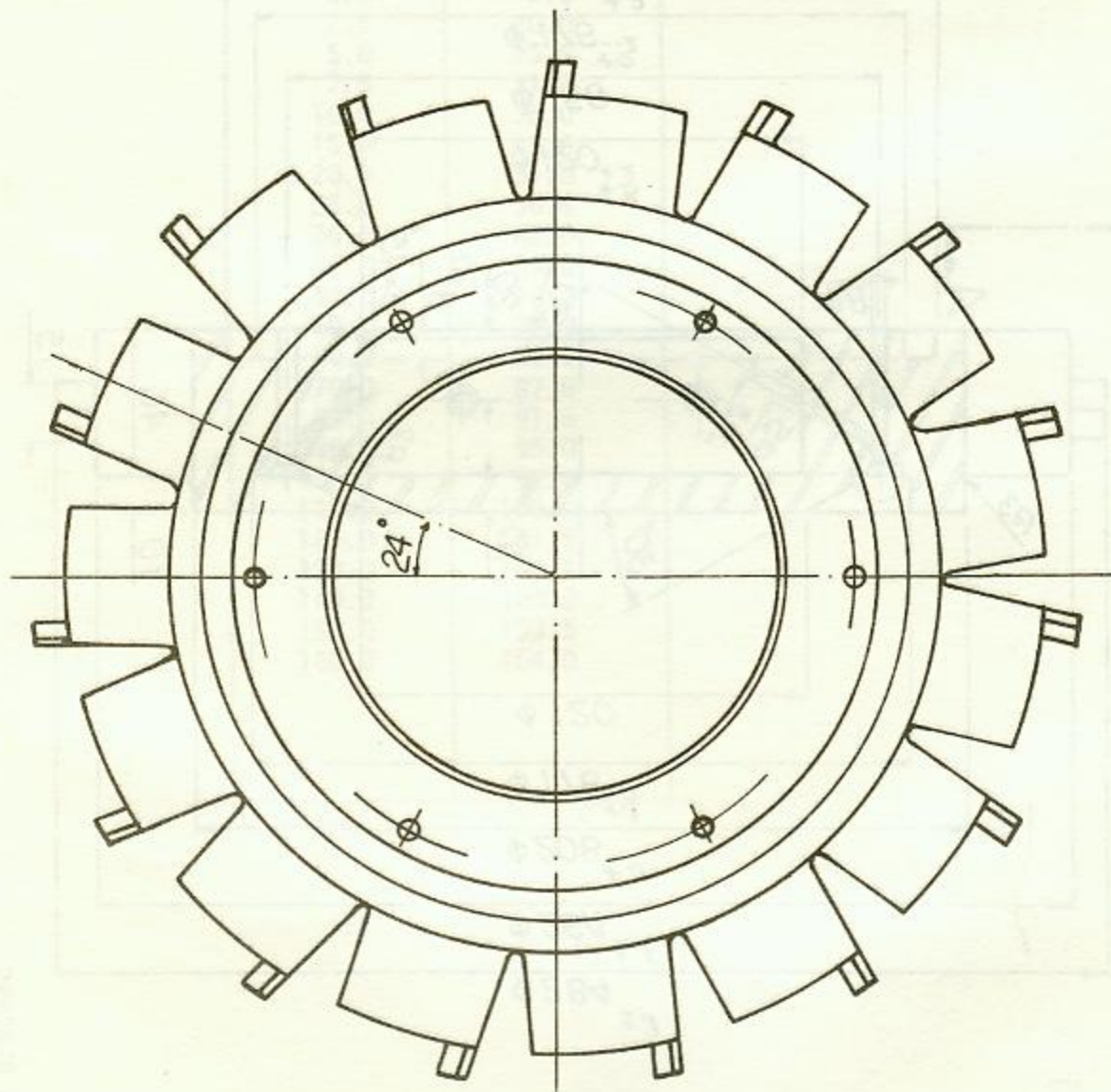
AF314

NOSE (1)



<i>X mm</i>	<i>Y mm</i>
0.0	0.0
2.5	20.0
5.0	25.5
7.5	31.5
10.0	36.0
15.0	45.0
20.0	51.0
25.0	56.5
30.0	62.0
35.0	66.0
40.0	70.0
50.0	77.0
60.0	82.0
70.0	87.0
80.0	91.5
90.0	95.0
100.0	98.0
110.0	100.0
120.0	101.5
130.0	102.5
140.0	103.0
150.0	103.5
160.0	104.0



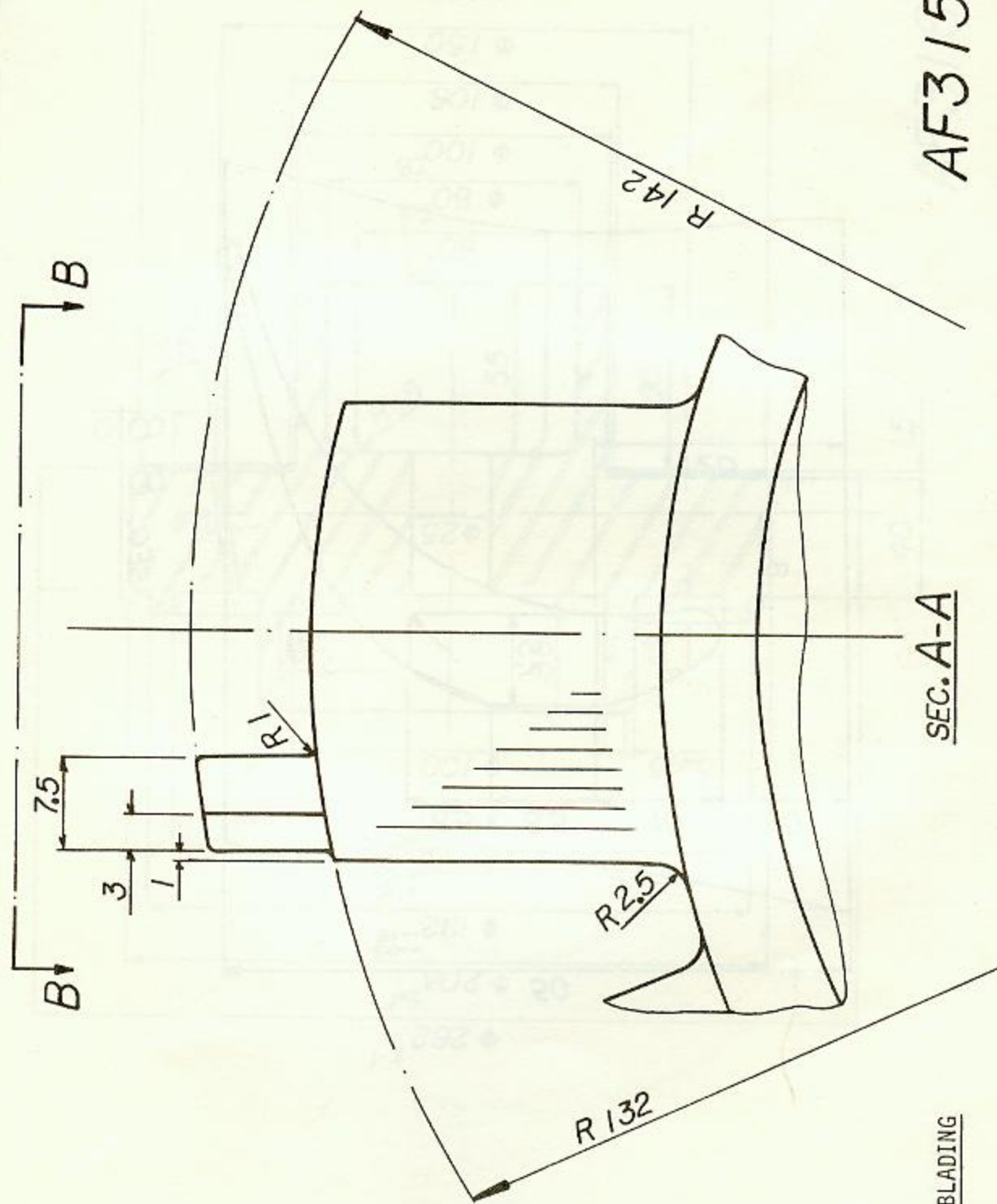


AF315 B

STATOR BLADING

AF312 D

AF315 C

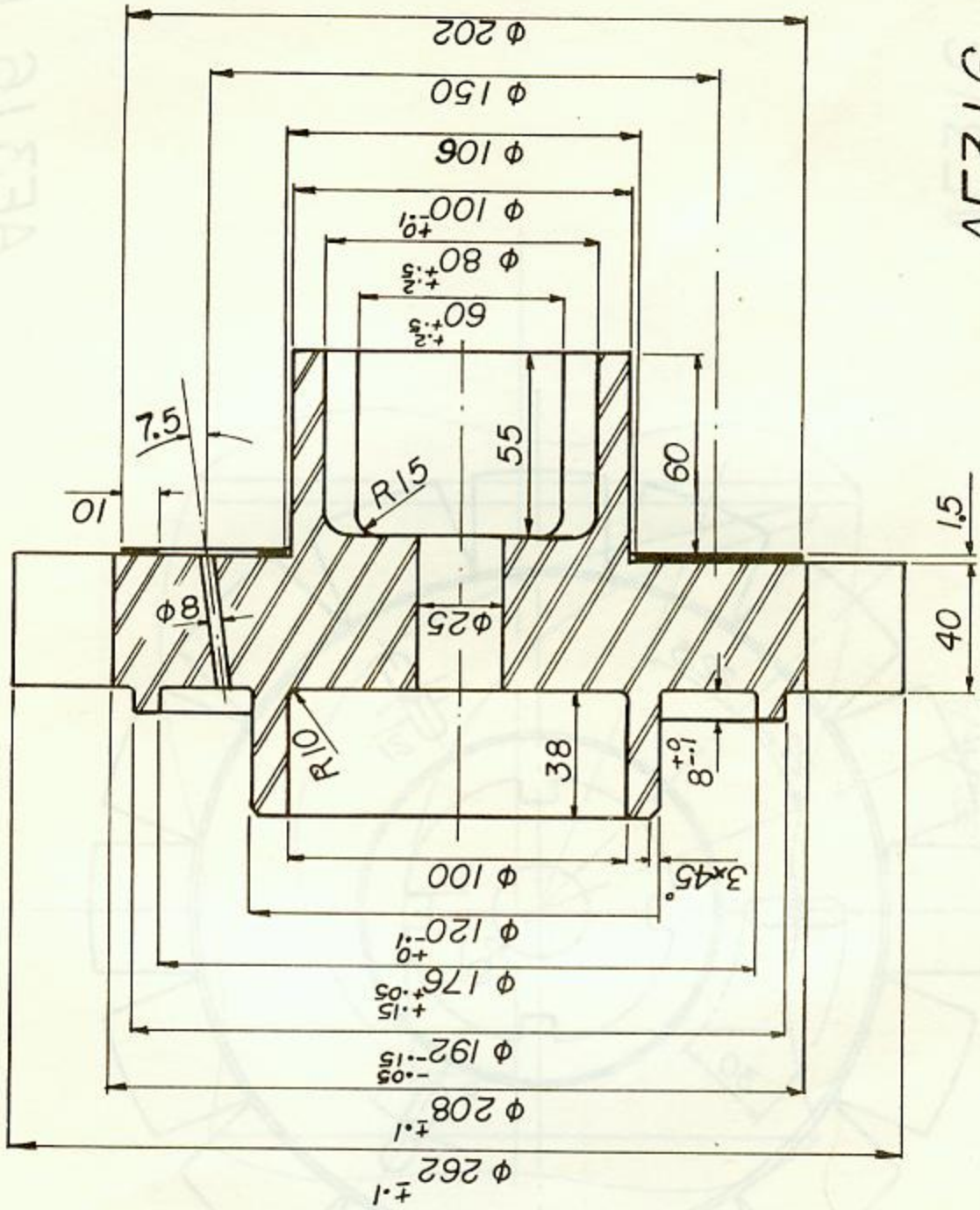


STATOR BLADING

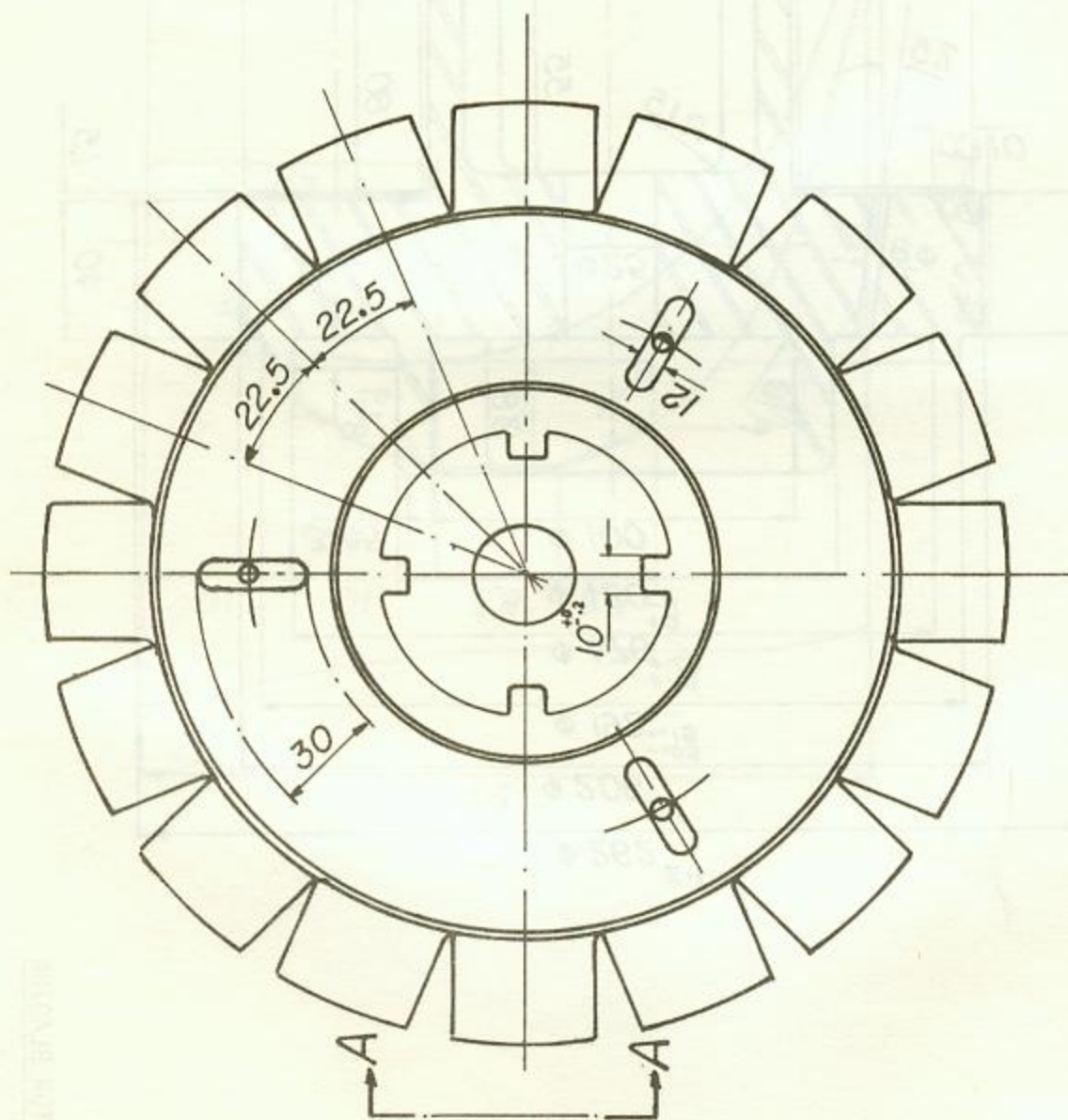
SEC. A-A



AF316 A

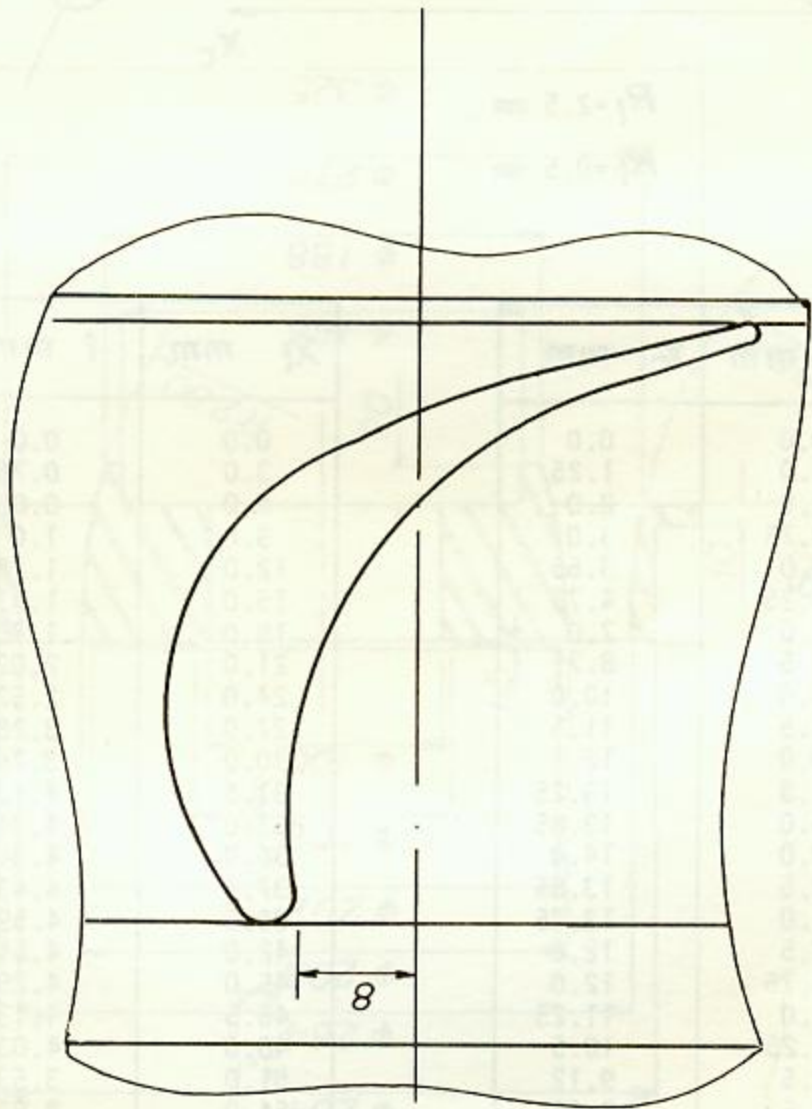


ROTOR BLADING



AF316 B

ROTOR BLADING



AF316 C

SEC. A-A

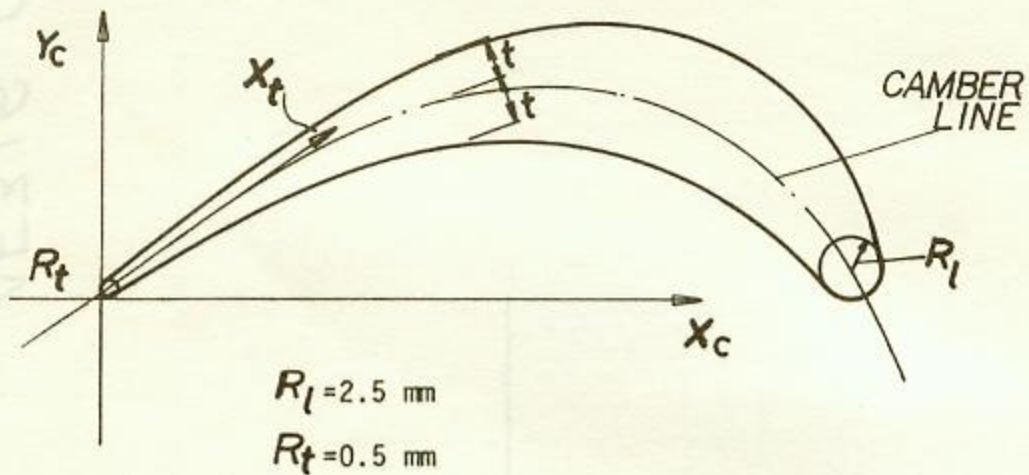
ROTOR BLADING

AF316

CHAMFER  
LINE

R1





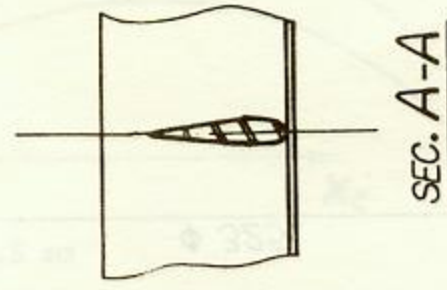
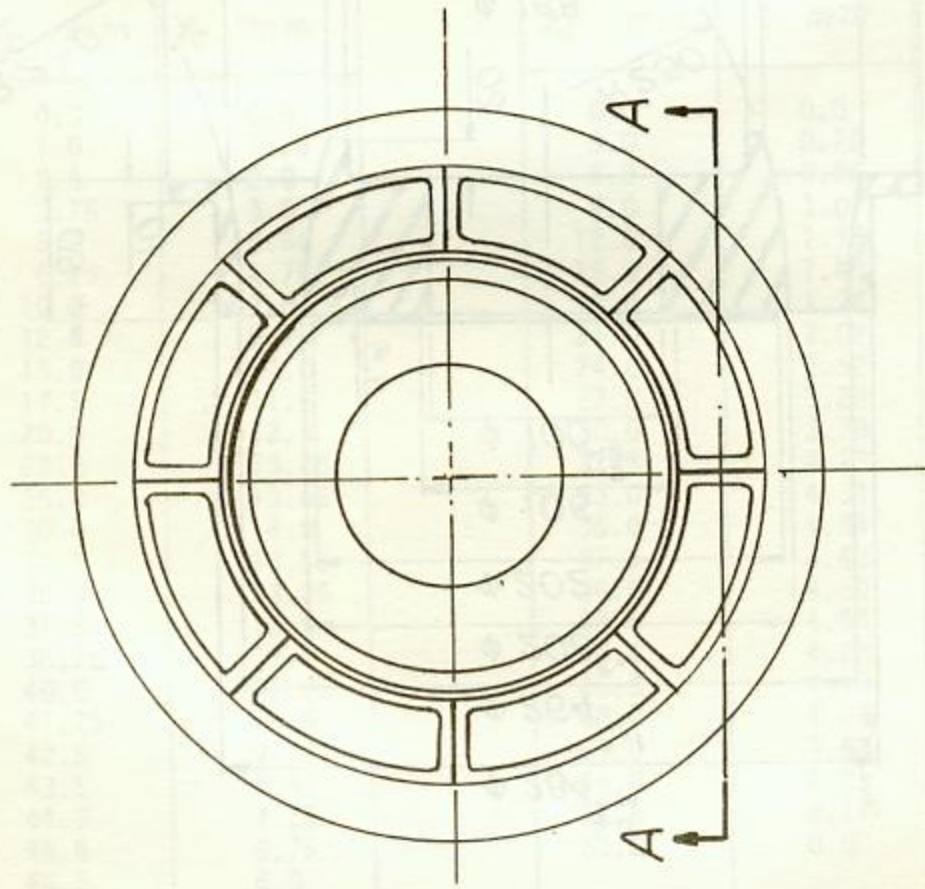
$X_c$ mm	$Y_c$ mm	$X_t$ mm	$t$ mm
0.0	0.0	0.0	0.0
1.0	1.25	3.0	0.76
2.5	2.0	6.0	0.86
3.75	3.0	9.0	1.0
5.0	3.65	12.0	1.18
6.25	4.75	15.0	1.43
10.0	7.0	18.0	1.76
12.5	8.75	21.0	2.02
15.0	10.0	24.0	2.52
17.5	11.5	27.0	3.28
20.0	12.5	30.0	3.78
22.5	13.25	31.5	4.13
25.0	13.85	33.0	4.34
30.0	14.0	36.0	4.34
32.5	13.85	37.5	4.43
35.0	13.25	39.0	4.59
37.5	12.6	42.0	4.54
38.75	12.0	45.0	4.28
40.0	11.25	46.5	4.13
41.25	10.5	48.0	4.03
42.5	9.12	51.0	3.53
43.5	8.62	54.0	2.83
44.5	7.75	57.0	2.17
45.5	6.75	60.0	0.0
46.5	6.0		
47.5	4.25		
48.75	2.0		
50.0	0.0		

AF317

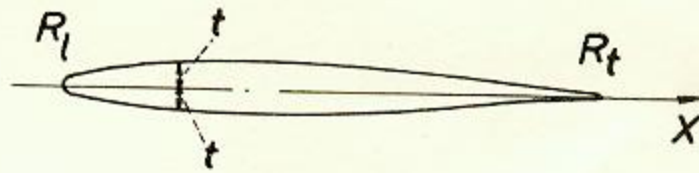
NOZZLE AND ROTOR BLADE SECTION



AF318 B



AF318 B



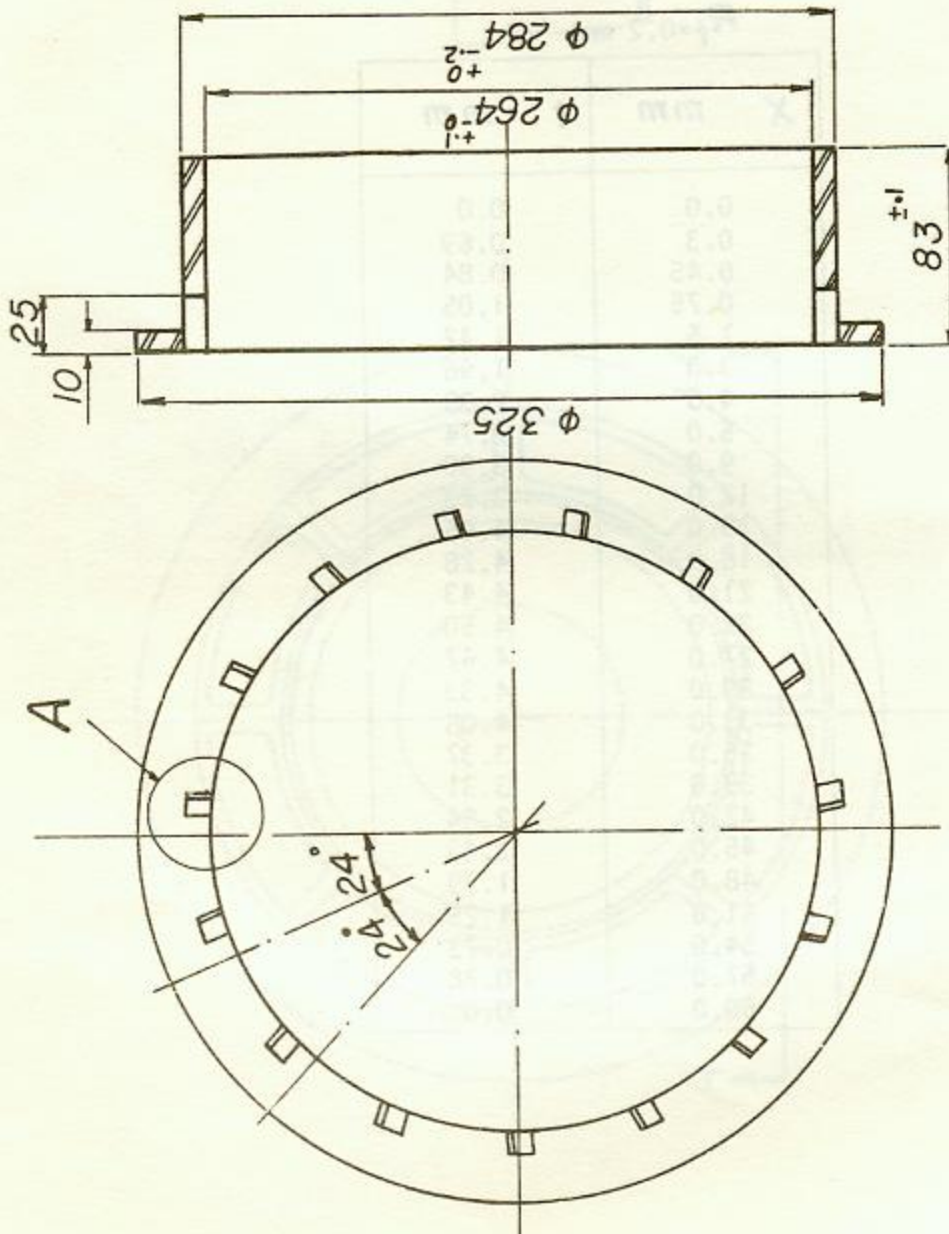
$$R_l = 1.0 \text{ mm}$$

$$R_t = 0.2 \text{ mm}$$

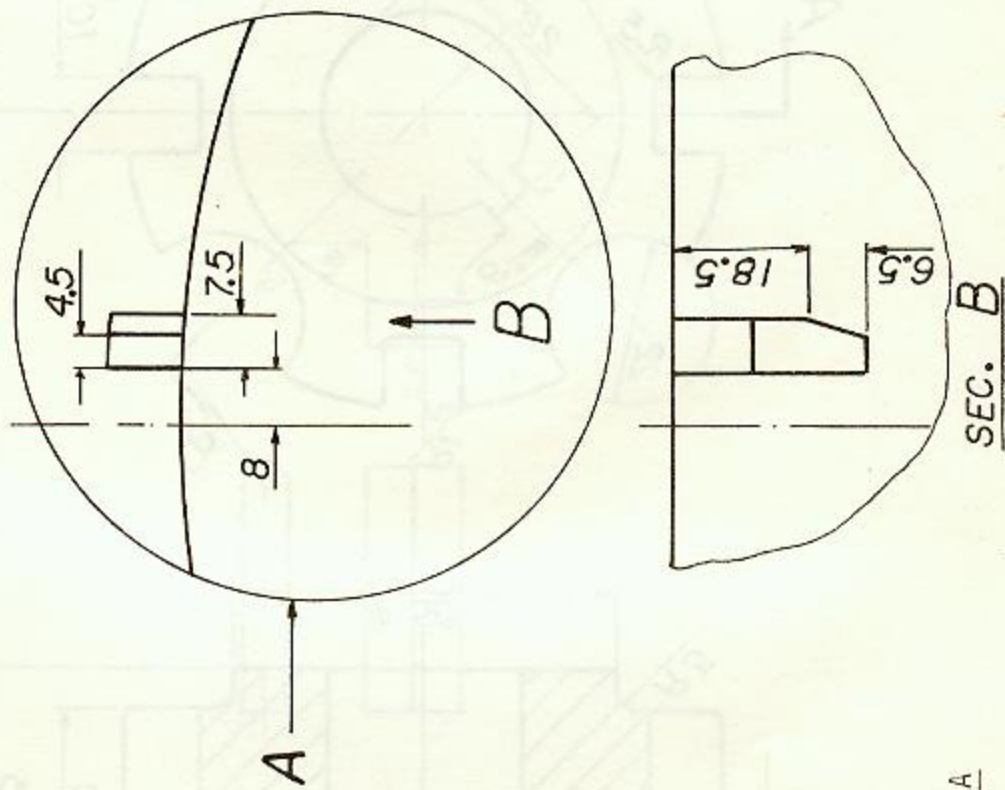
$X$	$mm$	$t$	$mm$
0.0		0.0	
0.3		0.69	
0.45		0.84	
0.75		1.05	
1.5		1.42	
3.0		1.96	
4.5		2.38	
6.0		2.74	
9.0		3.30	
12.0		3.73	
15.0		4.05	
18.0		4.28	
21.0		4.43	
24.0		4.50	
27.0		4.47	
30.0		4.33	
33.0		4.08	
36.0		3.37	
39.0		3.31	
42.0		2.84	
45.0		2.33	
48.0		1.79	
51.0		1.25	
54.0		0.73	
57.0		0.28	
60.0		0.0	

AF319 B

DIFFUSER-BLADE SECTION

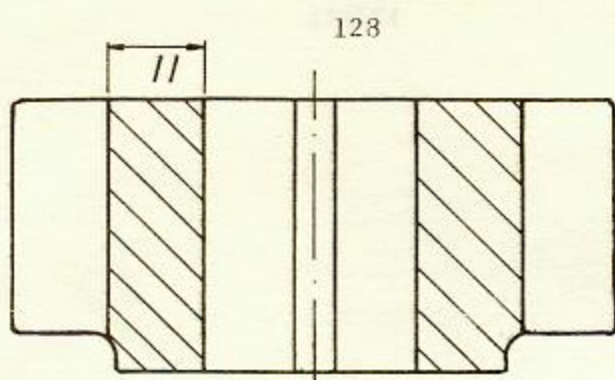


AF320 A

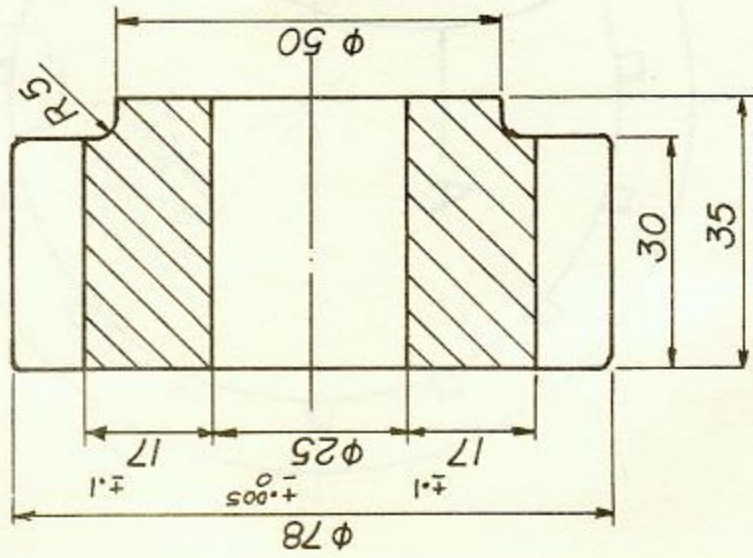
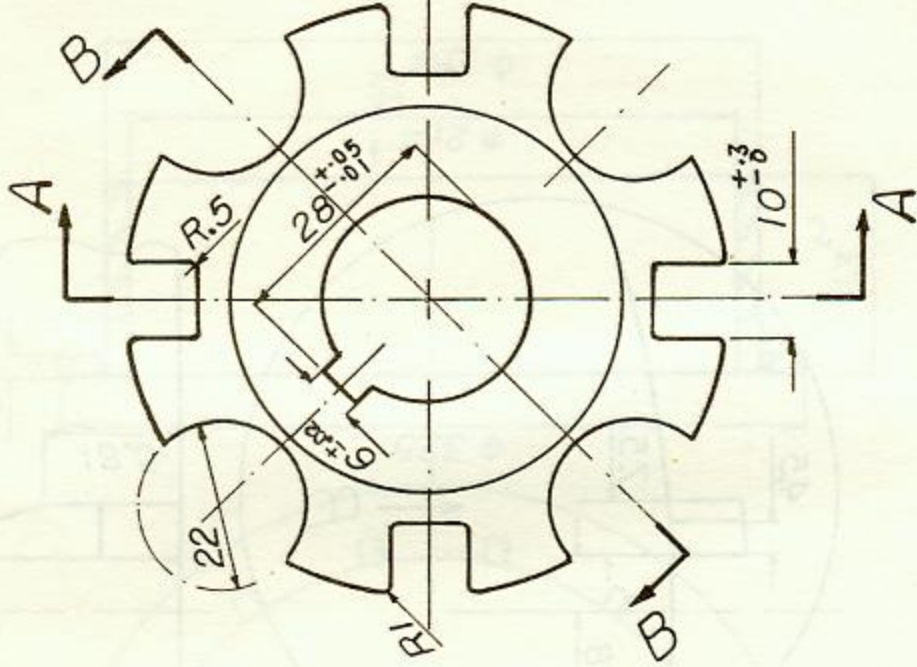


AF320 B

DETAIL OF "A" FROM AF320A



SEC. B-B



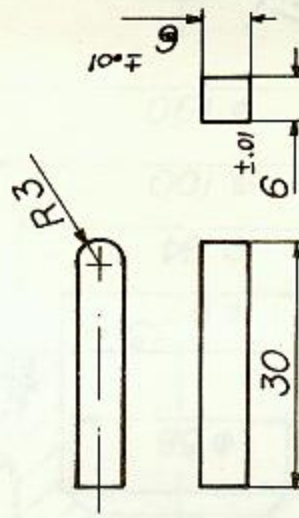
SEC. - A-A

AF321 A

SLOTTED DISK

AF321 B

3/16" ±0.0015

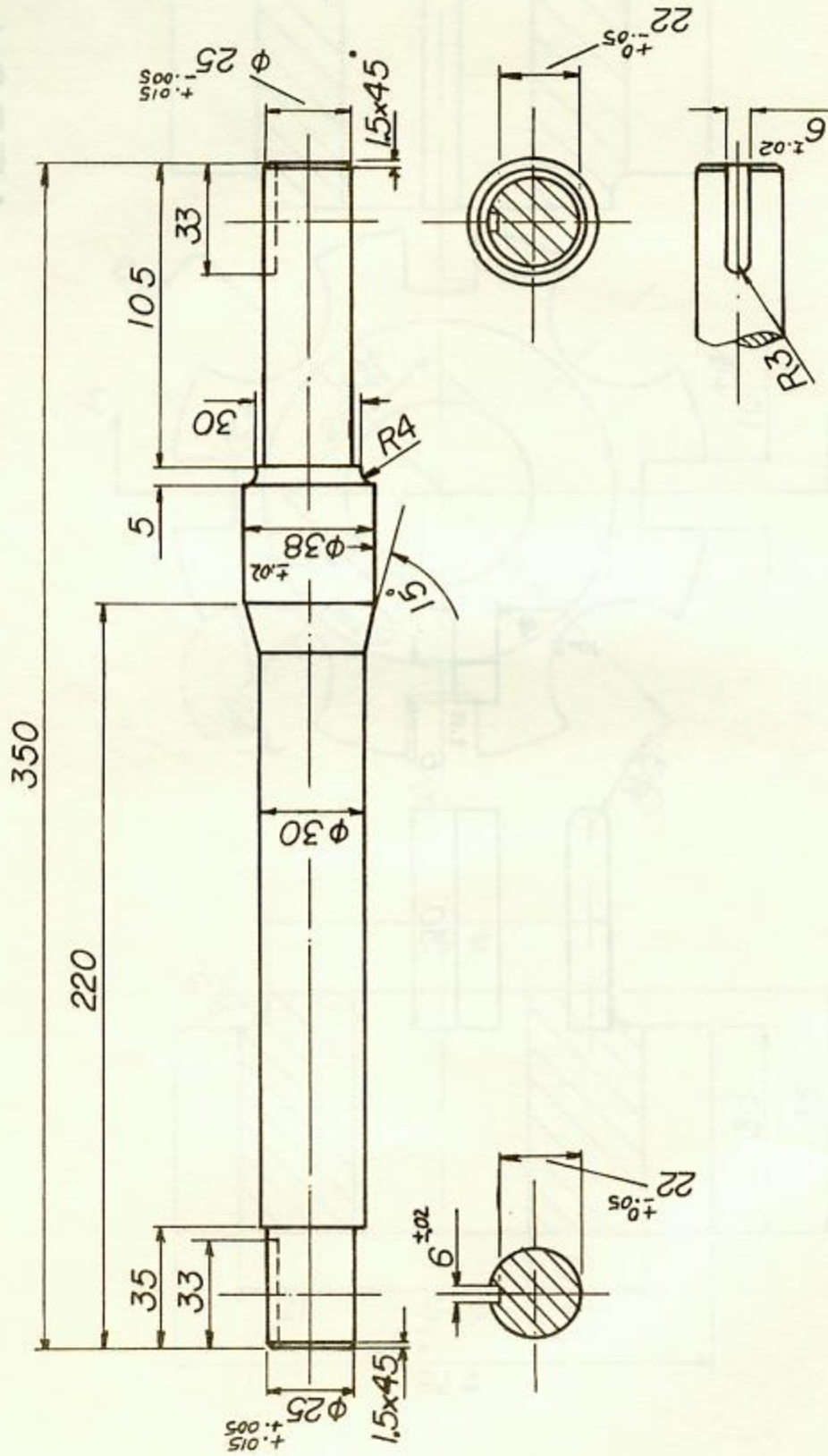


AF321 B

KEY



AF351 B



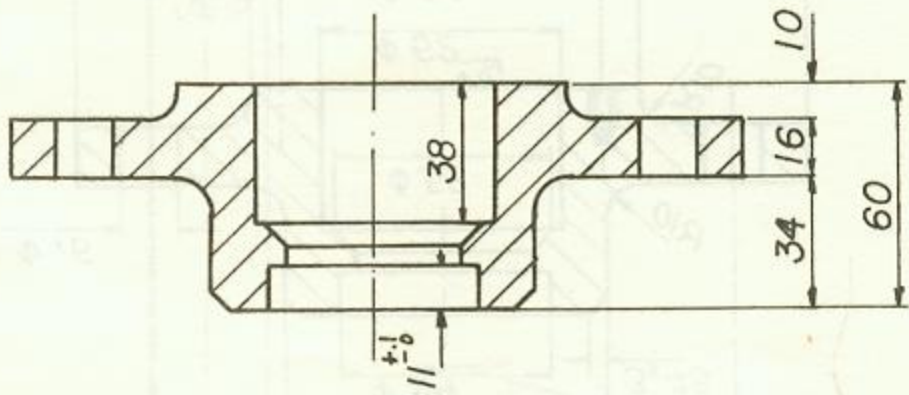
AF322

SHAFT

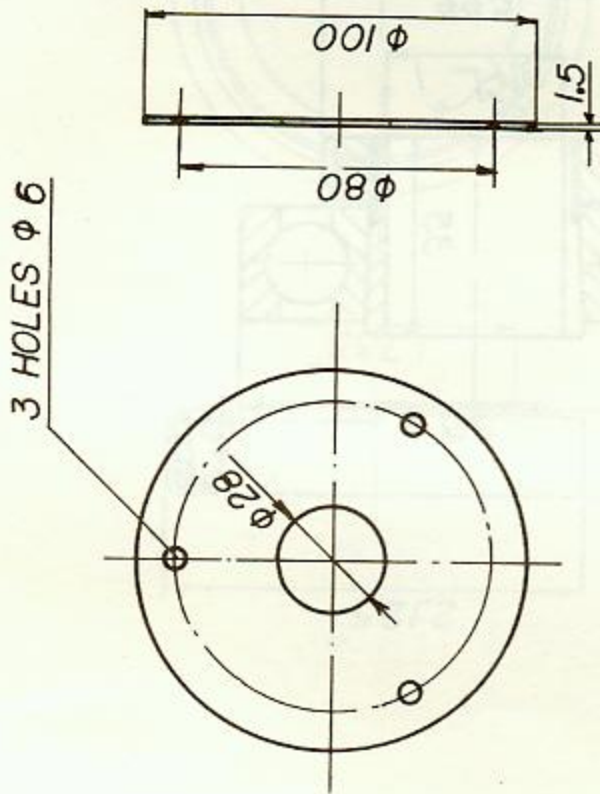


AF323 A

AF323 A



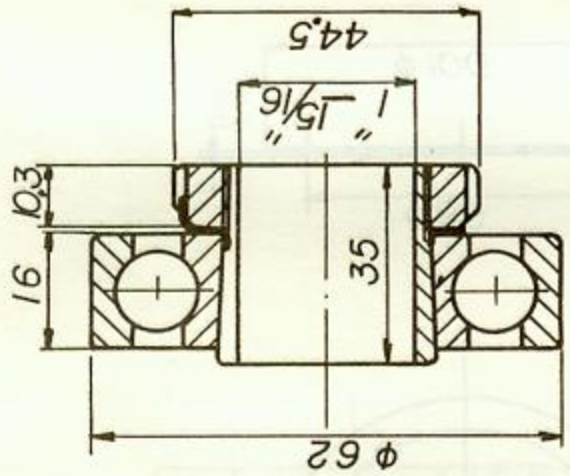
HUB HOUSING DETAIL (2 of 2)



AF323 B

FRONT CAP

AF323 B

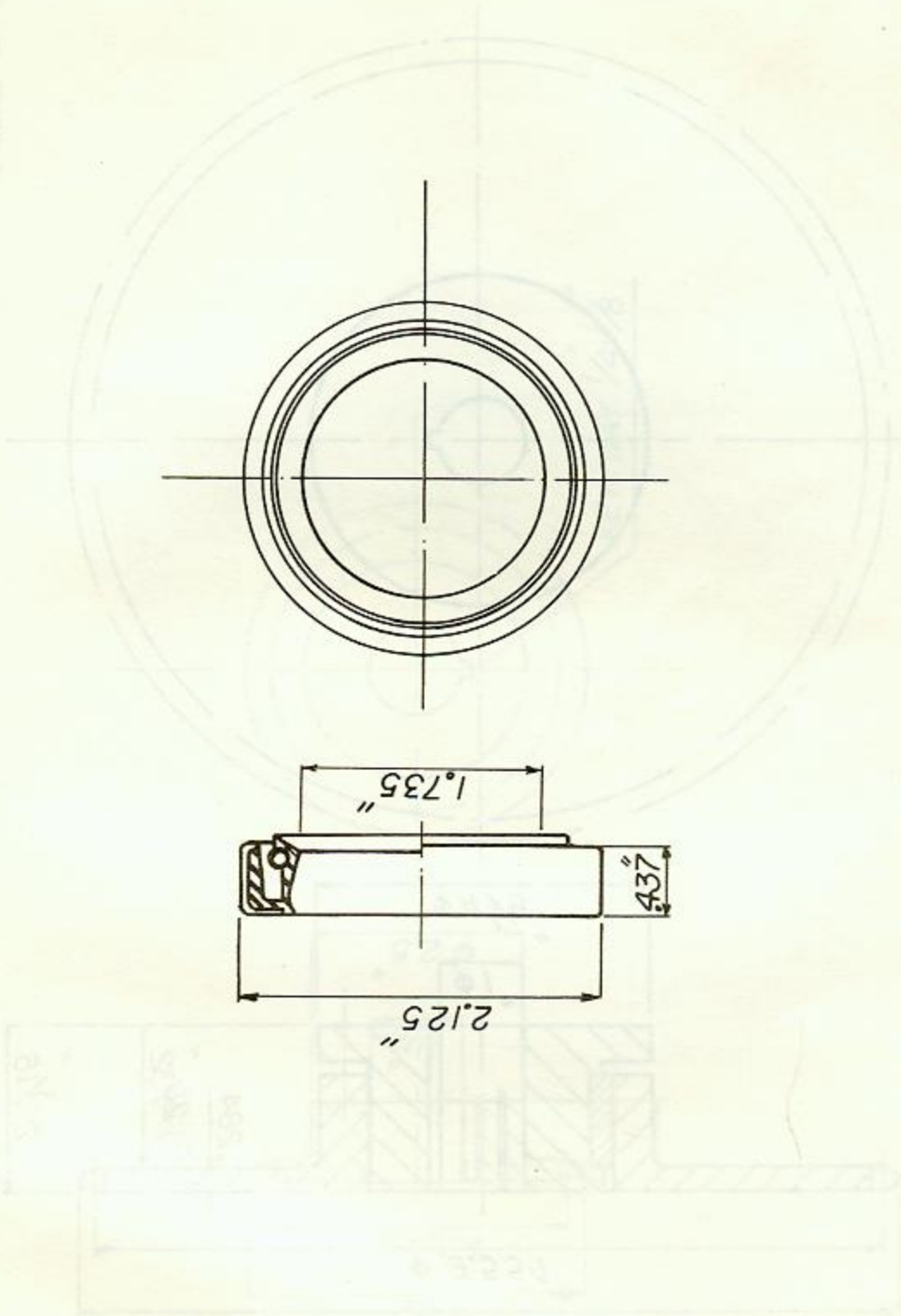


AF323 C

BALL BEARING

AF323A

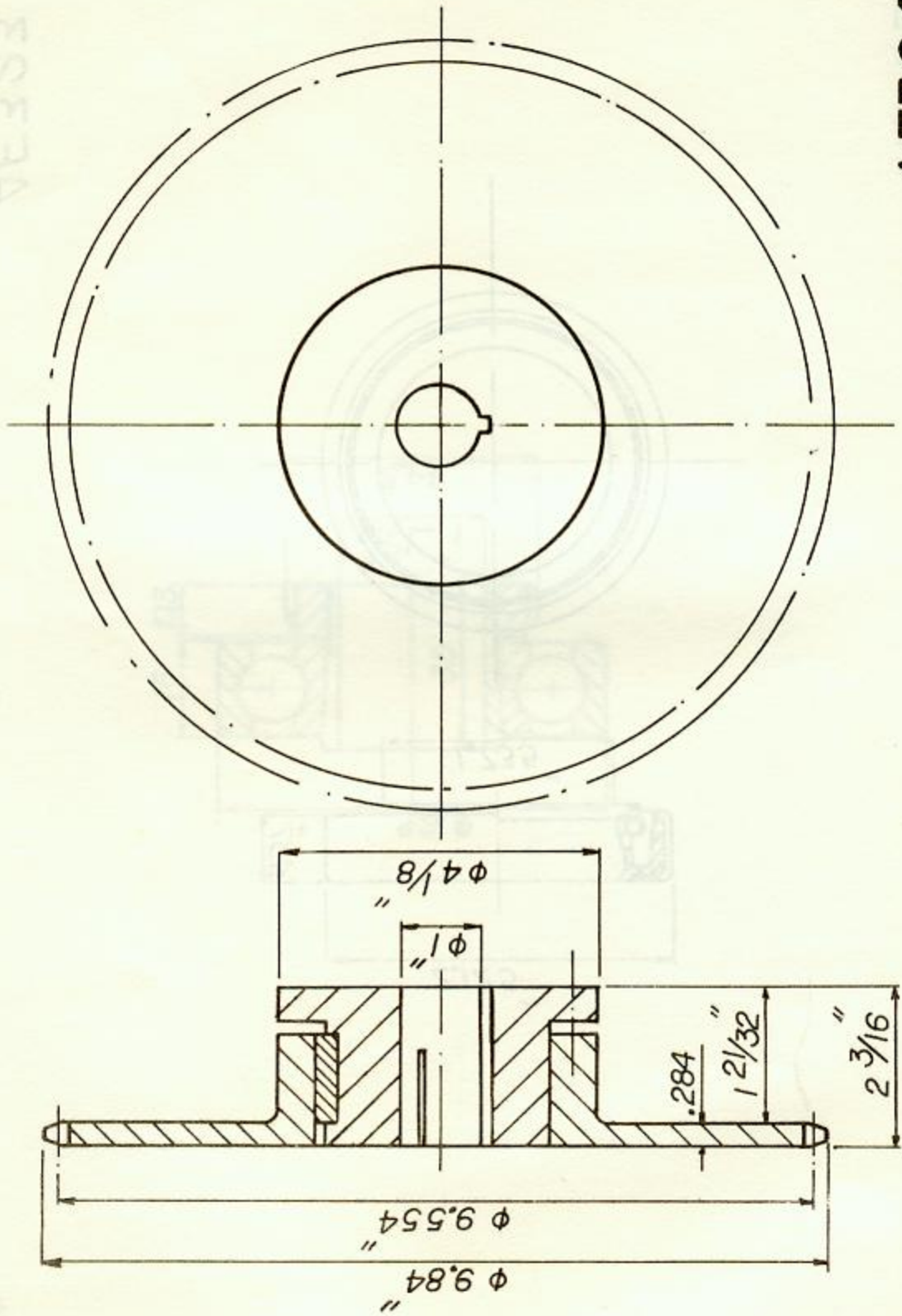
AF323 D



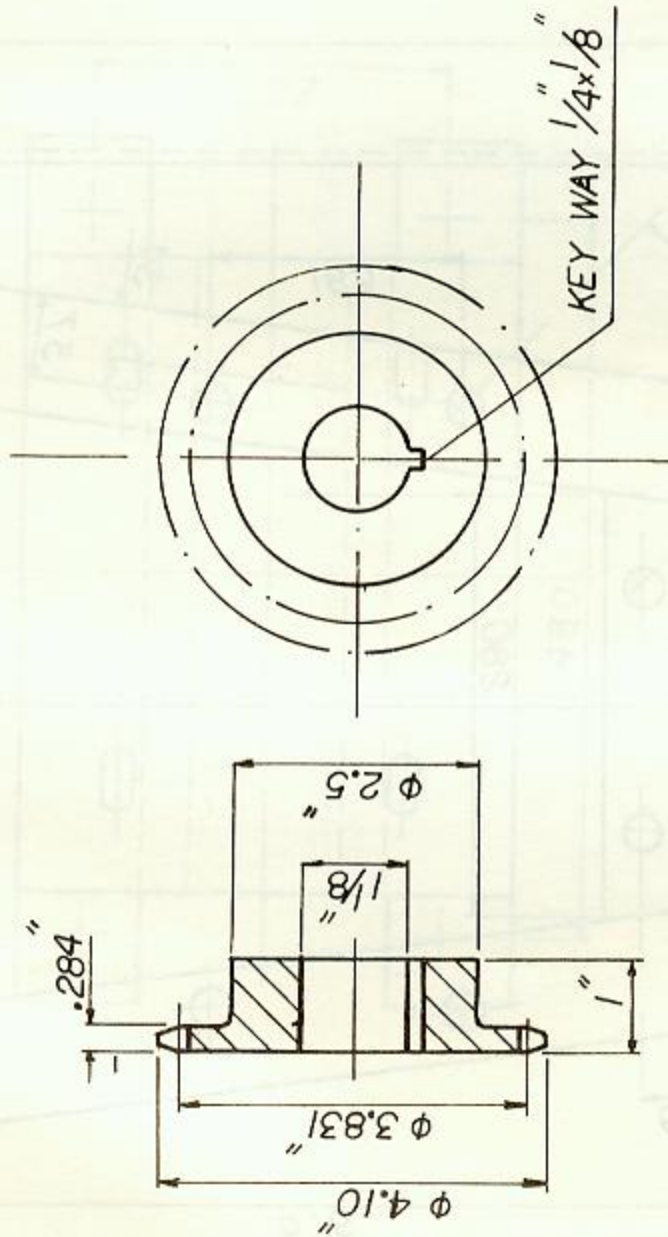
SEAL

AF352 D

AF324 C



BIG SPROCKET

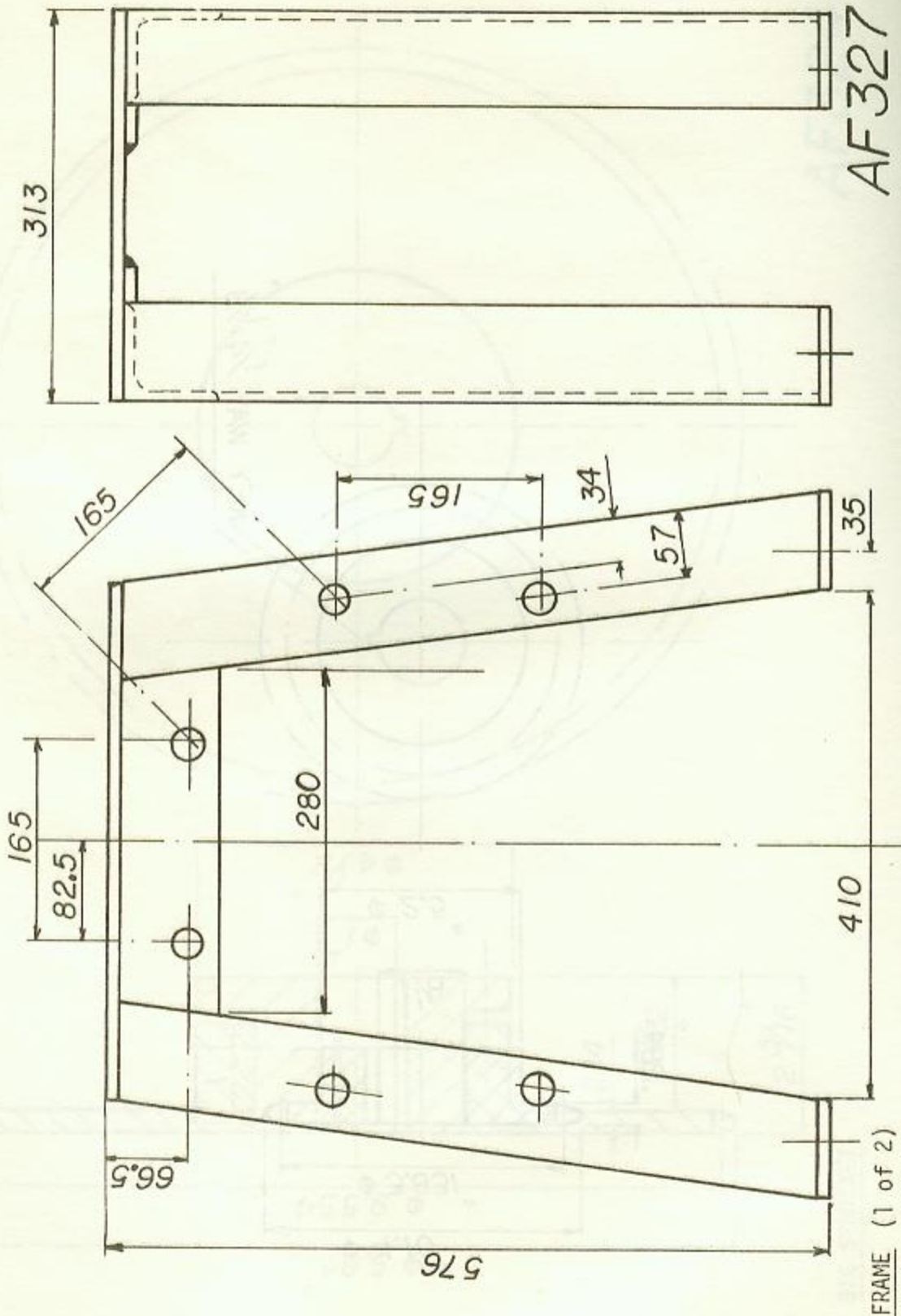


AF325

SMALL SPROCKET

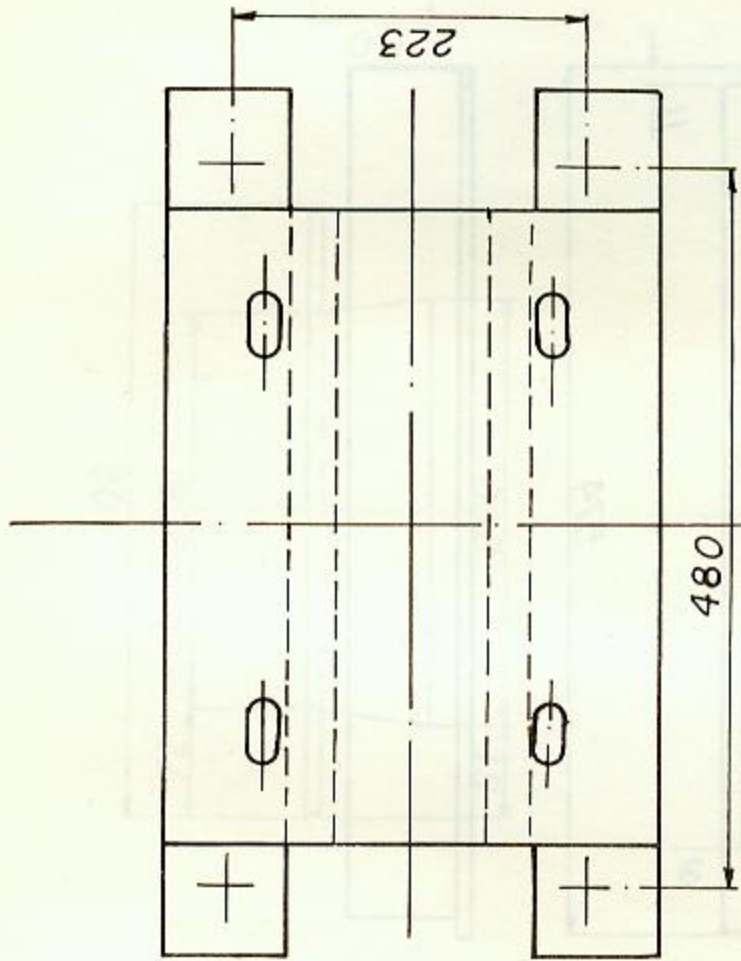


AF327



AF327

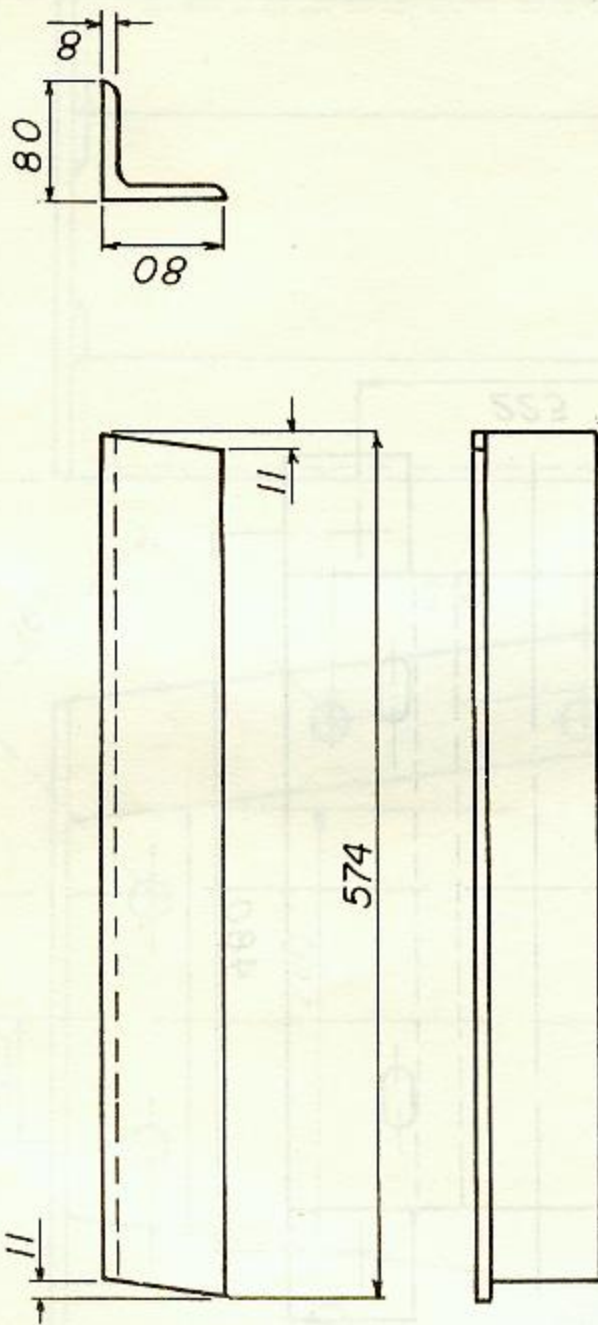
FRAME (1 of 2)



AF327

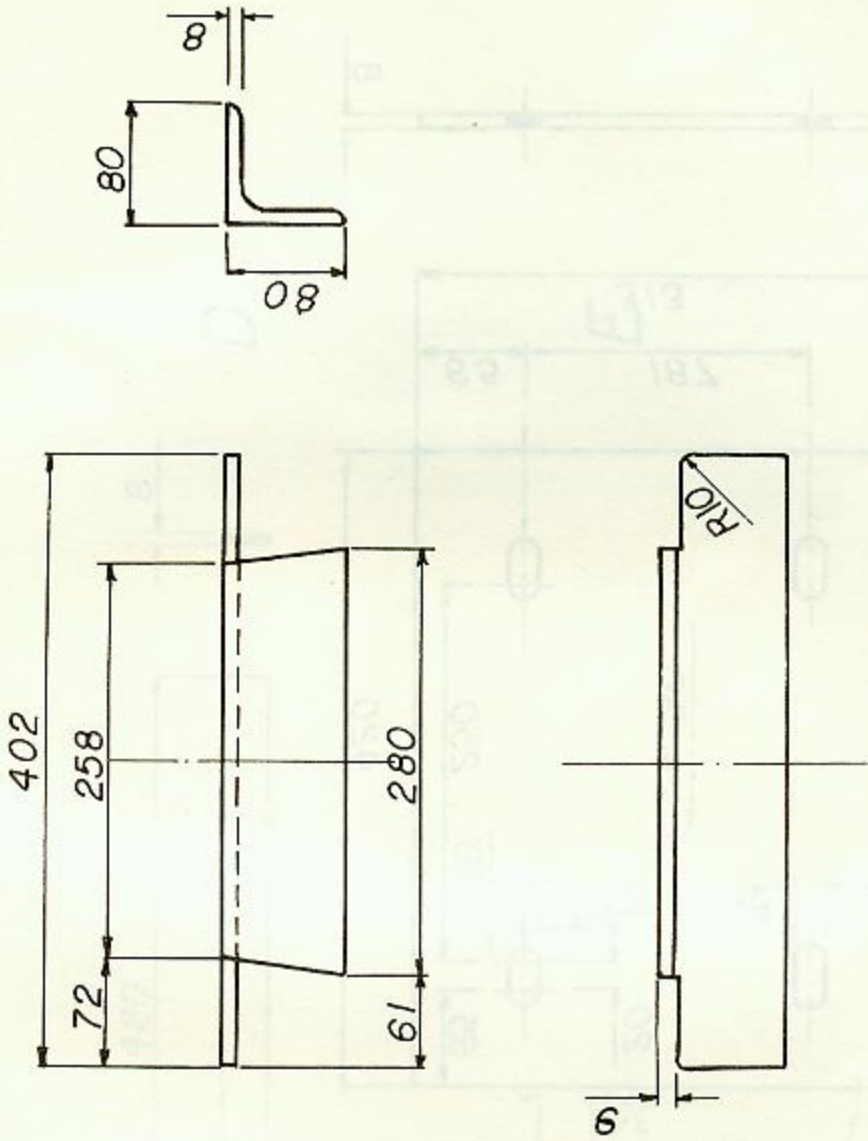
FRAME (plan view) 2 of 2

AF327A



AF327 A

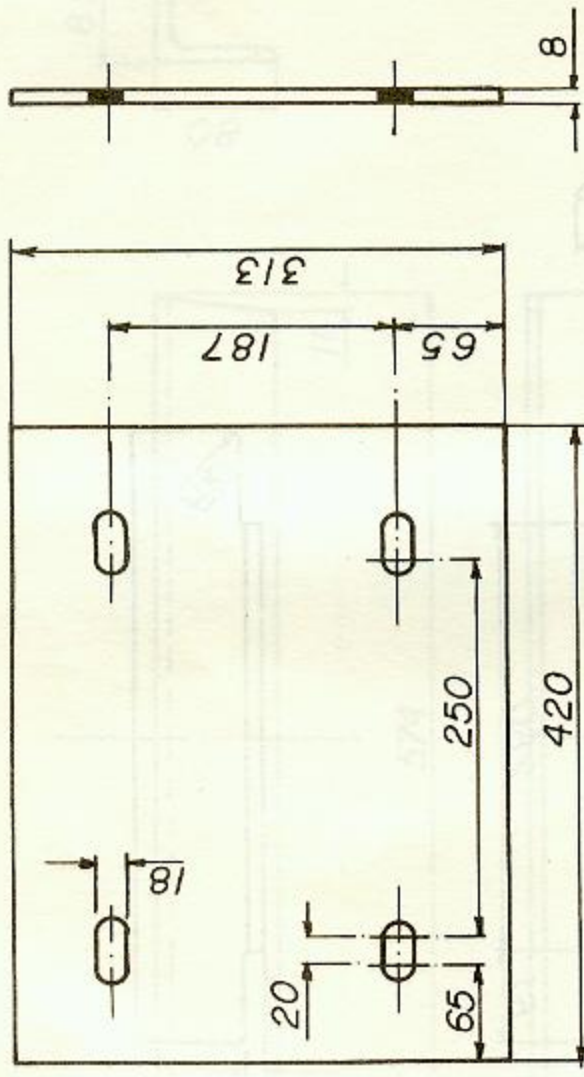
SIDE ANGLES



TOP ANGLE

AF327 B

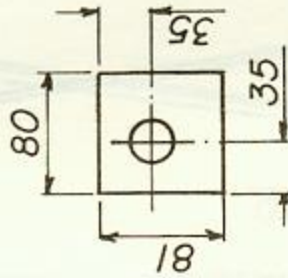
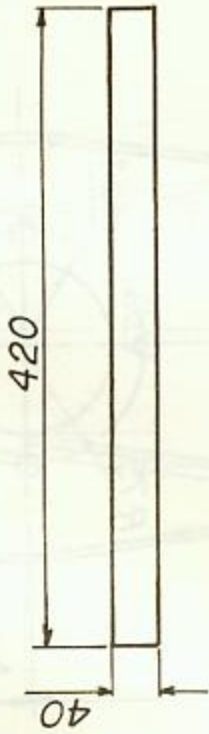
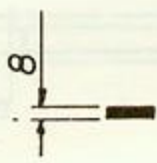
AF327 B



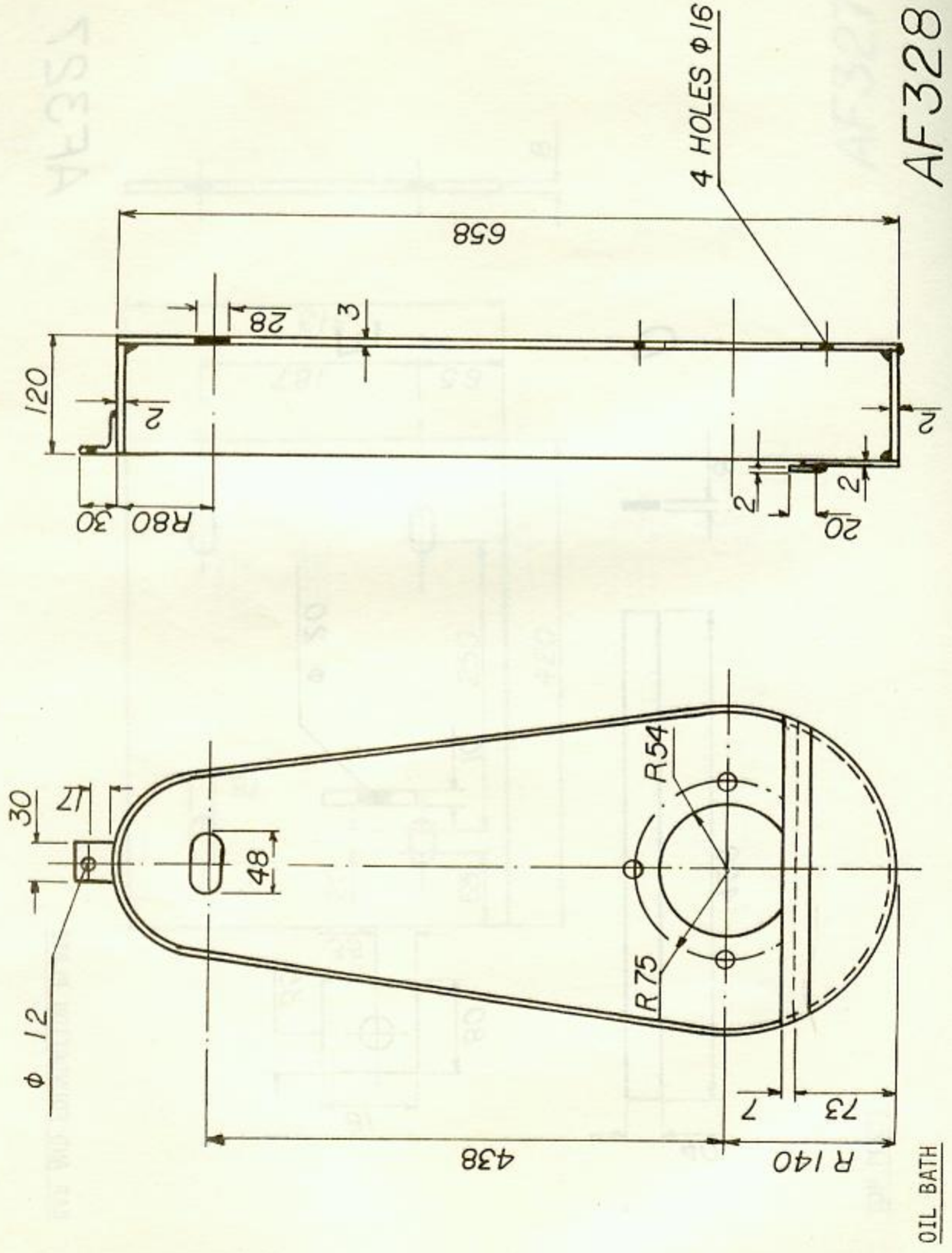
AF327 C

TOP PLATE

AF327 D  
E

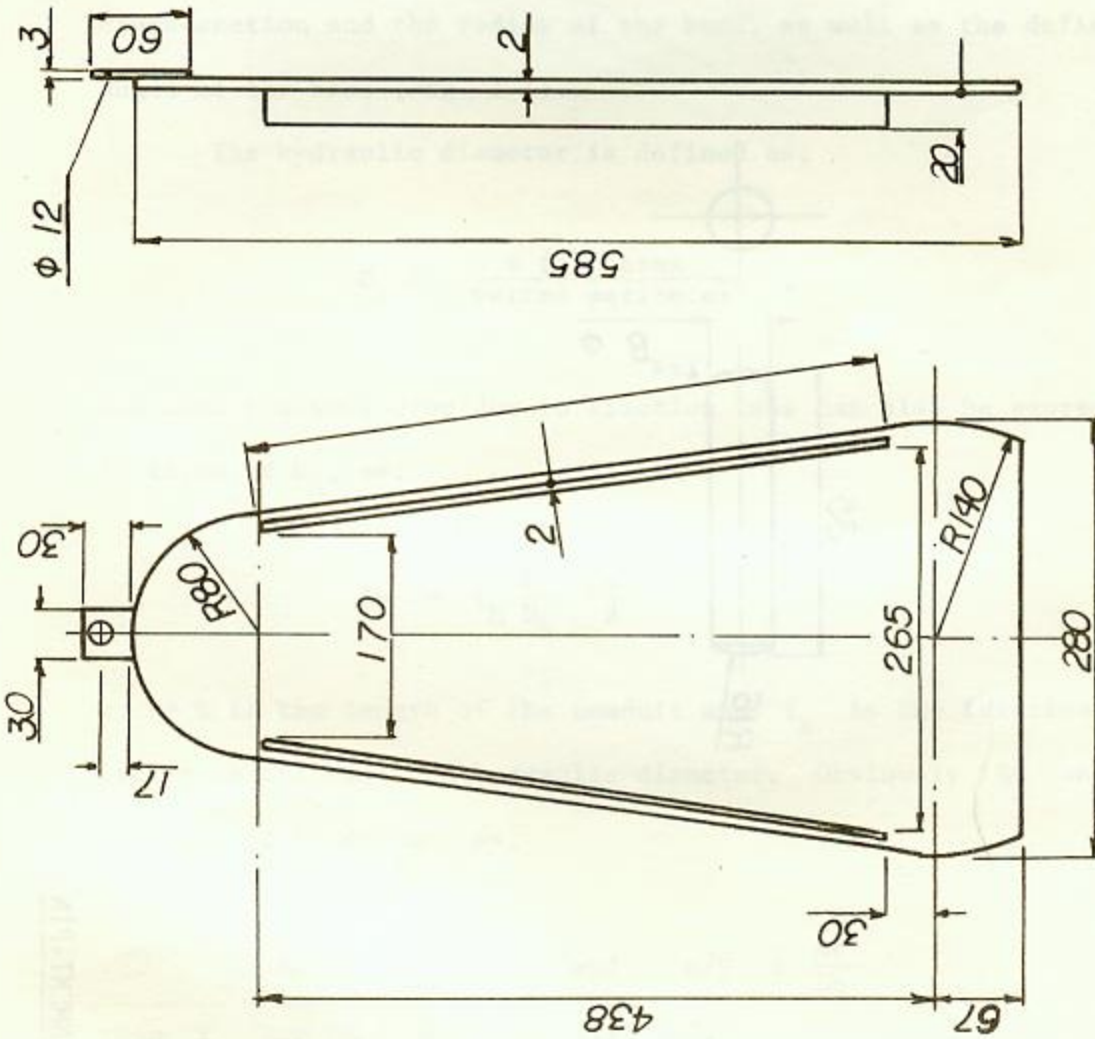


BAR AND FOUNDATION PLATE



AF329

AF329



OIL BATH COVER



## APPENDIX II

### FRICTION LOSS IN NONCIRCULAR CONDUITS

Pressure drop due to flow through a non-circular cross-section bend can be found from;

$$\Delta p = K \frac{\rho v^2}{2}$$

where  $K$  is the loss factor,  $v$  the average flow velocity and  $\rho$  is the mass density.  $K$  is a factor of hydraulic diameter of the cross-section and the radius of the bend, as well as the deflection angle of the bend (Fig. I-1).

The hydraulic diameter is defined as;

$$\Delta D_h \equiv \frac{4 \times \text{flow area}}{\text{wetted perimeter}} ,$$

and then pressure drop due to friction loss can also be expressed in terms of  $D_h$ , as:

$$\Delta p = f_h \frac{L}{D_h} \frac{\rho v^2}{2}$$

where  $L$  is the length of the conduit and  $f_h$  is the friction factor on the basis of hydraulic diameter. Obviously  $Re$  and  $\epsilon/D$  should be defined as,

$$Re \equiv \frac{v D_h}{4\nu} \quad \text{and} \quad \epsilon/D \equiv \frac{4\epsilon}{D_h}$$

then  $f_h$  can be found using Fig. I-2.

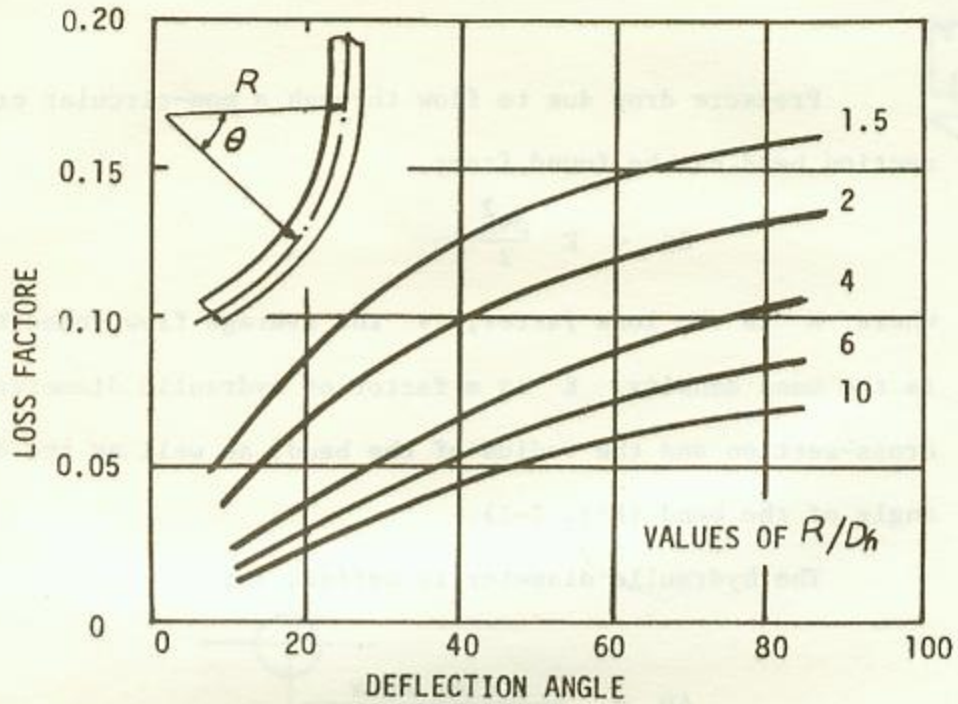


FIG. 1. LOSS FACTOR FOR BENDS. (ASCE, J. HYDRAULIC DIV., NOV. 65)

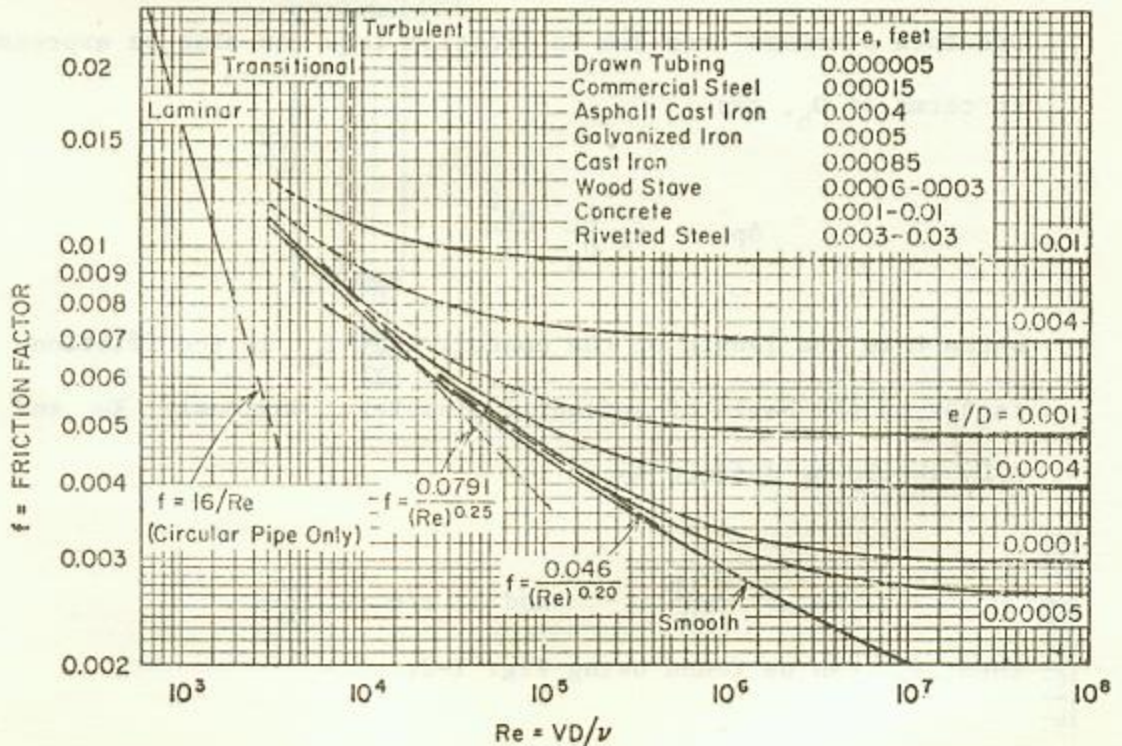


FIG. 2. FRICTION FACTOR  $f$  VS.  $Re$ . FOR DIFFERENT  $e/D$ . (W.M. Rohsenow and H.Y. Choi, Heat, Mass and Momentum Transfer p 58)

APPENDIX III  
EFFICIENCIES

The total-to-total efficiency of a turbine is defined as

$$\eta_{tt} \equiv \frac{\text{turbine output power}}{\text{enthalpy drop from inlet total pressure and temperature to outlet total pressure}}$$

This definition of efficiency is concerned with the blading hydraulic losses.

The total-to-static efficiency of a turbine is defined as,

$$\eta_{t-s} \equiv \frac{\text{Turbine output power}}{\text{enthalpy drop from inlet total pressure and temperature to outlet static pressure}}$$

This efficiency concerns the amount of energy going out of the turbine by drain flow plus the internal losses of the blading.

For a turbine as a machine an overall total-to-static efficiency of the machine can be defined which should include the disk friction and other mechanical losses. That is

$$\eta_{t-sm} \equiv \eta_{t-s} \times \eta_m$$

where  $\eta_m$  is the mechanical efficiency of the machine and defined as,

$$\eta_m \equiv \frac{T - T_{\text{loss}}}{T}$$

where  $T$  stands for shaft torque.

For a turbo-generator unit the efficiency of the generator should also be taken into account which is

$$\eta_g \equiv \frac{\text{output electrical energy}}{\text{input mechanical work}}$$

Then the overall efficiency of the unit will be defined as;

$$\eta_{t-su} \equiv \eta_{t-s} \times \eta_m \times \eta_g \cdot$$

See Fig. II-1 .

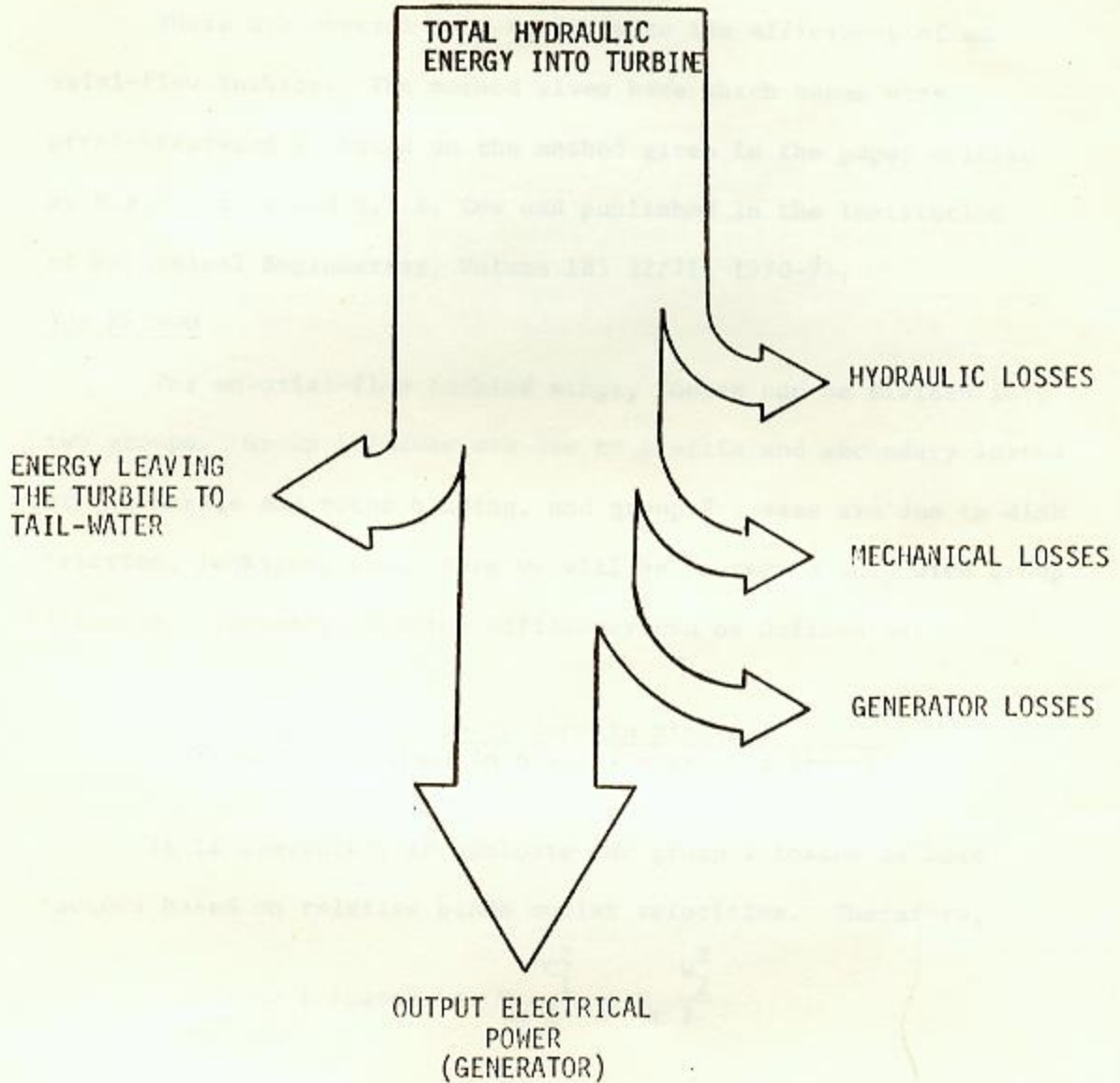


FIG. 1 -- SCHEME OF LOSSES IN WATER TURBO-GENERATORS.

## APPENDIX IV

### PERFORMANCE ESTIMATION OF AXIAL-FLOW TURBINES

There are several ways to evaluate the efficiency of an axial-flow turbine. The method given here which seems very straightforward is based on the method given in the paper written by H.R.M. Craig and H.J.A. Cox and published in the Institution of Mechanical Engineering, Volume 185 32/71, 1970-71.

#### THE METHOD

For an axial-flow turbine stage, losses can be divided into two groups. Group 1 losses are due to profile and secondary losses of the nozzle and rotor blading, and group 2 losses are due to disk friction, leakages, etc. Here we will be concerned only with group 1 losses. Therefore blading efficiency can be defined as

$$\eta_{t-tb} \equiv \frac{\text{work done in blading}}{\text{work done in blading} + \text{group 1 losses}}$$

It is convenient to evaluate the group 1 losses as loss factors based on relative blade outlet velocities. Therefore,

$$\text{Group 1 losses} = X_n \frac{C_1^2}{2} + X_r \frac{W_2^2}{2}$$

where  $X_n$  and  $X_r$  are the sum of loss factors due to profile and secondary losses etc. for the nozzle and rotor, respectively.

Then to take the losses due to tip leakage and etc. into account we have to multiply the value of blading efficiency by the area ratio defined as follows;

$$A_r \equiv \frac{\text{Rotor blade swept area}}{\text{annulus area}}$$

### Evaluation of loss factors

The blade loss factor is the sum of profile loss factor  $X_p$  and secondary loss factor  $X_s$ , where the former one is defined as

$$X_p \equiv X_{pb} N_{pi} N_{pr} N_{pt} + (\Delta X_p) + (\Delta X_p)_{s/e} + (\Delta X_p)_m$$

Each one of these are defined as:

- $X_{pb} \equiv$  basic profile loss
- $N_{pi} \equiv$  loss correction factor due to incidence
- $N_{pr} \equiv$  loss correction factor due to high Reynolds Number
- $N_{pt} \equiv$  loss correction factor due to trailing edge
- $(\Delta X_p)_t \equiv$  profile loss factor increment due to trailing edge
- $(\Delta X_p)_{s/e} \equiv$  profile loss factor increment due to back surface radius
- $(\Delta X_p)_m \equiv$  profile loss factor increment due to high Mach number

This method can acceptably be used for axial-flow water turbines of the kind that this report is concerned with. In this case for design-point preliminary design  $(\Delta X_p)_m$ ,  $(\Delta X_p)_{s/e}$  and  $N_{pi}$  would be zero and the simple form for  $X_p$  will be

$$X_p = X_{pb} N_{pr} N_{pt} + (\Delta X_p)_t$$

Each of these parameters can be found using curves given in Figs. III-2 to III-6. The Reynolds Number is defined on the blade opening as;

$$Re \equiv \frac{W_2 O_2}{\nu} \quad \text{or} \quad \frac{C_1 O_1}{\nu}$$

See Fig. III-1 for the terminology of the blades.

The secondary-loss factor can be found using Figures III-7 and III-8, where the secondary-loss factor  $X_s$  is defined as

$$X_s \equiv (N_s)_{h/b} \times (X_s)_b$$

where

$$(X_s)_b \equiv \text{basic secondary-loss factor}$$

$$(N_s)_{h/b} \equiv \text{secondary-loss ratio.}$$



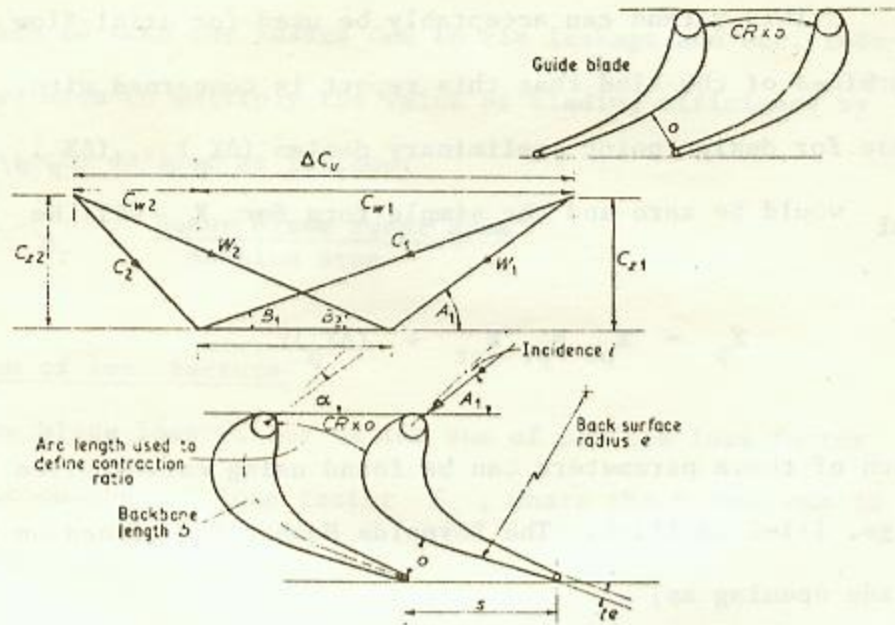


Fig. 1. Turbine blade and velocity triangle notation

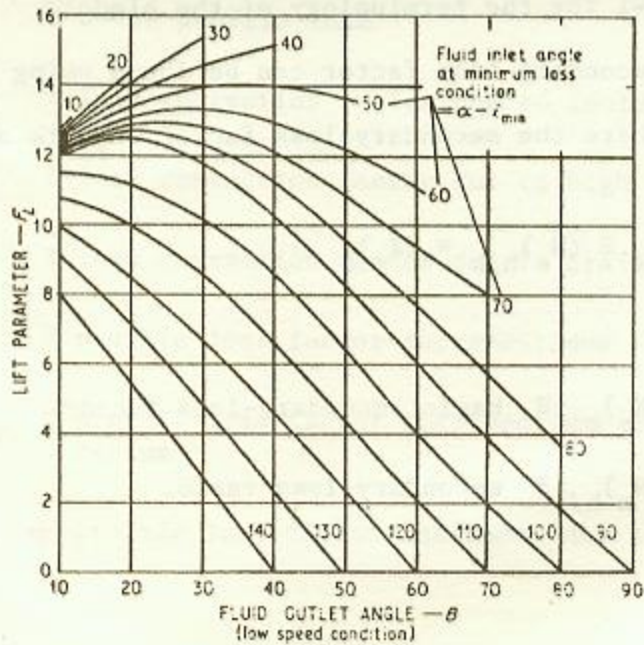


Fig. 2 . Lift parameter,  $F_L$

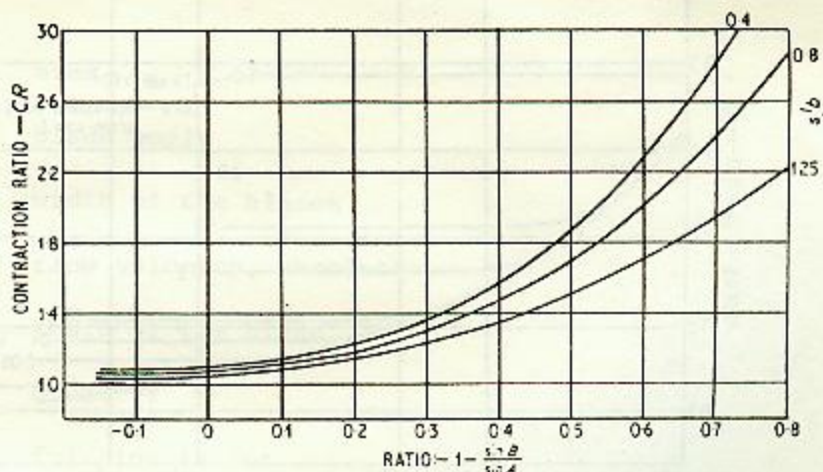


Fig. 3. Contraction ratio for average profiles

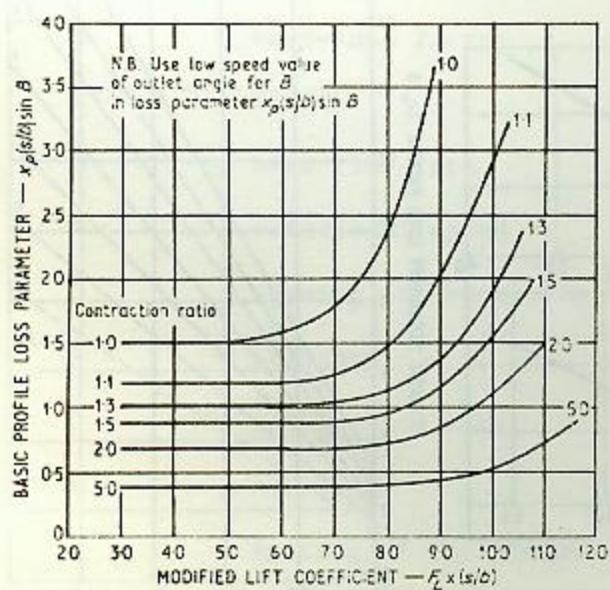


Fig. 4. Basic profile loss

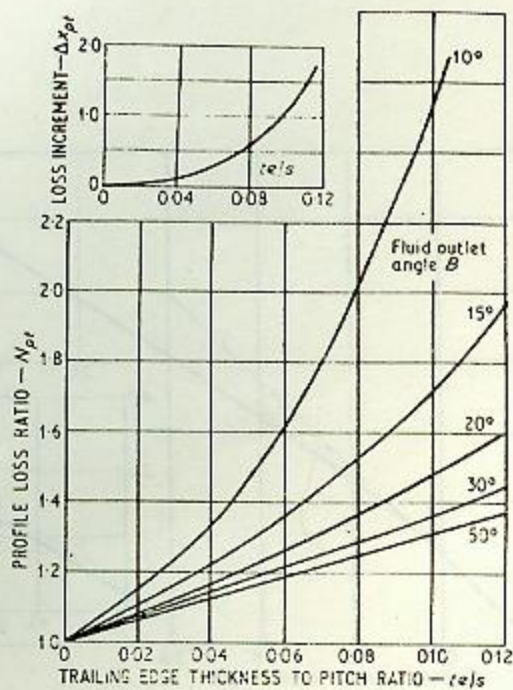


Fig. 5. Trailing edge thickness losses

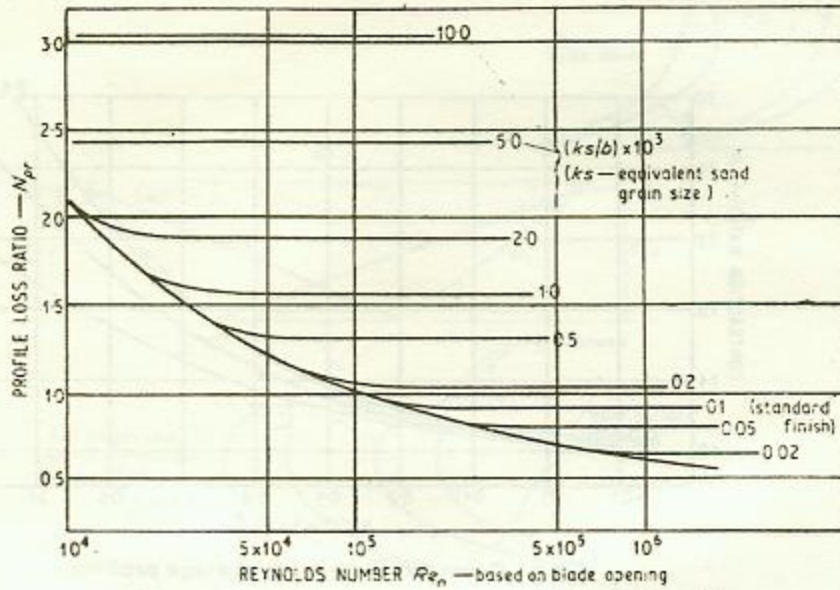


Fig. 6. Profile loss ratio against Reynolds number effect

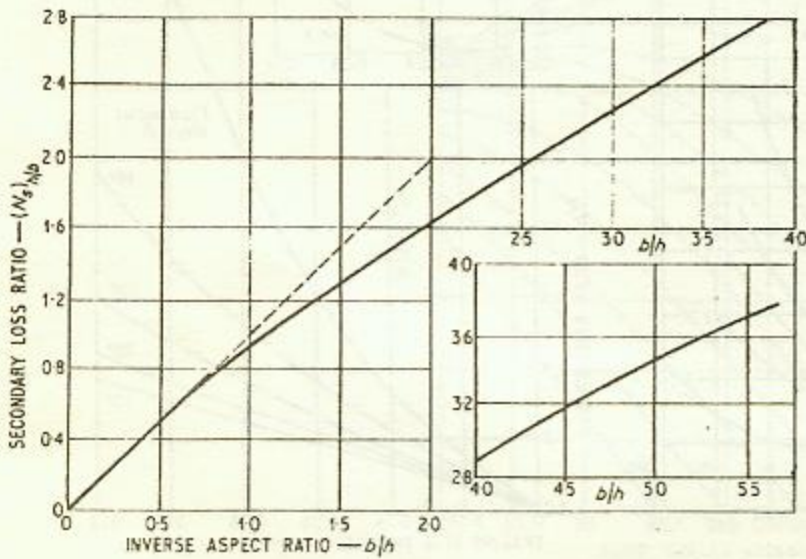


Fig. 7. Secondary loss-aspect ratio factor

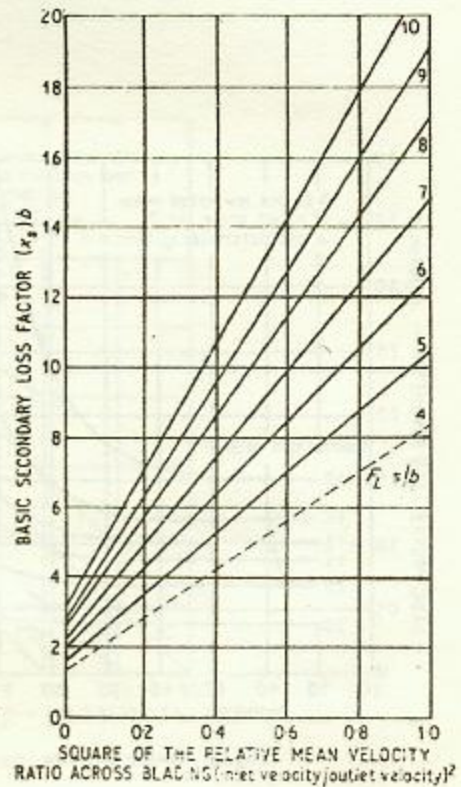


Fig. 8. Secondary loss-basic loss factor

## LIST OF SYMBOLS

A	area
B	blade angle
b	width of the blades
C	flow velocity, absolute
c	chord of the blade
d	diameter
f	friction factor
g	acceleration due to gravity
H	hydraulic head
h	blade height
h	enthalpy
i	incidence angle
K	head-loss factor
L	length
$\dot{m}$	mass flow rate
N	rotational speed
O	opening of the blades
P	pressure
Q	volume flow rate
r	radius
s	spacing of the blades
T	torque

...continued

## LIST OF SYMBOLS (continued)

$U$	blade tangential velocity
$W$	relative velocity, flow
$Z$	number of blades
$\alpha$	angle of absolute velocity
$\beta$	angle of relative velocity
$\Delta$	drop or rise of a variable
$\delta$	deviation angle
$\eta$	efficiency
$\theta$	turning angle
$\lambda$	stagger or setting angle
$\rho$	mass density
$\sigma$	solidity
$\phi$	flow coefficient
$\psi$	work coefficient
$\omega$	speed of revolution (angular velocity)

\* \* \*

SUBSCRIPTS

a	annulus
h	hub
i	inlet
ℓ	leading edge
m	mean value
n	nozzle
o	outlet
p	profile
r	rotor and radial direction
t	tip
x	axial direction
°	stagnation property
1	inlet to the blade
2	out of blade
θ	tangential direction

\* \* \*

## REFERENCES

- (1) Horlock, J.H. Axial Flow Turbines. Robert E. Kreiger Publishing Co., Huntington, New York, 1973.
- (2) Dunavent, J. C., and Erwin, J. R. Investigation of Related Series of Turbine Blade Profiles in Cascade. National Advisory Committee for Aeronautics, Washington, NACA. TN3802.
- (3) Craig, H. R. M., and Cox, H. J. A. Performance Estimation of Axial Flow Turbines. The Institution of Mechanical Engineers (Thermodynamics and Fluid Mechanics Group), Volume 185 32/71, 1970-71.

